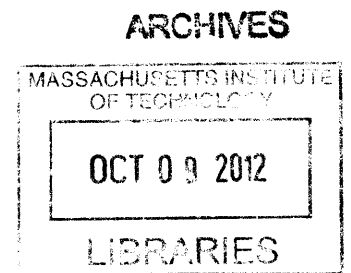


Human Adaptation of Avian Influenza Viruses

by

Karunya Srinivasan

Master of Science, Chemical Engineering 2001
Master of Science, Biology 2003
Rensselaer Polytechnic Institute



SUBMITTED TO THE DEPARTMENT OF BIOLOGICAL ENGINEERING IN PARTIAL FULFILLMENT OF
THE REQUIREMENTS FOR THE DEGREE OF

DOCTOR OF PHILOSOPHY IN BIOLOGICAL ENGINEERING
AT THE
MASSACHUSETTS INSTITUTE OF TECHNOLOGY

September 2012

© 2012 Massachusetts Institute of Technology. All Rights Reserved.

Author

.....

Karunya Srinivasan
Department of Biological Engineering
June 6, 2012

Certified by

.....

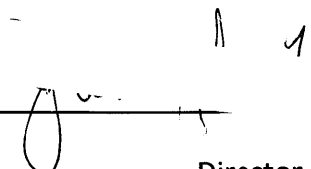
Ram Sasisekharan
Director & Edward Hood Taplin Professor of
Health Sciences & Technology
Thesis Supervisor

Accepted by

.....

Forest M. White
Associate Professor of Biological Engineering
Chair, Graduate Program


Thesis Committee Members:



James G Fox
Director and Professor of Division of Comparative Medicine
Thesis Committee Chair



Ram Sasisekharan
Director & Edward Hood Taplin Professor of
Health Sciences & Technology
Thesis Supervisor



Zachary H Shriver
Vice President of Research,
Visterra, Inc.
Thesis Committee Member

Human Adaptation of Avian Influenza Viruses

By

Karunya Srinivasan

Submitted to the Department of Biological Engineering on
June 6, 2012 in Partial Fulfillment of the Requirements
For the Degree of Doctor of Philosophy in Biological Engineering

Abstract

Human adaptation of avian influenza viruses pose an enormous public health challenge as the human population is predominantly naïve to avian influenza antigens. As such, constant surveillance is needed to monitor the circulating avian strains. Of particular importance are strains belonging to H5N1, H7N7, H7N2 and H9N2 subtypes that continue to circulate in birds worldwide and have on occasions caused infections in humans. A key step in influenza human adaptation is the accumulation of substitutions/mutations in the viral coat glycoprotein, hemagglutinin (HA), that changes HA's binding specificity and affinity towards glycan receptors in the upper respiratory epithelia (referred to as human receptors). Unlike for the H1, H2, H3 and more recently H5 HA a correlation between the quantitative binding of HA to human receptors and respiratory droplet transmissibility has not been established for H9 and H7 subtypes.

This thesis is a systematic investigation of determinants that mediate changes in HA-glycan receptor binding specificity, with focus on the molecular environments within and surrounding the glycan receptor binding site (RBS) of avian HAs, particularly the H9 and H7 subtypes. The glycan receptor binding properties of HA were studied using a combination of biochemical and molecular biology approaches including dose dependent glycan binding, human tissue staining and structural modeling. Using these complementary analyses, it is shown that molecular interactions between amino acids in and proximal to the RBS, including interactions between the RBS and the glycan receptor converge to provide high affinity binding of avian HA to human receptors. For the H9 HA $\alpha 2 \rightarrow 6$ glycan receptor-binding affinity of a mutant carrying Thr-189 \rightarrow Ala amino acid change correlated with the respiratory droplet transmission in ferrets conferred by this change. Further, it was demonstrated for the first time that two specific mutations; Gln226 \rightarrow Leu and Gly228 \rightarrow Ser in glycan receptor-binding site of H7 HA substantially increase its binding affinity to human receptors.

These approaches and findings contribute to a framework for monitoring the evolution of HA and the development of general rules that govern human adaption applicable to strains beyond ones currently under study.

Thesis Supervisor : Prof. Ram Sasisekharan

Acknowledgements

This thesis would not have been possible without the support and encouragement of many to whom I am immensely grateful.

First, I would like to thank my advisor Professor Ram Sasisekharan for his belief in me and for giving me the opportunity to work in his lab. My experiences interacting with him and the confidence he placed in me have helped me grow both as a graduate student and as a researcher who can independently handle her research and discuss the same with an elite audience.

I would like to thank my thesis committee chair Professor James Fox for his invaluable support and guidance. During the numerous meetings we have had through the course of my study his continued enthusiasm towards my work and unstinted support has been an inspiration.

Dr. Zachary Shriver, a member of my committee has contributed to my progress through his numerous insights on the practical applications of my work and sharing exciting updates from the world of biotech/pharma. I have gained much from our numerous exchanges, which prepared me to think more rigorously and learn to embrace the big picture.

I had a great experience being a teaching assistant to Professor John Essigmann and Prof. Darrell Irvine for the class 20.380 viz. "Biological Engineering Design" in Spring 2009. That spring semester I had a wonderful experience of working alongside senior year BE undergraduate students developing cutting research based projects to tackle numerous pathological conditions including malignant cancer.

Dr. Karthik Viswanathan is the first name that comes to mind as I proceed to enunciate the numerous folks associated with the Sasisekharan lab that helped with my research. His perspectives and pragmatic approach have been very useful over the years. I would like to thank Dr. Toomas Haller and Dr. Dave Evarone with whom I worked on the pectin project. I still remember my thoroughly entertaining conversations with Dr. Haller on subjects that ranged from pectin structure to hiking and biking trails in New Hampshire; the latter being as insightful as his meticulous advice on how to extract pectin from citrus fruits.

My list of former Sasisekharan lab members to thank for their support would be incomplete without the mention of Carol, a former graduate student in the lab. Apart from engaging conversations on knitting patterns (she hand kitted a wonderful pair of gloves for me that I still use for biking in cold weather) to teaching me how to make vegetarian sushi I cannot thank Carol enough for her wonderful sense of humor and calm demeanor.

As for current members of the lab, I would like to thank my colleagues Akila and Rahul for their guidance and help throughout my stay; Akila for sharing with me her wet bench skills and Rahul for showing me the nuances of structural modeling.

Among others, I would like to mention Luke Robinson with whom I closely interacted when involved in the pectin work. I am also grateful to Vidya, Kannan, Beam, Andrew, Jing, Nathan, Joann and Keith for their encouragement. A special thanks to my neighbor Boris for welcoming me with a beaming smile each day as I walked into the lab.

Last but not least, Ada is one person whose cheerful presence and alacrity made everything from administrative to academic surmountable. Thank you Ada!

During the course of my graduate work, I have needed to use numerous core facilities around campus. I would like to express my gratitude to Debby Pheasant (at the MIT Biophysical Core Facility) and Wendy Salmon (at the Keck Imaging Facility, Whitehead Inst) for their instructions, advice and assistance in understanding, operating and working with the instruments they managed.

As for the folks outside of MIT who have been with me through this journey I would like to first thank Dr. Margaret Levin at Galenea Corp, where I worked before heading over to MIT. Her unflinching enthusiasm towards the path I proposed to take and her confidence that I would be successful in the same proved of enormous help.

A special thanks to friends outside of the lab. Thank you Rashmi, Venkatesh, Janani, Diwakar, Raghu, Supraja (MadhuSri and Elsa) for the wonderful time that we have had over the years. Your friendship has been a pillar of support.

I cannot find words to express my gratitude to my family for their support. A special thanks to my in-laws and particularly my brother-in-law Mukund and his wife Lakshmi. I am also grateful to my cousins Ashwin, Anitha, Anusha and Anand and my nieces Nethra, Neha, Malavika, Nandita and nephew Siddharth for their encouragement. This journey was made possible by your support and conviction! I also would like to mention my extended family, Sudha, Sreekanth and nephews Sunil and Suhas in this context.

Saving the most important folks for the last 😊 I would like to thank my husband Aravind for everything; for being my friend/philosopher and guide and being by my side all through this journey. This moment would not have been possible without his confidence and encouragement. Thank you Aravind, for your patience and simply for being yourself! I couldn't ask for more!

Finally, I would also like to thank my mother, and my daughter, Niyathi, whose wonderful kisses and smiles went a long way in making this dissertation a reality. Niyathi, in particular for her patience and delightful company outside the lab that help me unwind after a long day at the bench. Thank you my dear little one!

Table of Contents

Abstract.....	3
Acknowledgements.....	4
1 Introduction	10
1.1 Summary	10
1.2 Influenza Viruses	12
1.2.1 Viral Genome	12
1.3 Influenza virus life cycle	13
1.4 Viral Evolution	13
1.4.1 Antigenic Drift	14
1.5 Genesis of Pandemic Influenza	14
1.6 Role of HA in host adaptation	14
1.7 A Topology based definition of HA-Glycan Interactions for a biological read out	15
1.8 Quantitative PCR	16
1.9 Reverse Genetics.....	16
1.10 Motivation for thesis and thesis outline	17
1.10.1 Quantitative Characterization of Glycan-Receptor Binding of H9N2 Influenza A Virus Hemagglutinin.....	17
1.10.2 Understanding receptor binding specificity of H7 Hemagglutinin containing strains of Influenza A virus	18
1.10.3 In Vitro platforms to screen/identify/isolate escape mutants Influenza viruses... ..	18
1.10.4 Decoding Pectins – Establishment of a structure-function relationship for complex glycans in cancer	19
1.11 Significance	19
1.12 References.....	20
2 Quantitative Characterization of Glycan-Receptor Binding of H9N2 Influenza A Virus Hemagglutinin.....	29
2.1 Summary	29
2.2 Introduction.....	30
2.3 Results	32
2.3.1 Characterization of glycan receptor-binding properties of WF10 and Qu88 HAs..	32
2.3.2 Molecular Interactions of WF10 and Qu88 HA with avian and human receptors .	33
2.3.3 Design of WF10 and Qu88 HA mutants and characterization of their glycan receptor-binding properties	34

2.4	Discussion.....	35
2.5	Materials and Methods.....	37
2.5.1	Cloning, baculovirus synthesis, expression and purification of HA.....	37
2.5.2	Homology based structural modeling of H9 HAs.....	38
2.5.3	Binding of recombinant WF10, Qu88 and mutant HAs to human tracheal and alveolar tissue sections.....	38
2.5.4	Dose dependent direct binding of WF10, Qu88 and mutant HAs.....	38
2.6	References.....	41
3	Quantitative Description of Glycan-Receptor Binding of Influenza A Virus H7 Hemagglutinin	49
3.1	Summary.....	49
3.2	Introduction.....	50
3.3	Results.....	52
3.3.1	Quantitative glycan-receptor binding affinities of H7N7 CC and FC HAs.....	52
3.3.2	Quantitative glycan-receptor binding affinities of H7N2 NY/107 HA.....	53
3.3.3	Quantitative glycan-binding affinity of H7N7 HAs double Gln226→Leu/Gly228→Ser mutations.....	53
3.3.4	Binding of H7 HAs to human respiratory tissues.....	54
3.4	Discussion.....	54
3.5	Materials and Methods.....	56
3.5.1	Cloning, baculovirus synthesis, expression and purification of HA.....	56
3.5.2	Dose dependent direct binding of FC, NY/107 and mutant HAs.....	56
3.5.3	Binding of recombinant FC and mFC: LS HAs to human tracheal and alveolar tissue sections	57
3.6	References.....	59
4	Characterization of Viral Escape Mutants by Sequencing and qPCR.....	67
4.1	Summary.....	67
4.2	Overview and Significance.....	69
4.3	Introduction.....	70
4.4	Results.....	71
	Quantitative PCR and genome sequencing as a screen for detection of escape mutants of Influenza viruses in response to pressure from neutralizing compounds.....	71
4.4.1	Method Development.....	71
4.5	Discussion.....	72

4.6	Materials and Methods.....	73
4.6.1	Infection: Calculations for Passage 1.....	73
4.6.2	Processing of vS/N for qRT-PCR and genome sequencing (Fig 4.2; Fig. 4.3 and 4.4 provide finer details).....	74
4.6.3	Processing of vRNA for sequencing the virus genome (Fig. 4.2, 4.3 and 4.4).....	75
4.7	References.....	77
5	Decoding Pectins – Establishment of a structure-function relationship for complex glycans in cancer.....	87
5.1	Summary.....	87
5.2	Introduction.....	88
5.2.1	Structural complexity of pectins.....	88
5.2.2	<i>In vitro</i> and <i>in vivo</i> inhibition of cancer cell growth with LMP treatment.....	89
5.2.3	Analytical tools to elucidate pectin structure.....	90
5.3	An integrated research design for the isolation, <i>in vitro</i> screening and structural characterization of pectic oligosaccharide fractions (POFs) with cancer inhibiting properties.....	91
5.3.1	Rationale.....	91
5.3.2	Strategy.....	92
5.4	Experimental Methods.....	95
5.4.1	Production of pectic derivatives by temperature and pH:.....	95
5.4.2	Capillary electrophoresis (CE).....	95
5.4.3	MALDI-MS.....	96
5.4.4	NMR.....	96
5.5	Acknowledgements.....	96
5.6	References.....	98
6	Summary and Significance of Thesis Research.....	111
6.1	Is Pandemic Influenza predictable?.....	111
6.2	Avian influenza viruses and the continuing risk of a future pandemic.....	111
6.3	Role of HA in Human Adaptation.....	112
6.4	Developing general rules for human adaptation, applicable to any Influenza strain.....	113
6.5	References.....	114

Table of Figures and Tables

Fig 1.1. Cartoon of Influenza A virus Mature Infectious Virion.	23
Fig 1.2. Human and Avian Sialylated Glycan Receptors for Influenza Viruses.	24
Fig 1.3. Antigenic Classification of Influenza viruses.	25
Fig 1.4. Life Cycle of Influenza viruses.	26
Fig 1.5. Genesis of Pandemic Influenza	27
Fig. 1.6 Microarray platforms for probing HA- Glycan interactions.	28
Fig.2.1 Glycan receptor-binding properties of WF10 and Qu88 HA. A,.....	43
Fig. 2.2. Structural model of H9 HA-glycan receptor complexes. A,	44
Fig.2.3. Glycan receptor-binding properties of mWF10:T189A and mWF10:L226Q. A,	45
Fig.2.4. Glycan receptor-binding specificity of mQu88:Q226L, mQu88:T189A and double mutant mQu88:Q226L/T189A HA.	46
Figure 2.5. Sialidase A treated sections of human trachea and alveolus stained with mQu88:Q226L/T189A and mQu88 HA respectively.	47
Table 2.1. Expanded nomenclature of glycans used in the glycan array	48
Fig 3.1. Glycan receptor-binding specificity of FC, CC, NY/107 and mNY/107:A135T HA.....	61
Fig. 3.2. Glycan receptor-binding specificity of Gln226→Leu/Gly228→Ser mutant of FC and CC.	62
Fig 3.3. Tissue binding specificity of FC and mFC:LS for human tracheal and alveolar sections..	63
Fig 3.4: Sequence Alignment of glycan-receptor binding site of H7 HAs.	64
Fig 3.5: Circular Dichroism Analysis of H7 wild type and mutant HAs used in the study.....	65
Fig 4.1 Characterization of viral escape mutants to understand viral evolution under selective pressure.	80
Fig 4.2 Rapid PCR based screen platform for detection of escape mutants to therapeutic pressure for Influenza Viruses.	81
Fig. 4.3 Expanding on the first three steps as outlined in Fig 4.2 viz 1. vS/N Harvest 2. vRNA Extraction and 3. cDNA Synthesis	82
Fig 4.4 Details on Steps 4 and 5 as outlined in Fig 4.2. (viz 4. Rnase H Digestion; ds DNA generation and 5. Agarose gel electrophoresis and gel purification).	83
Table 4.1. Sequencing Primers for the viral genome.....	84
Fig 4.5 A. HA gene amplified after processing vS/N. B. Validation of NA Primers.	85
Fig. 4.6 A. Sequencing guidelines in the context of Reverse Genetics. B. Amplification of HA, NA and M plasmids from v S/N of transfection reaction	86
Figure 5.1: Structural complexity of pectins (adapted from Gunning et al).....	101
Figure 5.2: LMP inhibits B16F10 cell growth <i>in vitro</i>	102
Figure 5.3. Inhibition of primary tumor growth by LMP.	103
Figure 5.4: LMP treatment inhibits tumor growth <i>in vivo</i>	104
Figure 5.5. CE analysis of APTS-labeled oligosaccharides from LMP.....	105
Figure 5.6. Flow chart of the strategy for Specific Aim 1.....	106
Figure 5.7. Overview of pectin-degrading enzymes (adapted from Gunning et al. [35]).	107
Figure 5.8. Overview of structural information garnered from analytical techniques.	108
Figure 5.9. Schematic of transition.	109

1 Introduction

1.1 Summary

In the context of recently emerged novel influenza strains through reassortment, avian influenza subtypes such as H5N1, H7N7, H7N2, H7N3 and H9N2 pose a constant threat in terms of their adaptation to the human host. Among these subtypes, it was recently demonstrated that mutations in H5 and H9 hemagglutinin (HA) in the context of lab-generated reassorted viruses conferred aerosol transmissibility in ferrets (a property shared by human adapted viruses). It has been previously demonstrated that the quantitative binding affinity of HA to $\alpha 2 \rightarrow 6$ sialylated glycans (human receptors) is one of the important factors governing human adaptation of HA. Although the H7 subtype has infected humans causing varied clinical outcomes from mild conjunctivitis to severe respiratory illnesses, it is not clear where the HA of these subtypes stand in regard to human adaptation since its binding affinity to glycan receptors has not yet been quantified.

The molecular interactions of HA with avian and human receptors have been captured using a topology-based definition of glycan receptors [1]. Glycan array platforms comprised of representative avian and human receptors have been widely employed to study the glycan receptor binding of HAs and whole viruses [2-5]. The relative binding affinities of recombinant HAs of avian- (such as H1N1 and H5N1) and human-adapted (such as H1N1 and H3N2) viruses to avian and human receptors have been quantified by analyzing these HAs (or whole viruses) in a dose-dependent manner on glycan array platforms[1, 6-8]. Furthermore, the glycan array binding properties of the HAs have been shown to correlate with their binding to physiological glycan-receptors in human respiratory tissues [9]. Importantly, it has been shown that the human receptor-binding affinity of H1N1 HAs correlated with the efficiency of airborne viral transmission in the ferret animal model [[6, 7]], which is an established model to evaluate viral transmissibility in humans [[7, 10-12]. Such a relationship has yet to be shown for the avian H9 and H7 subtypes. Given increasing number of isolated incidents of human infections by

contemporary strains a detailed analysis of how far these strains have evolved and more importantly how their affinity compares with pandemic and epidemic strains of Influenza A viruses with proven mammalian host transmissibility is addressed in this thesis.

The last part of this thesis focuses on developing in vitro platforms that mimic antigenic drift of the virus in an attempt to map viral evolution and better understand the proclivity of the virus to undergo certain changes in vivo than others. To this end, reverse genetics, quantitative PCR and genome sequencing protocols were tools explored to address the probability of mutation predicted *in silico* appearing in a natural population.

These approaches/findings contribute to a framework for monitoring the evolution of HA and the development of general rules that govern human adaption applicable to strains beyond ones currently under study.

1.2 Influenza Viruses

Influenza viruses belong to the Orthomyxoviridae family of single stranded enveloped RNA viruses. There are three genera of Influenza viruses (viz A, B and C) classified based on the nucleoproteins and matrix proteins of the virus. The influenza A viruses are classified based on two surface proteins Hemagglutinin (HA) and Neuraminidase (NA) as these proteins are primarily responsible for the antigenic changes observed in these viruses. There are 17 known HAs and 9 NAs that have been isolated from their natural reservoir. Based on their antigenicity Influenza viruses are classified into two groups (1 and 2) which are further divided into five clades (Fig. 3). The virions are ~80-120 nm spherical particles with a segmented genome of 8 strands of negative sense RNA that code for 12 viral proteins (HA, NA, matrix proteins M1 and M2, viral polymerases PB1, PB1-F2, PB1-N40, PB2 and PA, Non-structural proteins NS1 and NS2, Nucleoprotein NP)[13]. There are ~400 HA homotrimers and ~100 NA homotetramers on the surface of the mature virion. Widely circulating human influenza viruses are limited to two HA (H1 and H3) and two NA (N1 and N2) subtypes while wild aquatic birds are the predominant hosts for the remaining subtypes (Fig. 1.1)[14].

1.2.1 Viral Genome

The influenza A virus genome consists of eight single-stranded RNAs that encode 11 or 12 proteins. These are nuclear export protein (NEP; also known as NS2) and the host antiviral response antagonist non-structural protein 1 (NS1), which are encoded by the NS segment; the matrix protein M1 and the ion channel M2, which are encoded by the M segment; the receptor-binding protein haemagglutinin (HA), the sialic acid-destroying enzyme neuraminidase (NA), nucleoprotein (NP), and the components of the RNA-dependent RNA polymerase complex (PB1, PB2 and PA), all expressed from their respective genome segments; and the newly identified N40 protein, which is expressed from the PB1 segment and has an unknown function. In addition, some viruses express the pro-apoptotic protein PB1-F2, which is encoded by a second ORF in the PB1 segment. Within the virion, each of the eight viral segments forms a viral ribonucleoprotein (RNP) complex: viral RNA is wrapped around NP, and this structure is then bound to the viral polymerase complex.

1.3 Influenza virus life cycle

The first step in the life cycle of the virus is attachment to host cell receptors mediated by HA. The viral HA attaches to host cell receptors that contain terminal α -2,6-linked or α -2,3-linked sialic acid (α -2,6-SA or α -2,3-SA) moieties, and the virus enters the cell by receptor-mediated endocytosis. Cleavage of HA by cellular proteases exposes the HA peptide for fusion between viral envelope and the endosomal membrane. Acidification of the endocytic vesicle opens the M2 ion channel, resulting in proton flux into the inside of the virion, a process that is required for proper uncoating of the RNP complexes that contain the viral genome. Acidification of the endosome also triggers the pH-dependent fusion step that is mediated by HA and results in the cytoplasmic release of the RNP complexes. These translocate to the nucleus, where the RNA-dependent RNA polymerase transcribes and replicates the negative-sense viral RNA ((-)vRNA), giving rise to three types of RNA molecules: the complementary positive-sense RNA ((+)cRNA), which it uses as a template to generate more vRNA; negative-sense small viral RNAs (svRNAs), which are thought to regulate the switch from transcription to replication; and the viral mRNAs, which are exported to the cytoplasm for translation. Viral proteins that are needed in replication and transcription are translocated back to the nucleus, and progeny RNPs are then exported to the cytoplasm for packaging, assisted by M1 and NEP. Viral HA, NA and M2 are transported by the *trans*-Golgi secretory pathway, and the mature proteins arrive at the plasma membrane, where M1 assists in the formation of virus particles. Budding then occurs, and release from the host cells is mediated by the neuraminidase activity of NA, which destroys the SA of the cellular and viral glycoproteins that would otherwise retain the new virions at the cell surface (Fig. 1.4)[9, 15].

1.4 Viral Evolution

The epidemiological success of Influenza viruses can be largely attributed to the rapid antigenic change that they continuously undergo [16]. The error-prone viral polymerase has a mutation rate of one nucleotide exchange per genome or per replication cycle. [17]. In case of selective pressures from neutralizing antibodies, chemical antivirals mutants with selective advantages (to facilitate escape from neutralization) may be singled out and become the dominant variant in the viral quasi species in that host or population.

1.4.1 Antigenic Drift

Antigenic Drift refers to slight changes in the viral surface proteins (point mutations that typically involve one or two amino acid changes) that allow the viruses to evade human immune responses. It may take 3-5 years for a given subtype to gradually accumulate enough point mutations to cause disease when it re-infects a previously exposed population. Antigenic drift causes epidemics.

1.5 Genesis of Pandemic Influenza

Of the known 16 HAs and 9 NAs that make up all known Influenza virus strains only a small subset circulate in the human population; the others being endemic to the natural reservoir for these viruses wild aquatic birds. The few known instances of acquisition of human tropism by avian strains have led to enormous global health consequences the most recent of being the 2009 H1N1 Swine flu pandemic[18] (Fig. 1.5).

1.6 Role of HA in host adaptation

Interspecies transmission of Influenza viruses is a polygenic event with the entire genome programmed for efficient replication and transmission in the new host species which explains why only a small subset of the 144 subtype combinations thrive in mammalian hosts. Host restriction is partly mediated by the viral surface glycoprotein hemagglutinin (HA) which binds to sialylated glycan receptors, complex glycans terminated by N-acetylneuraminic acid (Neu5Ac) expressed on the host cell surface. Attachment is mediated via trimerized mature viral HA with monovalent complexes between HA and host glycans being weak and easily dissociated. Attachment is further stratified by the glycosidic linkage to the penultimate galactose and the composition of the further inner fragments of the sialyloligosaccharides present at the cell surface. Thus, it is conceivable that host restriction is imposed by the variety of different sialyloligosaccharides expressed with restriction to tissue and species in the different hosts of the virus. Glycans terminating in Neu5Ac that is $\alpha 2 \rightarrow 6$ -linked to the penultimate sugar are predominantly expressed in human upper respiratory epithelia and serve as receptors for human-adapted influenza A viruses (henceforth referred to as human receptors). Binding to human receptors consequently allows the virus to replicate in the

respiratory epithelium in addition to allowing the virus to be conveyed via respiratory droplets when the infected individual sneezes. On the other hand, glycans terminating in Neu5Ac that is $\alpha 2 \rightarrow 3$ -linked to the penultimate sugar residue, serve as receptors for the avian-adapted influenza viruses (henceforth referred to as avian receptors) and are typically found to replicate in the gastrointestinal tract of birds allowing these avian strains to spread via fecal-to-oral route[19, 20] (Fig 1.2).

When avian influenza viruses are transmitted from avian reservoir hosts to highly susceptible poultry like chickens and turkeys only mild symptoms are induced with the birds remaining mostly asymptomatic except in cases of coinfection with other strains or the virus mutating without warning to a highly pathogenic strain consequently resulting in complete mortality. Poultry species like the waterfowl, quail and turkey support multiple cycles of infection and recent studies have shown the birds to have a human receptor distribution in the upper respiratory epithelium consequently allowing these avian HAs to mutate towards adaptation to their new hosts which results in the acquisition of human receptor specificity increasing the likelihood of transmission to humans in immediate contact with the birds (Fig 5).

1.7 A Topology based definition of HA-Glycan Interactions for a biological read out

Given the importance of HA-glycan interaction in governing infection and transmissibility numerous tools have been used to discern a particular strain's pandemic potential based on the receptor binding specificity of HA. Agglutination assays, Fetuin capture assays, crystal structures of HA with glycans and more recently advances in chemical and chemoenzymatic synthesis of glycans have allowed fine exploration of the HA-glycan interactions [9]. However, one limitation of these tools is that the viral titers or HA concentrations used are often very high and only look at $\alpha 2-3$ or $\alpha 2-6$ glycans and often times proving inconsistent in explaining the apparent differences in transmission capabilities of numerous strains that have similar profiles or preferences discerned by these assay platforms.

The molecular interactions of HA with avian and human receptors have been captured using a topology-based definition of glycan receptors [1]. Glycan array platforms comprised of representative avian and human receptors have been employed to study the glycan receptor

binding of HAs and whole viruses [2-5]. The relative binding affinities of recombinant HAs of avian- (such as H1N1 and H5N1) and human-adapted (such as H1N1 and H3N2) viruses to avian and human receptors have been quantified by analyzing these HAs (or whole viruses) in a dose-dependent manner on glycan array platforms[1, 6-8]. Furthermore, the glycan array binding properties of the HAs have been shown to correlate with their binding to physiological glycan-receptors in human respiratory tissues [9]. Importantly, it has been shown that the human receptor-binding affinity of H1N1 HAs correlated with the efficiency of airborne viral transmission in the ferret animal model [[6, 7]], which is an established model to evaluate viral transmissibility in humans [[7, 10-12] as these animals have similar glycan structures to humans including a predominance of a2-6 glycans in their upper respiratory tract epithelium.

1.8 Quantitative PCR

Molecular based techniques for detecting Influenza viruses have become an integral component of human and animal surveillance programs over the last two decades. The recent pandemic of swine origin (H1N1) and the continuing circulation of highly pathogenic avian influenza viruses have further stressed the need for rapid and accurate identification of viral species. To this end, there has been remarkable progress on the detection and molecular characterization of influenza virus infection in clinical, mammalian and domestic poultry and wild bird samples in recent years. The application of these techniques including reverse transcriptase PCR, real-time PCR, microarrays and other nucleic acid sequencing based amplifications has been extensively documented. This thesis refers to numerous excellent reviews on the applications of such tools/techniques in Influenza virus research [21-23]. Real time PCR was used to evaluate IC50 changes in response to drugs/therapeutic compounds in an effort to map viral evolution in this thesis.

1.9 Reverse Genetics

The term reverse genetics simply refers to the generation of a whole infectious virus particle from cDNAs of individual virus genes. The ability to generate any combination of internal genes and surface proteins is an excellent tool for systematic exploration of the contribution/role of the various components of the virus in virulence and transmissibility. While the glycan array

platform described above allows testing of engineered mutants of HA, using reverse genetics one could engineer a live virus bearing the mutant surface glycoprotein and explore transmission in vivo thus completing the entire cycle[24-28].

1.10 Motivation for thesis and thesis outline

The 2009 Swine origin Influenza pandemic was a gentle reminder that in spite of extensive research our ability to predict when or how severe or even the subtype for the next pandemic still remains poor[29]. The continuing spread of the high pathogenic H5N1 virus in several continents leading to numerous fatalities has raised the pandemic stakes significantly. Although overshadowed by H5N1 outbreaks, there have been several other poultry epizoonotics involving human respiratory infections; H9N2 and H7 subtype viruses being prominent players in this category[30-33].

Fundamental questions on how influenza viruses switch hosts from wild birds to domesticated poultry, pigs or horses and eventually to humans remain unanswered, especially those regarding changes that would allow human-to-human transmission capabilities[34, 35]. With data suggesting that the 1918 virus was avian-like prior to human adaptation and that the H2N2 and H3N2 pandemics in '57 and '68 were reassortments with the '18 and '57 respectively; the need to analyze systematically the possibility of both a de novo human adaptation by a hitherto avian strain and reassortment become important for pandemic preparedness.

Broadly divided into the following major sections, this thesis addresses the aforementioned inadequacies via the use and development of novel in vitro platforms for the study of Influenza viruses:

1.10.1 Quantitative Characterization of Glycan-Receptor Binding of H9N2 Influenza A Virus Hemagglutinin

The glycan receptor-binding properties of both H9N2 viruses isolated from avian species and reassorted viruses comprising of wild-type and mutant forms of H9 HA have been studied by screening them on glycan array platforms [36]. Such screening analyses served as a quick readout for the number of different types of glycans that can bind to the virus at a fixed high

viral titer and limited biochemical information on glycan affinity and specificity. Previously, the Sasisekharan lab had demonstrated that correlating glycan-receptor binding properties from such screening assays to transmissibility of virus had major limitations [8]. Instead, deriving quantitative parameters from a dose-dependent binding to representative human and avian receptors to compare relative human:avian receptor binding affinities correlated with the respiratory droplet transmissibility of the virus was a better way to get a handle on human adaptation [8, 37, 38]. Such a correlation remains to be determined for the H9 subtype in the context of the reassorted viruses that show respiratory droplet transmission in ferrets and this section delves into the evaluation of the pandemic potential of contemporary H9N2 strains.

1.10.2 Understanding receptor binding specificity of H7 Hemagglutinin containing strains of Influenza A virus

As with H9N2 strains, screening initiatives have been undertaken to elucidate the glycan binding preferences for H7 subtype viruses.

This section is an investigation of glycan-receptor binding properties of avian H7 subtype HAs given that this subtype has been known to infect and cause disease in humans. Using a combination of structural modeling, glycan array and human tissue binding analyses in this study; glycan-receptor binding specificity and affinity of wild-type and mutant forms of H7 HAs was quantitatively characterized. Such a quantitative description of glycan-binding properties of H7 HAs has not been reported earlier.

1.10.3 In Vitro platforms to screen/identify/isolate escape mutants Influenza viruses

While the aforementioned sections primarily focus on the use of recombinant proteins for receptor specificity and affinity evaluations the question/s of whether the same conclusions would hold good in vivo remain. In an effort to develop an in vitro platform that mimics the physiological representation of HA this section proposes the use of reverse genetics for mutational analysis of HA. In addition, quantitative PCR as a tool for escape mutant detection could be use in tandem to hone our understanding of the direction of evaluation of these complex viruses that would aid in vaccine and drug development.

1.10.4 Decoding Pectins – Establishment of a structure-function relationship for complex glycans in cancer

This final part of this thesis, is focused on taking lesson from the structure and conformational analysis of glycan-protein interactions of influenza A virus hemagglutinin to its sialylated glycan receptors to the another disease modality viz cancer.

The use of a similar framework to isolate the test carbohydrate oligosaccharides as cancer therapeutics is discussed.

1.11 Significance

To improve the ability to predict influenza pandemics it is necessary to use quantitative tools and complementary analyses to gain a better understanding of host-switching events. Enhanced surveillance and prospective analysis of strains in circulation are crucial in a complex ecological system. The need for development of cost-effective and rapid readout platforms that would help make intelligent choices on how best to evaluate the risk posed by Influenza viruses would be important when addressing a global health challenge. To this end a structure-function relationship paradigm proposed in this thesis attempts to address the aforementioned challenges in a systematic fashion. Presented are two studies, the first being the study of the relationship between the Influenza virus surface glycoprotein HA and its glycan receptors and the second being the study of the role of complex carbohydrates in cancer.

1.12 References

- 1 Basler, C. F. (2007) Influenza viruses: basic biology and potential drug targets. *Infect Disord Drug Targets*. **7**, 282-293
- 2 Bouvier, N. M. and Palese, P. (2008) The biology of influenza viruses. *Vaccine*. **26 Suppl 4**, D49-53
- 3 Shriver, Z., Raman, R., Viswanathan, K. and Sasisekharan, R. (2009) Context-specific target definition in influenza A virus hemagglutinin-glycan receptor interactions. *Chem Biol*. **16**, 803-814
- 4 Nayak, D. P., Hui, E. K. and Barman, S. (2004) Assembly and budding of influenza virus. *Virus Res*. **106**, 147-165
- 5 Taubenberger, J. K. and Kash, J. C. (2011) Insights on influenza pathogenesis from the grave. *Virus Res*. **162**, 2-7
- 6 Taubenberger, J. K. and Morens, D. M. (2010) Influenza: the once and future pandemic. *Public Health Rep*. **125 Suppl 3**, 16-26
- 7 Neumann, G. and Kawaoka, Y. (2011) The first influenza pandemic of the new millennium. *Influenza Other Respi Viruses*. **5**, 157-166
- 8 Ge, S. and Wang, Z. (2011) An overview of influenza A virus receptors. *Crit Rev Microbiol*. **37**, 157-165
- 9 Viswanathan, K., Chandrasekaran, A., Srinivasan, A., Raman, R., Sasisekharan, V. and Sasisekharan, R. (2010) Glycans as receptors for influenza pathogenesis. *Glycoconj J*. **27**, 561-570
- 10 Chandrasekaran, A., Srinivasan, A., Raman, R., Viswanathan, K., Raguram, S., Tumpey, T. M., Sasisekharan, V. and Sasisekharan, R. (2008) Glycan topology determines human adaptation of avian H5N1 virus hemagglutinin. *Nat Biotechnol*. **26**, 107-113
- 11 Wei, C. J., Boyington, J. C., Dai, K., Houser, K. V., Pearce, M. B., Kong, W. P., Yang, Z. Y., Tumpey, T. M. and Nabel, G. J. (2010) Cross-neutralization of 1918 and 2009 influenza viruses: role of glycans in viral evolution and vaccine design. *Sci Transl Med*. **2**, 24ra21
- 12 Stevens, J., Blixt, O., Paulson, J. C. and Wilson, I. A. (2006) Glycan microarray technologies: tools to survey host specificity of influenza viruses. *Nat Rev Microbiol*. **4**, 857-864
- 13 Stevens, J., Blixt, O., Chen, L. M., Donis, R. O., Paulson, J. C. and Wilson, I. A. (2008) Recent avian H5N1 viruses exhibit increased propensity for acquiring human receptor specificity. *J Mol Biol*. **381**, 1382-1394
- 14 Childs, R. A., Palma, A. S., Wharton, S., Matrosovich, T., Liu, Y., Chai, W., Campanero-Rhodes, M. A., Zhang, Y., Eickmann, M., Kiso, M., Hay, A., Matrosovich, M. and Feizi, T. (2009) Receptor-binding specificity of pandemic influenza A (H1N1) 2009 virus determined by carbohydrate microarray. *Nat Biotechnol*. **27**, 797-799
- 15 Hensley, S. E., Das, S. R., Bailey, A. L., Schmidt, L. M., Hickman, H. D., Jayaraman, A., Viswanathan, K., Raman, R., Sasisekharan, R., Bennink, J. R. and Yewdell, J. W. (2009) Hemagglutinin receptor binding avidity drives influenza A virus antigenic drift. *Science*. **326**, 734-736
- 16 Maines, T. R., Jayaraman, A., Belser, J. A., Wadford, D. A., Pappas, C., Zeng, H., Gustin, K. M., Pearce, M. B., Viswanathan, K., Shriver, Z. H., Raman, R., Cox, N. J., Sasisekharan, R.,

- Katz, J. M. and Tumpey, T. M. (2009) Transmission and pathogenesis of swine-origin 2009 A(H1N1) influenza viruses in ferrets and mice. *Science*. **325**, 484-487
- 17 Srinivasan, A., Viswanathan, K., Raman, R., Chandrasekaran, A., Raguram, S., Tumpey, T. M., Sasisekharan, V. and Sasisekharan, R. (2008) Quantitative biochemical rationale for differences in transmissibility of 1918 pandemic influenza A viruses. *Proc Natl Acad Sci U S A*. **105**, 2800-2805
- 18 Belser, J. A., Szretter, K. J., Katz, J. M. and Tumpey, T. M. (2009) Use of animal models to understand the pandemic potential of highly pathogenic avian influenza viruses. *Adv Virus Res*. **73**, 55-97
- 19 Belser, J. A., Gustin, K. M., Maines, T. R., Blau, D. M., Zaki, S. R., Katz, J. M. and Tumpey, T. M. (2011) Pathogenesis and transmission of triple-reassortant swine H1N1 influenza viruses isolated before the 2009 H1N1 pandemic. *J Virol*. **85**, 1563-1572
- 20 Bouvier, N. M. and Lowen, A. C. (2010) Animal Models for Influenza Virus Pathogenesis and Transmission. *Viruses*. **2**, 1530-1563
- 21 Ozawa, M. and Kawaoka, Y. (2011) Taming influenza viruses. *Virus Res*. **162**, 8-11
- 22 Kiraly, J. and Kostolansky, F. (2009) Reverse genetics and influenza virus research. *Acta Virol*. **53**, 217-224
- 23 Cheng, C. S., Shu, Y. L. and Zhang, Z. Q. (2007) [Advances in research of reverse genetics of influenza virus]. *Bing Du Xue Bao*. **23**, 68-71
- 24 Neumann, G. and Kawaoka, Y. (2001) Reverse genetics of influenza virus. *Virology*. **287**, 243-250
- 25 Merkulov, V. A., Lebedev, V. N., Plekhanova, T. M., Maksimov, V. A., Korovkin, S. A. and Mironov, A. N. (2009) [Using reverse genetics method for developing recombinant strains of influenza viruses acceptable for use as live attenuated vaccines]. *Zh Mikrobiol Epidemiol Immunobiol*, 111-117
- 26 Neumann, G., Noda, T. and Kawaoka, Y. (2009) Emergence and pandemic potential of swine-origin H1N1 influenza virus. *Nature*. **459**, 931-939
- 27 Chmielewski, R. and Swayne, D. E. (2011) Avian influenza: public health and food safety concerns. *Annu Rev Food Sci Technol*. **2**, 37-57
- 28 Alexander, D. J. (2006) Avian influenza viruses and human health. *Dev Biol (Basel)*. **124**, 77-84
- 29 Alexander, D. J. (2008) Avian influenza - diagnosis. *Zoonoses Public Health*. **55**, 16-23
- 30 Capua, I. and Alexander, D. J. (2007) Avian influenza infections in birds--a moving target. *Influenza Other Respi Viruses*. **1**, 11-18
- 31 Medina, R. A. and Garcia-Sastre, A. (2011) Influenza A viruses: new research developments. *Nat Rev Microbiol*. **9**, 590-603
- 32 Taubenberger, J. K., Morens, D. M. and Fauci, A. S. (2007) The next influenza pandemic: can it be predicted? *JAMA*. **297**, 2025-2027
- 33 Wan, H., Sorrell, E. M., Song, H., Hossain, M. J., Ramirez-Nieto, G., Monne, I., Stevens, J., Cattoli, G., Capua, I., Chen, L. M., Donis, R. O., Busch, J., Paulson, J. C., Brockwell, C., Webby, R., Blanco, J., Al-Natour, M. Q. and Perez, D. R. (2008) Replication and transmission of H9N2 influenza viruses in ferrets: evaluation of pandemic potential. *PLoS One*. **3**, e2923

- 34 Jayaraman, A., Pappas, C., Raman, R., Belser, J. A., Viswanathan, K., Shriver, Z., Tumpey, T. M. and Sasisekharan, R. (2011) A single base-pair change in 2009 H1N1 hemagglutinin increases human receptor affinity and leads to efficient airborne viral transmission in ferrets. *PloS one*. **6**, e17616
- 35 Viswanathan, K., Koh, X., Chandrasekaran, A., Pappas, C., Raman, R., Srinivasan, A., Shriver, Z., Tumpey, T. M. and Sasisekharan, R. (2010) Determinants of glycan receptor specificity of H2N2 influenza A virus hemagglutinin. *PLoS One*. **5**, e13768

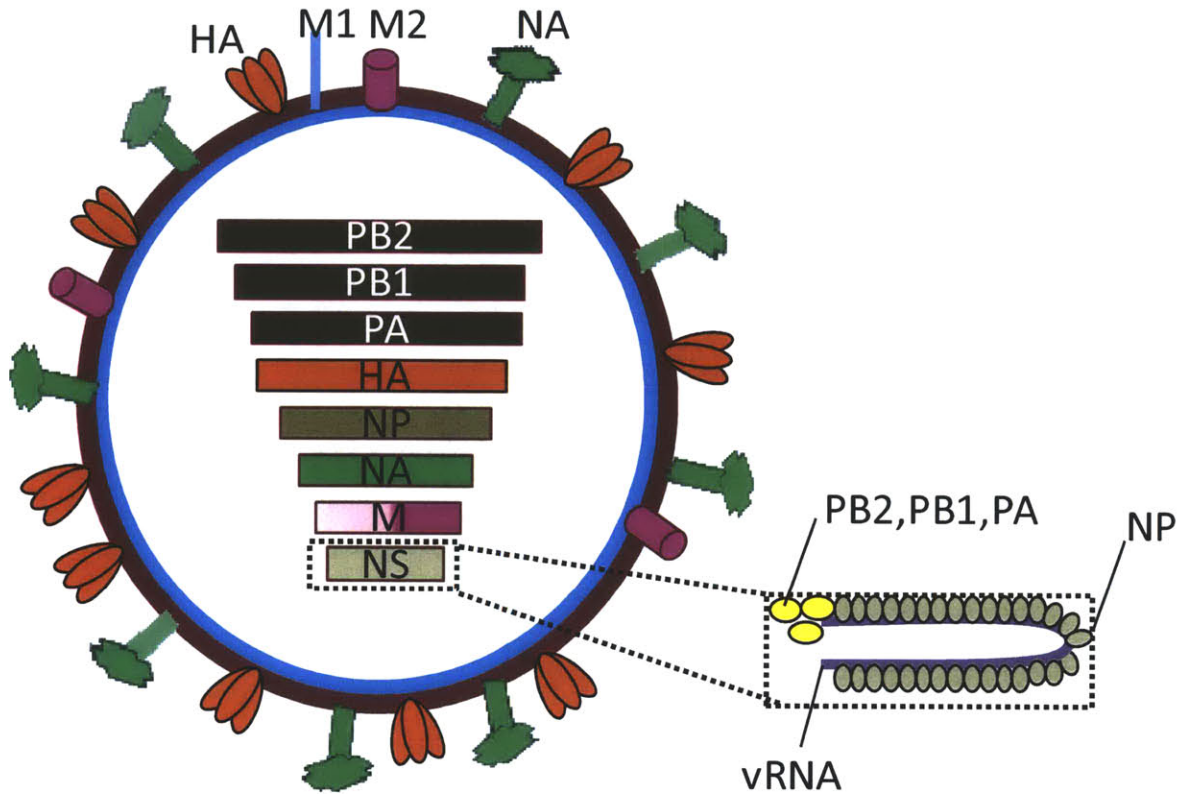
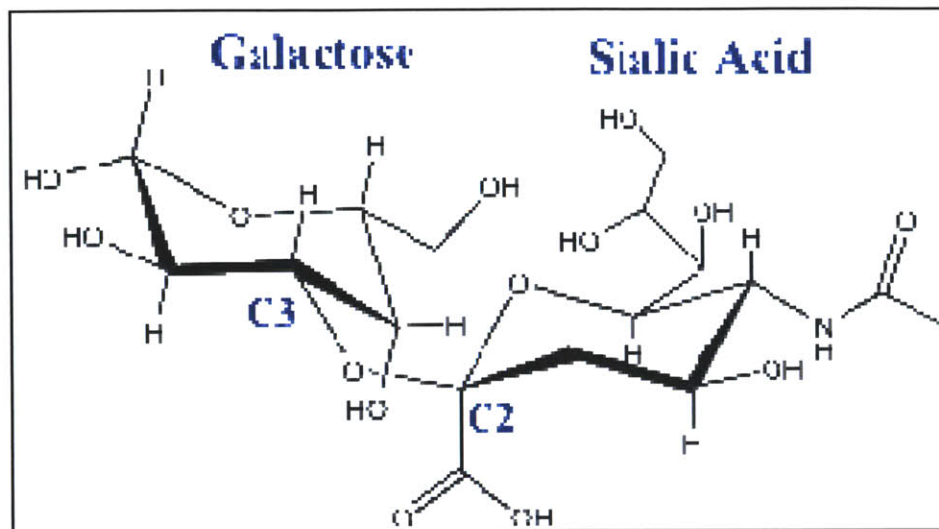


Fig 1.1. Cartoon of Influenza A virus Mature Infectious Virion.

The Influenza surface glycoproteins, HA and NA that form the basis for classification of the various strains are shown. M2, a component of the viral envelope and the 8 different gene segments that are encapsulated by the viral envelope are seen.

Inset: the vRNP that consists of the viral RNA wound around NP.

HUMAN



AVIAN

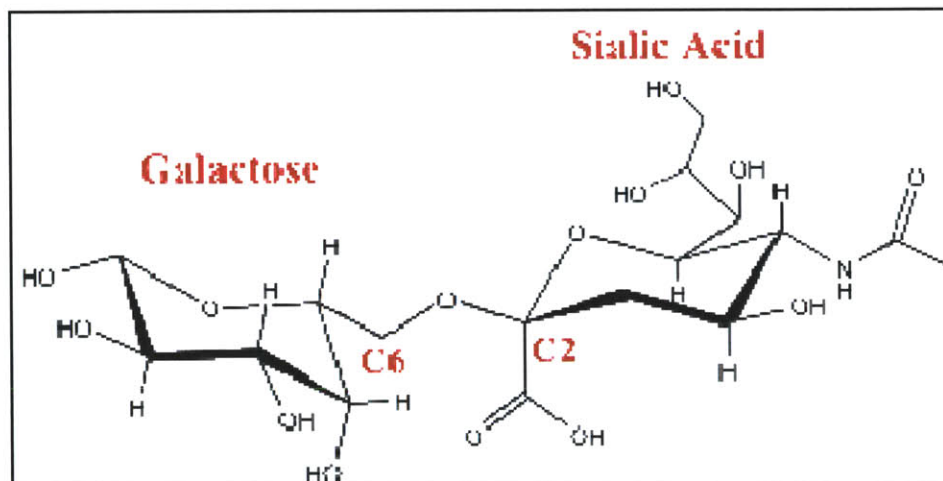


Fig 1.2. Human and Avian Sialylated Glycan Receptors for Influenza Viruses.

Receptors that are α 2-3 linked (avian; shown in red) or α 2-6 linked (human; shown in blue).

GROUP	HA	NA
1	H1,H2,H5,H6,H8,H9,H11,H12,H13,H16, H17	N1, N4, N5 and N8
2	H3,H4,H7,H10,H14,H15	N2, N3, N6, N7 and N9

Fig 1.3. Antigenic Classification of Influenza viruses.

The 17 known HAs and 9 NAs that comprise all known strains of Influenza viruses are broadly classified into two groups (viz 1 and 2) based on their antigenicity.

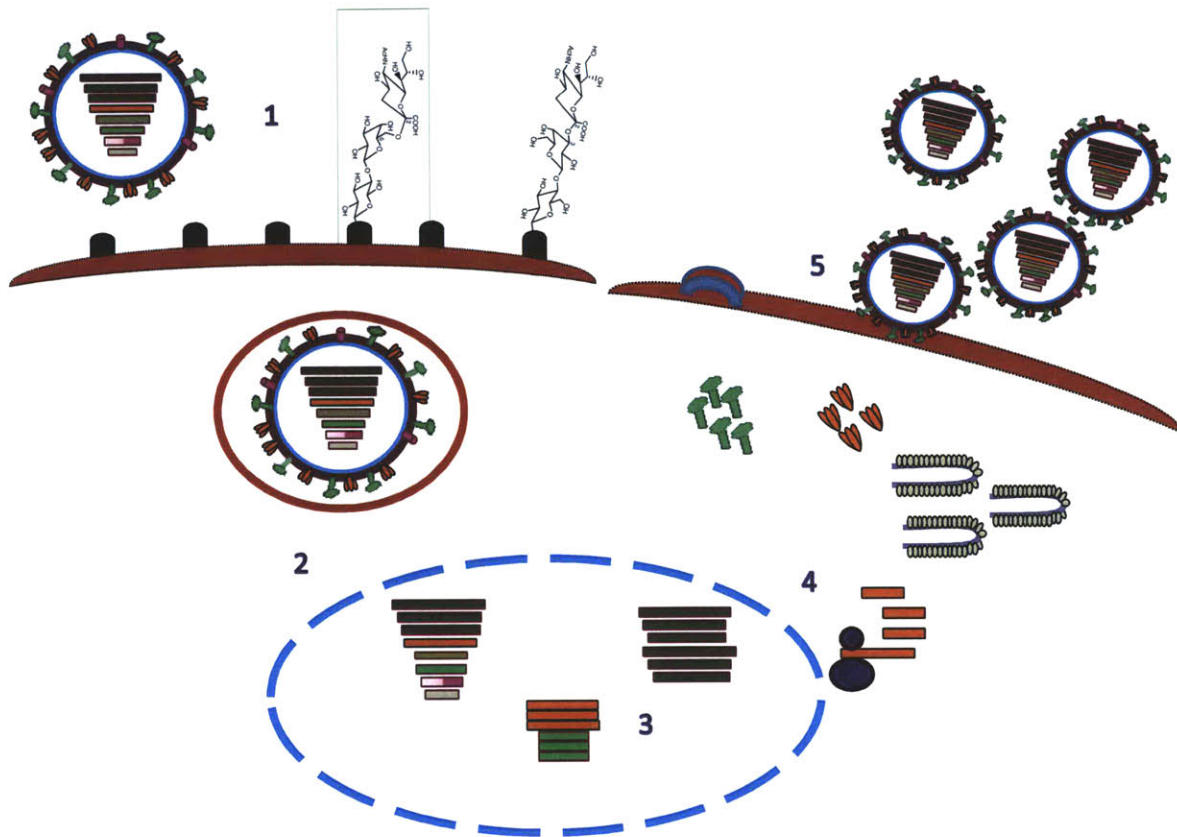


Fig 1.4. Life Cycle of Influenza viruses.

The influenza virus life cycle can be divided into the following stages: 1. entry into the host cell with attachment to host cell receptors mediated by Hemagglutinin; 2. entry of vRNPs into the nucleus preceded by pH dependent fusion step; 3. transcription and replication of the viral genome; 4. export of the vRNPs from the nucleus; and 5. assembly and budding of newly formed nascent virions at the host cell plasma membrane

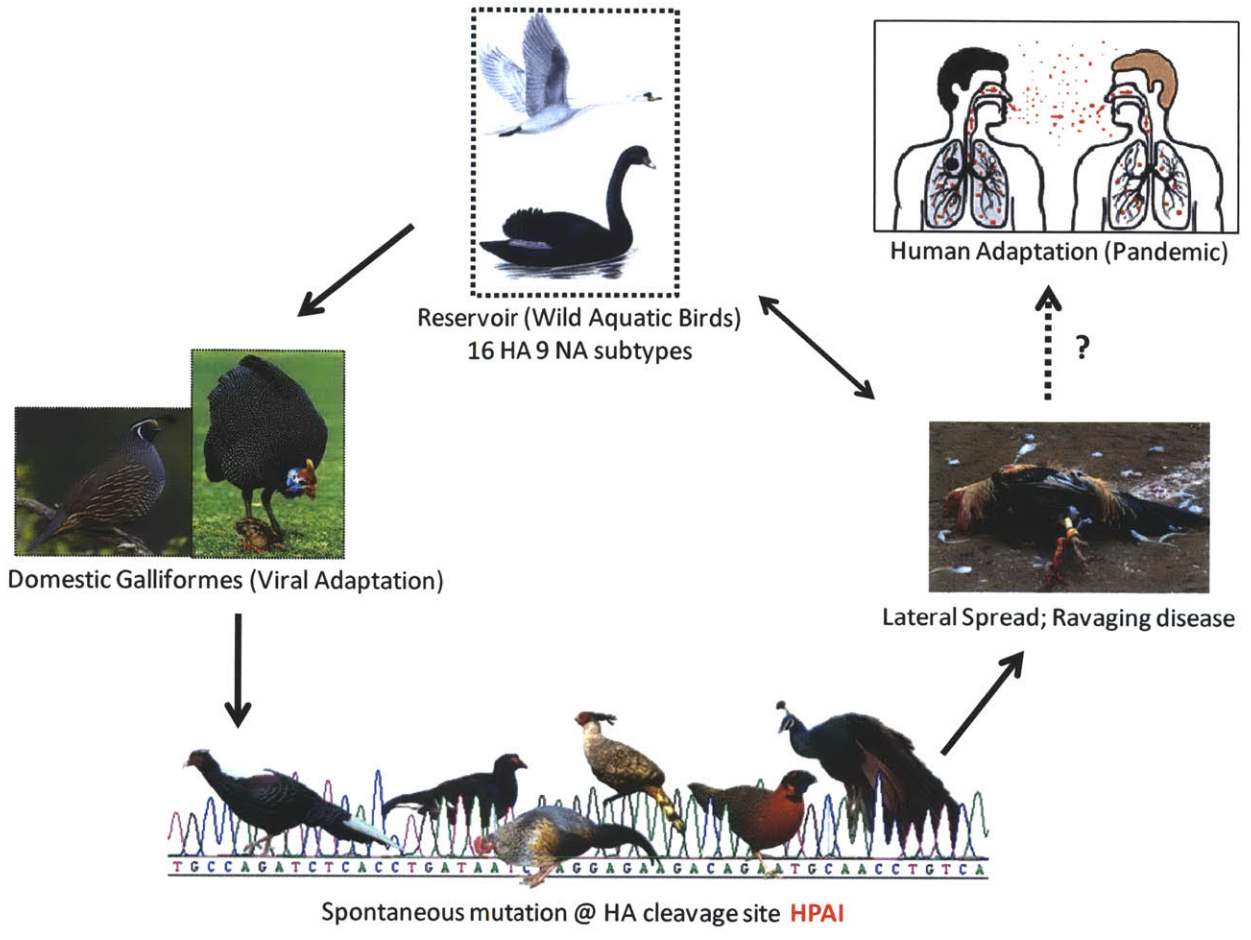


Fig 1.5. Genesis of Pandemic Influenza

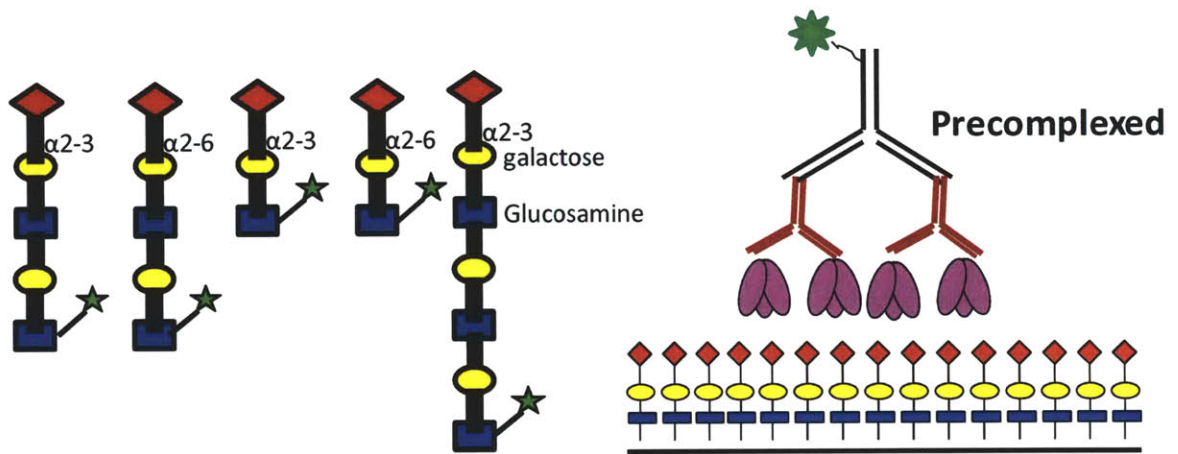
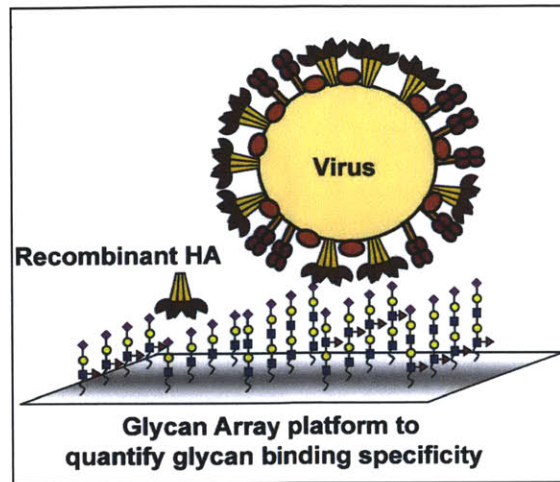


Fig. 1.6 Microarray platforms for probing HA- Glycan interactions.

2 Quantitative Characterization of Glycan-Receptor Binding of H9N2 Influenza A Virus Hemagglutinin

2.1 Summary

Avian influenza subtypes such as H5, H7 and H9 are yet to adapt to the human host so as to establish airborne transmission between humans. However, lab-generated reassorted viruses possessing hemagglutinin (HA) and neuraminidase (NA) genes from an avian H9 isolate and other genes from a human-adapted (H3 or H1) subtype acquired two amino acid changes in HA and a single amino acid change in NA that confer respiratory droplet transmission in ferrets. We previously demonstrated for human-adapted H1, H2 and H3 subtypes that quantitative binding affinity of their HA to $\alpha 2 \rightarrow 6$ sialylated glycan receptors correlates with respiratory droplet transmissibility of the virus in ferrets. Such a relationship remains to be established for H9 HA. In this study, we performed a quantitative biochemical characterization of glycan receptor binding properties of wild-type and mutant forms of representative H9 HAs that were previously used in context of reassorted viruses in ferret transmission studies. We demonstrate here that distinct molecular interactions in the glycan receptor-binding site of different H9 HAs affect the glycan-binding specificity and affinity. Further we show that $\alpha 2 \rightarrow 6$ glycan receptor-binding affinity of a mutant H9 HA carrying Thr-189 \rightarrow Ala amino acid change correlates with the respiratory droplet transmission in ferrets conferred by this change. Our findings contribute to a framework for monitoring the evolution of H9 HA by understanding effects of molecular changes in HA on glycan receptor-binding properties.

2.2 Introduction

Among subtypes of influenza A viruses isolated from avian species, H5N1, H7N2, H7N3 and H9N2 have been known to infect humans but are yet to adapt to human host so as to establish airborne human-to-human transmission. In the past few years, novel influenza strains such as 2009 H1N1 and 2010 H3N2 that naturally emerged from multiple reassortment of viral gene segments between avian, swine and human isolates were able to successfully adapt to human host [29, 39]. In the context of these novel strains, the avian influenza subtypes pose a significant threat of human adaptation [40]. With the human population predominantly naïve to these avian influenza antigens, constant surveillance with particular focus on molecular changes geared towards human host adaptation becomes vital in this era of pandemics [41].

The adaptation of influenza A viruses to human host has been studied extensively in model animal systems such as ferrets [12, 42]. One of the important factors governing human adaptation of the virus is the gain in its ability to transmit via respiratory droplets in the ferret animal model [12, 42]. The transmissibility of human-adapted pandemic influenza strains, 1918 H1N1, 1957 H2N2 and 2009 H1N1, in ferrets has been demonstrated to correlate with the specificity and quantitative affinity of the viral surface glycoprotein hemagglutinin (HA) binding to $\alpha 2 \rightarrow 6$ sialylated glycans (or *human receptors*) [8, 37, 38]. These human receptors are predominantly expressed in upper respiratory epithelium of humans and ferrets [43, 44]. The HA of influenza viruses isolated from avian species typically binds to $\alpha 2 \rightarrow 3$ sialylated glycans (or *avian receptors*) [44]. Therefore, the gain in the ability of HA from an avian isolate (such as H5, H7, H9, etc.) to preferentially bind to human receptors (high relative binding affinity to human receptor over avian receptor) is implicated as one of the important factors for the human adaptation of the virus [9].

H9 is unique among avian subtypes since its HA has naturally acquired a mutation in the 226 position (based on H3 numbering) in glycan-receptor binding site (RBS) from Gln to Leu [45]. Leu-226 is predominantly found in human-adapted H2 and H3 HAs and is critically involved in their binding to human receptors. It was demonstrated that among different avian H9N2 isolates, those with Leu-226 in the RBS showed a similar tropism of preferentially infecting non-ciliated human airway epithelial cells (characteristic of human-adapted viruses) [45]. Although

the H9N2 virus is yet to adapt to a human host, reassorted viruses carrying HA and NA from a H9N2 virus isolated from a wild terrestrial bird (A/Guinea Fowl/Hong Kong/WF10/99 or WF10) and other genes from human-adapted H3N2 [46] or 2009 pandemic H1N1 [47] have been able to transmit via respiratory droplet in ferrets by acquiring as few as two amino acid changes, Thr-189→Ala (in RBS) and Gly-192→Arg in HA.

The glycan receptor-binding properties of both H9N2 viruses isolated from avian species and reassorted viruses comprising of wild-type and mutant forms of H9 HA have been studied by screening them on glycan array platforms [36]. Such screening analyses served as a quick readout for the number of different types of $\alpha 2 \rightarrow 3$ and $\alpha 2 \rightarrow 6$ sialylated glycans that bind to the virus at a fixed high viral titer and limited biochemical information on glycan affinity and specificity. Previously, we demonstrated that correlating glycan-receptor binding properties from such screening assays to transmissibility of virus has major limitations [8]. Instead, we demonstrated that deriving quantitative parameters from a dose-dependent binding to representative human and avian receptors to compare relative human:avian receptor binding affinities correlated with the respiratory droplet transmissibility of the virus [8, 37, 38]. Such a correlation remains to be determined for the H9 subtype in the context of the reassorted viruses that show respiratory droplet transmission in ferrets.

In this study, we focused on investigating the glycan receptor-binding specificity and affinity of H9 HAs from the representative avian isolates WF10 and A/Quail/Hong Kong/A28945/88 (Qu88) that had been recombinantly constructed via reverse genetics for ferret transmissibility studies carried out previously [36, 46, 47]. We first quantified glycan-receptor binding specificity of WF10 and Qu88 HAs using a dose-dependent glycan array assay mentioned above [8]. We then constructed homology-based structural models of these HAs to investigate the effect of these mutations on the glycan-receptor binding of HA. We finally made these mutations on WF10 and Qu88 HAs and experimentally quantified the glycan receptor-binding affinities of these mutant HAs. Our results demonstrated and corroborated that the mutations on H9 HAs that were found to confer respiratory droplet transmission in the ferret model also substantially increased human receptor-binding specificity and affinity in comparison to those of wild-type HAs.

2.3 Results

As stated earlier, WF10 and Qu88 H9 HAs were chosen as representative HAs for characterization of glycan-receptor binding properties. These HAs are isolated from different avian hosts. While WF10 is from guinea fowl (wild terrestrial bird), Qu88 is from a strain that has been established in domestic poultry in China. WF10 HA has Leu-226 in the RBS while Qu88 has Gln-226 [45]. As pointed out earlier, reassorted viruses comprising of WF10 HA acquired additional mutations in the HA that conferred the viruses with the ability to transmit via respiratory droplets in ferrets after repeated passaging in these animals [46].

2.3.1 Characterization of glycan receptor-binding properties of WF10 and Qu88 HAs

We previously developed a dose-dependent glycan array binding assay to quantitatively characterize glycan receptor binding affinity of HA by calculating an apparent binding constant K_d' [1, 8]. WF10 HA was recombinantly expressed and analyzed using this assay. WF10 HA showed a highly specific binding to a representative human receptor, 6'SLN-LN (**Fig. 2.1A**). Although the WF10 virus showed binding to both avian and human receptors in previous glycan array screening studies [36], our results indicate that its quantitative binding affinity to human receptor is orders of magnitude higher than that to avian receptor.

The K_d' ~300 pM for WF10 HA binding to 6'SLN-LN is 5 fold higher than that of 2009 H1N1 HA (K_d' ~ 1.5 nM) [37] and 60-fold lower than that of 1918 H1N1 and 1958 H2N2 (K_d' ~ 5 pM) HA [8, 38]. The human receptor-binding property of WF10 based on the glycan array was consistent with its extensive staining of apical surface of human tracheal epithelium, which predominantly expresses human receptors (**Fig. 2.1B**).

Qu88 HA, on the other hand showed predominant binding to avian receptors 3'SLN-LN and 3'SLN-LN-LN (K_d' 30pM) with minimal binding to human receptors (**Fig. 2.1C**). Therefore not only does the Qu88 virus preferentially bind to higher number of avian receptors as observed in previous glycan array screening studies [36], the quantitative avian receptor-binding affinity of Qu88 is orders of magnitude higher than its human receptor-binding affinity. Furthermore, the avian receptor-binding property of Qu88 HA was consistent with its extensive staining of human alveolar tissue section (**Fig. 2.1D**), which predominantly expresses these receptors [44].

2.3.2 Molecular Interactions of WF10 and Qu88 HA with avian and human receptors

To better understand the contrasting glycan-binding properties of WF10 and Qu88 HAs we analyzed the molecular interactions of these HAs with representative avian and human receptors. The X-ray crystal structures of a swine H9 HA and its complexes with an avian (LSTa) and human receptor (LSTc) [48] were used to generate structural models of Qu88-LSTa and WF10-LSTc complexes (Fig. 2.2). Analysis of these structural complexes shows differences in amino acids that constitute the glycan receptor-binding site (RBS) of WF10 and Qu88 HAs. Specifically, there are differences in residues at positions 156 and 226 (numbering is based on H3 HA) and also orientation of side chain of Asn-193. There is also a difference in amino acid at the 137 position (which is not shown in the figure for the sake of clarity) wherein WF10 has Arg while Qu88 has Lys at this position.

In the case of RBS of Qu88 HA, Gln-226 is positioned to make ionic contact with glycosidic oxygen atom of Neu5Ac α 2 \rightarrow 3Gal linkage. On the other hand, in WF10, Leu-226 is positioned to make van der Waals contact with C-6 atom of Neu5Ac α 2 \rightarrow 6Gal linkage. The difference in nature of contacts involving amino acid position 226 is one of the molecular features that explain the differences in the glycan receptor-binding specificity of WF10 and Qu88 HAs. The residue at 156 position appear to be involved in making contacts with the human receptor and not the avian receptor and therefore changes in this position is likely to affect binding of HA to human receptors. The orientation of side chain of Asn-193 is such that it is positioned to make contact with human receptor (in WF10-LSTc complex) and not the avian receptor (in Qu88-LSTa complex). There appear to be interconnected networks of inter-residue interactions involving the following sets of residue positions, (136, 137, and 226), (186, 222, and 227), (183,186, 187, 189, and 190) and (187, 189, 193, 156). These interaction networks are likely to govern the orientation of the side chains of the residues at the corresponding positions in the network, which in turn would govern contacts with glycan receptor. Therefore, differences in the amino acids at positions 137, 156, 183, 186, 187, 189, 193, 222, 226, and 227 between different H9 HAs would impinge on the quantitative glycan receptor-binding specificity of the HAs.

One of the observed mutations in WF10 HA in the reassorted virus that shows airborne transmission in ferrets is Thr-189 \rightarrow Ala. Although Thr-189 does not make direct contacts with

both avian and human receptor, this position is a part of two critical amino acid interaction networks involving key residues at positions 190, 193 and 156 that are involved in making contact with the glycan receptor. Therefore, we postulated that the Thr-189→Ala mutation, in the context of a given HA, would alter binding to both avian and human receptors by affecting side chain orientation of residues (in a given HA) that make contact with these receptors.

2.3.3 Design of WF10 and Qu88 HA mutants and characterization of their glycan receptor-binding properties

To experimentally test the effect of changes in the amino acid positions (based on the above structural analysis) on the glycan receptor-binding properties of WF10 and Qu88 H9 HAs, we designed the following mutant forms of these HAs. We designed two mutant forms of WF10 HA; mWF10:T189A (to investigate the effect of Thr-189→Ala mutation on human receptor-binding) and mWF10:L226Q (to determine if Leu-226→Gln mutation would change its binding preference from human to avian receptor). In the case of Qu88 HA, we defined three mutant forms; mQu88:T189A (to establish if changes to Thr-189 would affect avian receptor-binding), mQu88:Q226L (to determine if Gln-226→Leu mutation would change its binding preference from avian to human receptor), and mQu88:Q226L/T189A (to explore if the additional Thr189→Ala mutation would further modulate human receptor-binding of mQu88:Q226L). The amino acid changes were made to WF10 and Qu88 using site-directed mutagenesis and the glycan-receptor binding properties of the mutant HAs were characterized using glycan array and human tissue binding analyses.

mWF10:T189A showed a more specific binding to 6'SLN-LN than WF10 HA where binding to other representative glycan receptors at > 40 µg/ml concentration was minimal when compared to WF10 HA at the same concentration (**Fig. 2.3A**). However the K_d' for the 6'SLN-LN binding of the mutant was the same as that of WF10 HA. Staining of mWF10:T189A HA on human upper respiratory tracheal tissue sections revealed a pattern similar to that observed with WT WF10 viz., extensive binding of the protein to the apical side and weak to no binding to the human deep lung alveolar tissue (**Fig. 2.3A**). The single amino acid change in mWF10:L226Q mutant, on the other hand, completely reversed its glycan-binding preference from human to avian receptors (with $K_d' \sim 30$ pM for 3'SLN-LN and 3'SLN-LN-LN) (**Fig. 2.3B**). Tissue binding

assay was consistent with the observed glycan specificity with no tracheal tissue staining observed and extensive alveolar tissue binding (Fig. 2.3B).

In the case of Qu88 HA, a single amino acid change in the mQu88:Q226L mutant completely changed its glycan-binding preference from avian to human receptors viz 6'SLN-LN (Fig. 2.4A). Furthermore, the $K_d' \sim 50$ pM for 6'SLN-LN binding of this mutant HA indicates that it shows a 5-fold increase in binding affinity to human receptor relative to the WF10 HA (which has Leu at 226 position). In fact the K_d' of mQu88:Q226L is in the same range as that of HAs from seasonal influenza strains [8]. Notably, both WF10 and mQu88:Q226L viruses showed similar pattern of binding to both avian and human receptors in the glycan array screening assays performed earlier [36]. Therefore, the glycan array screening of these viruses at single high titer was unable to capture these key differences and nuances in their quantitative human receptor-binding affinity.

The additional Thr-189→Ala change in the mQu88:Q226L/T189A mutant leads to an increase in the binding specificity to 6'SLN-LN where binding to other glycan receptors at 40 µg/ml was minimal when compared to mQu88:Q226L at the same concentration (Fig. 2.4B). The $K_d' \sim 60$ pM for 6'SLN-LN binding of mQu88:Q226L/T189A was in the same range as that of mQu88:Q226L. Both these mutant HAs showed extensive staining to apical surface of human tracheal epithelium consistent with their human-receptor binding properties on the glycan array (Fig. 2.4A and B). The third mutant mQu88:T189A increased specificity to 3'SLN-LN and 3'SLN-LN-LN without altering the K_d' (~ 30 pM) when compared to that calculated for the wild-type Qu88 HA (Fig. 2.4C). Consistent with its glycan array-binding properties, mQu88:T189A also showed extensive staining to human alveolar tissues (Fig. 2.4C).

2.4 Discussion

In this study we investigated glycan-receptor binding properties of avian H9N2 HA given that this subtype has been known to infect and cause disease in humans. Using a combination of structural modeling, glycan array and human tissue binding analyses in this study we quantitatively characterized glycan-receptor binding specificity and affinity of wild-type and mutant forms of WF10 and Qu88 HAs. To our knowledge, such a quantitative description of glycan-binding properties of H9 HA has not been reported earlier.

While Qu88 does show measurable binding to human receptors at concentrations higher than 5 $\mu\text{g/ml}$, its binding to avian receptors is substantially higher. This relative binding preference to avian receptor is typical of what we have observed with avian-adapted HAs including H5 HA [1, 8, 38]. It is important to note that WF10, which is as HA derived from an avian isolate, showed highly preferential binding to human receptors.

Although the $K_d' \sim 300 \text{ pM}$ for WF10 HA binding to human receptor is 5 fold higher than that of 2009 H1N1 HA [37], a reassorted virus with HA and NA from WF10 and other internal genes from a human-adapted H3N2 virus did not show respiratory droplet transmission in ferrets [46]. Repeated passaging of this reassorted virus in ferrets led to a strain (RCP10) that had additional mutations in HA and NA and transmitted via respiratory droplets in ferrets. One of the mutations Thr-189 \rightarrow Ala is in the RBS of H9 HA while the other mutation is in HA2 close to the transmembrane region (unlikely to impact RBS features and hence receptor binding). It was demonstrated that both these mutations are needed for conferring respiratory droplet transmission. Our structural model of WF10 HA – human receptor complex showed that the amino acid in 189 position would indirectly influence glycan-receptor binding through inter-residue interactions. We demonstrated that Thr189 \rightarrow Ala mutation in WF10, mQ88:Q226L and Qu88 HAs increases binding specificity. The fact that the Thr-189 \rightarrow Ala mutation is needed for respiratory droplet transmission highlights the role of improving human receptor specificity in the context of other genes in a reassorted virus in conferring airborne transmissibility. To our knowledge, the effect of the amino acid change at the 189 position on the glycan-binding property of H9 HAs has not been reported earlier.

The contribution of Gln-226 to avian receptor binding and Leu-226 to human receptor binding was corroborated by the preferential avian receptor binding of mWF10:L226Q and human receptor-binding of mQu88:Q226L mutants respectively. Unlike H2 and H3 subtypes where change in receptor binding preference from avian to human receptor has been associated with at least two mutations Q226L and G228S, it appears that in the case of H9 HA a single mutation Q226L might be sufficient to alter its glycan-receptor binding properties. Based on the calculated K_d' , the mQu88:Q226L mutant shows 5-fold higher affinity to human receptor than WF10. This suggests that Leu-226 in context of His-156 and Lys-137 in the Qu88 RBS provides a

more optimal environment than Leu-226 in the context of Gln-156 and Arg-137 in WF10 RBS for achieving a higher quantitative human receptor affinity. Therefore, this study provides an important framework to understand key mutations such as Gln226→Leu in the context of the entire RBS in different H9 HAs to appropriately monitor the evolution of H9 viruses.

In summary, our results demonstrate that H9 HAs from avian isolates such as WF10 show binding affinity and specificity to human receptors characteristic of HAs from human-adapted subtypes such as H1, H2 and H3. While H9N2 subtype is yet to adapt to the human host, reassorted strains with H9 HA and NA have acquired as few as 2 amino acid changes in HA and a single Ile-28→Val change in NA to confer respiratory droplet transmission in ferrets (characteristic trait of human-adapted viruses). Such an outcome has not been possible with HAs from other avian subtypes. The 2 mutations in WF10 HA are much fewer than those reported for H5 HA in the context of reassorted strains that transmit via respiratory droplets between ferrets. Given that natural triple reassortments have led to novel swine-origin H1N1 (2009 H1N1) [29] and H3N2 [39], it is important to monitor H9 HA and NA from strains such as WF10 in the context of their potential natural reassortment with other subtypes. Our study contributes to a framework that facilitates monitoring of molecular changes in RBS of H9 HA that govern its human-receptor binding properties.

2.5 Materials and Methods

2.5.1 Cloning, baculovirus synthesis, expression and purification of HA

Briefly, recombinant baculoviruses with WF10 or Qu88 gene and mutants off of each background, were used to infect (MOI=1) suspension cultures of Sf9 cells (Invitrogen, Carlsbad, CA) cultured in BD Baculogold Max-XP SFM (BD Biosciences, San Jose, CA). The infection was monitored and the conditioned media was harvested 3–4 days post-infection. The soluble HA from the harvested conditioned media was purified using Nickel affinity chromatography (HisTrap HP columns, GE Healthcare, Piscataway, NJ). Eluting fractions containing HA were pooled, concentrated and buffer exchanged into 1X PBS pH 8.0 (Gibco) using 100K MWCO spin columns (Millipore, Billerica, MA). The purified protein was quantified using BCA method (Pierce).

2.5.2 Homology based structural modeling of H9 HAs

Using the SWISS-MODEL web-based automated homology-modeling platform (<http://swissmodel.expasy.org/>) the structural models of WF10, and Qu88 were constructed. The template structure chosen by SWISS-MODEL was that of crystal structure of A/swine/Hong Kong/9/98 H9N2 HA (PDB ID: 1JSD). The co-crystal structures of A/swine/Hong Kong/98 HA with representative avian (PDB ID: 1JSH) and human (PDB ID: 1JSI) receptors were used to build structural models of WF10 and Qu88 in complex with glycan receptors.

2.5.3 Binding of recombinant WF10, Qu88 and mutant HAs to human tracheal and alveolar tissue sections

Paraffinized human tracheal (US BioChain) tissue sections were deparaffinized, rehydrated and incubated with 1% BSA in PBS for 30 minutes to prevent non-specific binding. HA was pre-complexed with primary antibody (mouse anti 6X His tag, Abcam) and secondary antibody (Alexa fluor 488 goat anti mouse, Invitrogen) in a molar ratio of 4:2:1, respectively, for 20 minutes on ice. The tissue binding was performed over different HA concentrations by diluting the pre-complexed HA in 1% BSA-PBS. Tissue sections were then incubated with the HA-antibody complexes for 3 hours at RT. The tissue sections were counterstained by propidium iodide (Invitrogen; 1100 in TBST). The tissue sections were mounted and then viewed under a confocal microscope (Zeiss LSM 700 laser scanning confocal microscopy). Sialic-acid specific binding of HAs to tissue sections was confirmed by loss of staining after pre-treatment with Sialidase A (recombinant from *Arthrobacter ureafaciens*, Prozyme), This enzyme has been demonstrated to cleave the terminal Neu5Ac from both Neu5Ac α 2 \rightarrow 3Gal and Neu5Ac α 2 \rightarrow 6Gal motifs. In the case of sialidase pretreatment, tissue sections were incubated with 0.2 units of Sialidase A for 3 hours at 37°C prior to incubation with the proteins. The loss of staining of a representative HA after sialidase pretreatment is shown in Fig. 2.5.

2.5.4 Dose dependent direct binding of WF10, Qu88 and mutant HAs

To investigate the multivalent HA-glycan interactions a streptavidin plate array comprising of representative biotinylated α 2 \rightarrow 3 and α 2 \rightarrow 6 sialylated glycans was used as described previously [8]. 3'SLN, 3'SLN-LN, 3'SLN-LN-LN are representative avian receptors. 6'SLN and

6'SLN-LN are representative human receptors (see **Table 2.1**). The biotinylated glycans were obtained from the Consortium of Functional Glycomics through their resource request program. Streptavidin-coated High Binding Capacity 384-well plates (Pierce) were loaded to the full capacity of each well by incubating the well with 50 μ l of 2.4 μ M of biotinylated glycans overnight at 4°C. Excess glycans were removed through extensive washing with PBS. The trimeric HA unit comprises of three HA monomers (and hence three RBS, one for each monomer). The spatial arrangement of the biotinylated glycans in the wells of the streptavidin plate array favors binding to only one of the three HA monomers in the trimeric HA unit. Therefore in order to specifically enhance the multivalency in the HA-glycan interactions, the recombinant HA proteins were pre-complexed with the primary and secondary antibodies in the molar ratio of 4:2:1 (HA: primary: secondary). The identical arrangement of 4 trimeric HA units in the pre-complex for all the HAs permit comparison between their glycan binding affinities. A stock solution containing appropriate amounts of Histidine tagged HA protein, primary antibody (Mouse anti 6X His tag IgG) and secondary antibody (HRP conjugated goat anti Mouse IgG (Santacruz Biotechnology) in the ratio 4:2:1 and incubated on ice for 20 min. Appropriate amounts of pre-complexed stock HA were diluted to 250 μ l with 1% BSA in PBS. 50 μ l of this pre-complexed HA was added to each of the glycan-coated wells and incubated at room temperature for 2 hours followed by the above wash steps. The binding signal was determined based on HRP activity using Amplex Red Peroxidase Assay (Invitrogen, CA) according to the manufacturer's instructions. The experiments were done in triplicate. Minimal binding signals were observed in the negative controls including binding of pre-complexed unit to wells without glycans and binding of the antibodies alone to the wells with glycans. The binding parameters, cooperativity (n) and apparent binding constant (K_d'), for HA-glycan binding were calculated by fitting the average binding signal value (from the triplicate analysis) and the HA concentration to the linearized form of the Hill equation:

$$\log\left(\frac{y}{1-y}\right) = n * \log([HA]) - \log(K_d')$$

where y is the fractional saturation (average binding signal/maximum observed binding signal). The theoretical y values calculated using the Hill equation:

$$y = \frac{[HA]^n}{[HA]^n + K_d'}$$

(for the set of n and Kd' parameters) were plotted against the varying concentration of HA to obtain the binding curves for the representative human receptor (6'SLN-LN).

2.6 References

1. Neumann G, Noda T, Kawaoka Y (2009) Emergence and pandemic potential of swine-origin H1N1 influenza virus. *Nature* 459: 931-939.
2. Pearce MB, Jayaraman A, Pappas C, Belser JA, Zeng H, et al. (2012) Pathogenesis and transmission of swine origin A(H3N2)v influenza viruses in ferrets. *Proceedings of the National Academy of Sciences of the United States of America* 109: 3944-3949.
3. Malik Peiris JS (2009) Avian influenza viruses in humans. *Revue scientifique et technique* 28: 161-173.
4. Medina RA, Garcia-Sastre A (2011) Influenza A viruses: new research developments. *Nature reviews Microbiology* 9: 590-603.
5. Belser JA, Katz JM, Tumpey TM (2011) The ferret as a model organism to study influenza A virus infection. *Disease models & mechanisms* 4: 575-579.
6. Bouvier NM, Lowen AC (2010) Animal Models for Influenza Virus Pathogenesis and Transmission. *Viruses* 2: 1530-1563.
7. Jayaraman A, Pappas C, Raman R, Belser JA, Viswanathan K, et al. (2011) A single base-pair change in 2009 H1N1 hemagglutinin increases human receptor affinity and leads to efficient airborne viral transmission in ferrets. *PloS one* 6: e17616.
8. Viswanathan K, Koh X, Chandrasekaran A, Pappas C, Raman R, et al. (2010) Determinants of Glycan Receptor Specificity of H2N2 Influenza A Virus Hemagglutinin. *PLoS One* 5: e13768.
9. Srinivasan A, Viswanathan K, Raman R, Chandrasekaran A, Raguram S, et al. (2008) Quantitative biochemical rationale for differences in transmissibility of 1918 pandemic influenza A viruses. *Proc Natl Acad Sci U S A* 105: 2800-2805.
10. Jayaraman A, Chandrasekharan A, Viswanathan K, Raman R, Fox JG, et al. (2012) Decoding the distribution of glycan receptors for human-adapted influenza A viruses in ferret respiratory tract. *PLoS ONE* In Press.
11. Ge S, Wang Z (2011) An overview of influenza A virus receptors. *Critical reviews in microbiology* 37: 157-165.
12. Shriver Z, Raman R, Viswanathan K, Sasisekharan R (2009) Context-specific target definition in influenza a virus hemagglutinin-glycan receptor interactions. *Chem Biol* 16: 803-814.
13. Wan H, Perez DR (2007) Amino acid 226 in the hemagglutinin of H9N2 influenza viruses determines cell tropism and replication in human airway epithelial cells. *Journal of virology* 81: 5181-5191.
14. Sorrell EM, Wan H, Araya Y, Song H, Perez DR (2009) Minimal molecular constraints for respiratory droplet transmission of an avian-human H9N2 influenza A virus. *Proceedings of the National Academy of Sciences of the United States of America* 106: 7565-7570.
15. Kimble JB, Sorrell E, Shao H, Martin PL, Perez DR (2011) Compatibility of H9N2 avian influenza surface genes and 2009 pandemic H1N1 internal genes for transmission in the ferret model. *Proceedings of the National Academy of Sciences of the United States of America* 108: 12084-12088.
16. Wan H, Sorrell EM, Song H, Hossain MJ, Ramirez-Nieto G, et al. (2008) Replication and transmission of H9N2 influenza viruses in ferrets: evaluation of pandemic potential. *PloS one* 3: e2923.

17. Chandrasekaran A, Srinivasan A, Raman R, Viswanathan K, Raguram S, et al. (2008) Glycan topology determines human adaptation of avian H5N1 virus hemagglutinin. *Nat Biotechnol* 26: 107-113.
18. Ha Y, Stevens DJ, Skehel JJ, Wiley DC (2001) X-ray structures of H5 avian and H9 swine influenza virus hemagglutinins bound to avian and human receptor analogs. *Proc Natl Acad Sci U S A* 98: 11181-11186.

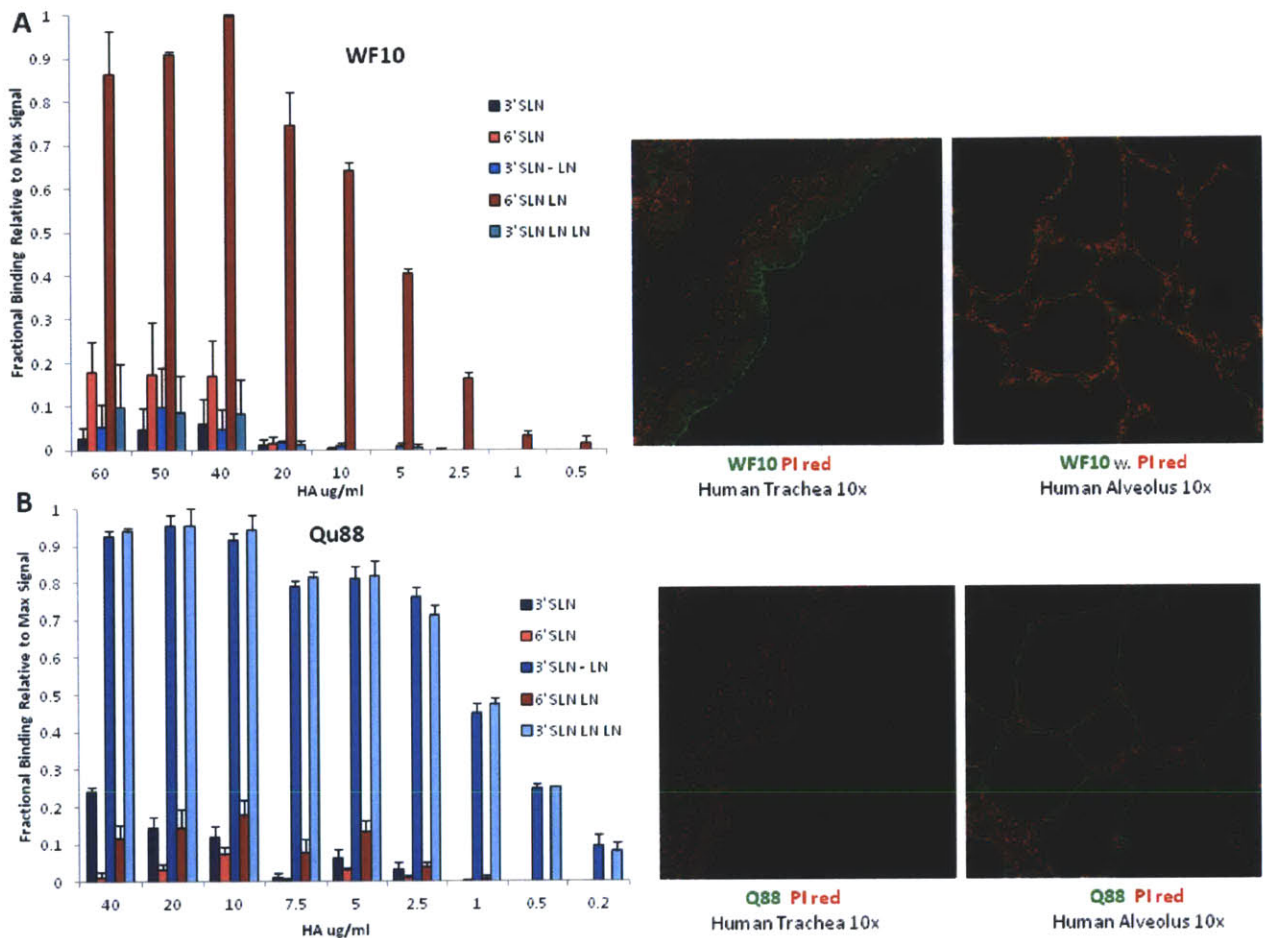


Fig.2.1 Glycan receptor-binding properties of WF10 and Qu88 HA.

A, Dose-dependent direct binding of WF10 HA to glycan array (*left*) shows that it binds specifically to a representative human receptor (6'SLN-LN). Tissue staining (*right*) shows extensive staining of apical surface of human tracheal epithelia and minimal observable staining of alveolar tissue section by WF10 HA (in green) shown against propidium iodide staining (in red). B, Dose-dependent direct glycan array binding of Qu88 HA (*left*) shows specific binding to avian receptors (3'SLN-LN and 3'SLN-LN-LN). The panel on the right shows poor staining of apical surface of human tracheal epithelia and extensive staining of alveolar tissue section by Qu88 HA (in green) shown against propidium iodide staining (in red).

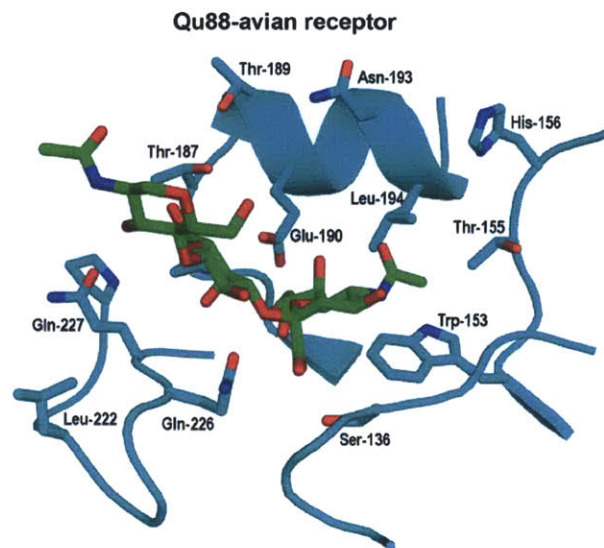
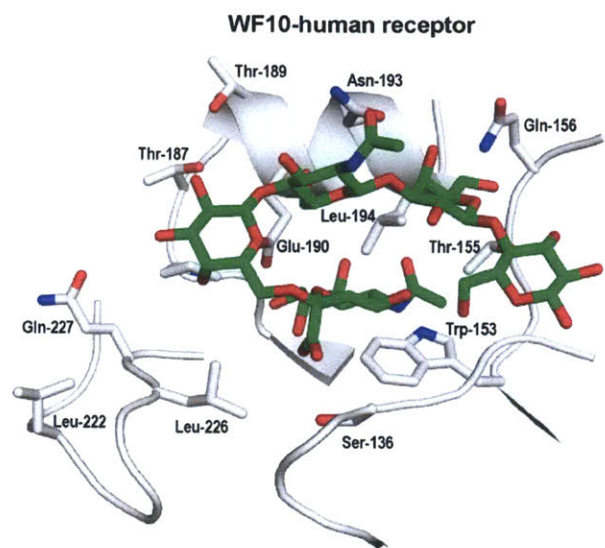
A**B**

Fig. 2.2. Structural model of H9 HA-glycan receptor complexes.

A, Structural model of Qu88 HA with an avian receptor. The glycan receptor-binding site of HA is shown as a cartoon (carbon atom colored in *cyan*) with side chains of key residues in the RBS shown in stick representation. B, Structural model of WF10 with human receptor. The glycan receptor-binding site of HA is shown as a cartoon (carbon atom colored in *gray*) with side chains of key residues in the RBS shown in stick representation. The glycan receptor is shown in stick representation (carbon atom colored in *green*)

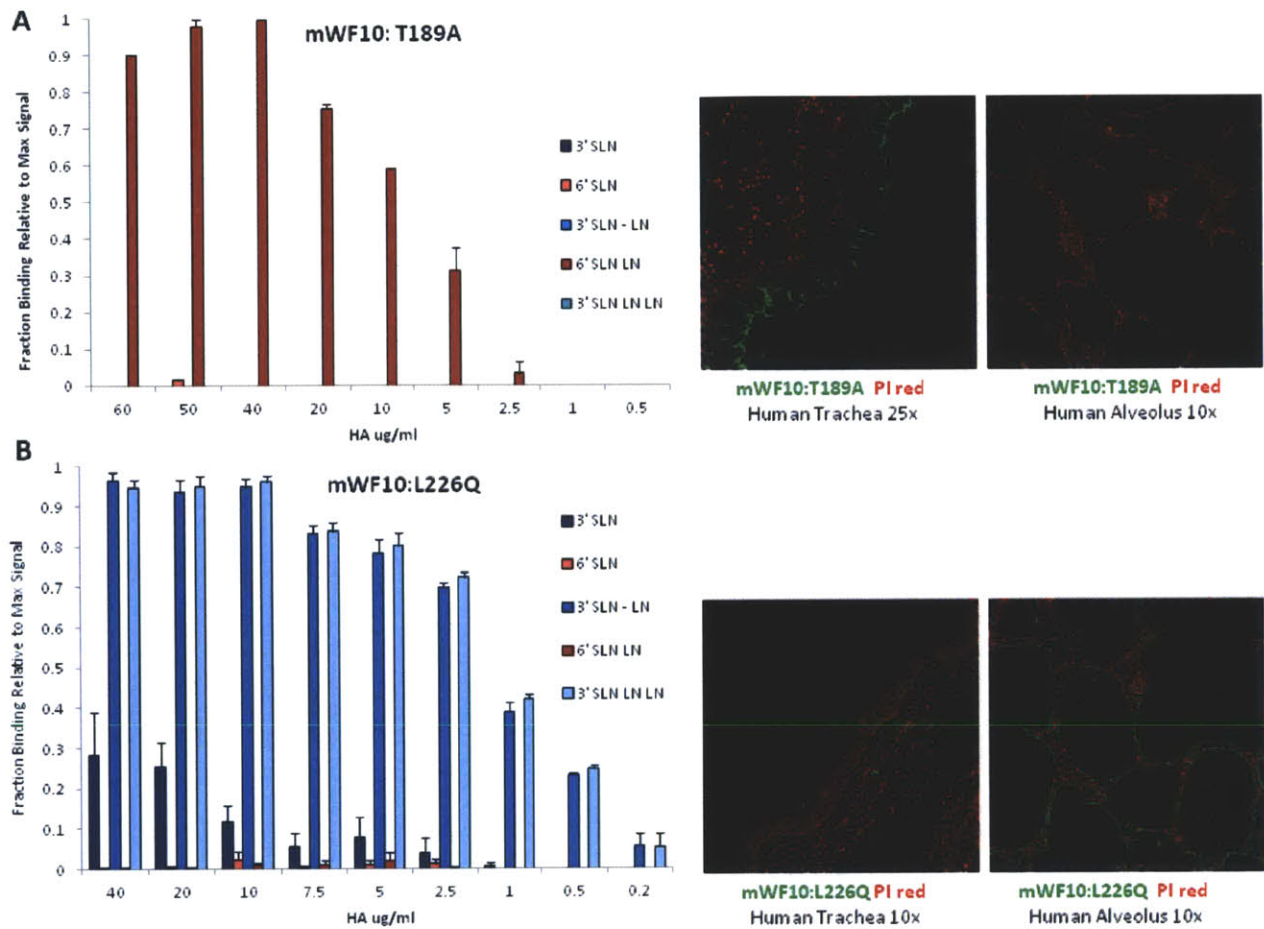


Fig.2.3. Glycan receptor-binding properties of mWF10:T189A and mWF10:L226Q.

A, Dose-dependent direct glycan array binding of mWF10:T189A HA (*left*) shows increased specificity to the human receptor 6'SLN-LN when compared to WF10 in Figure 1A. Tissue-binding of mWF10:T189A HA (*right*) shows extensive staining (in *green* against propidium iodide in *red*) of apical surface of human tracheal section and minimal staining of human alveolar section consistent with human receptor-binding specificity. B, Dose-dependent direct glycan array binding of mWF10:L226Q HA (*left*) shows a complete reversal in binding from human to avian receptors (3'SLN-LN and 3'SLN-LN-LN). The panel on right, shows poor staining of apical surface of human tracheal epithelia and extensive staining of human alveolar sections by mWF10:L226Q HA (in *green*) shown against propidium iodide staining (in *red*).

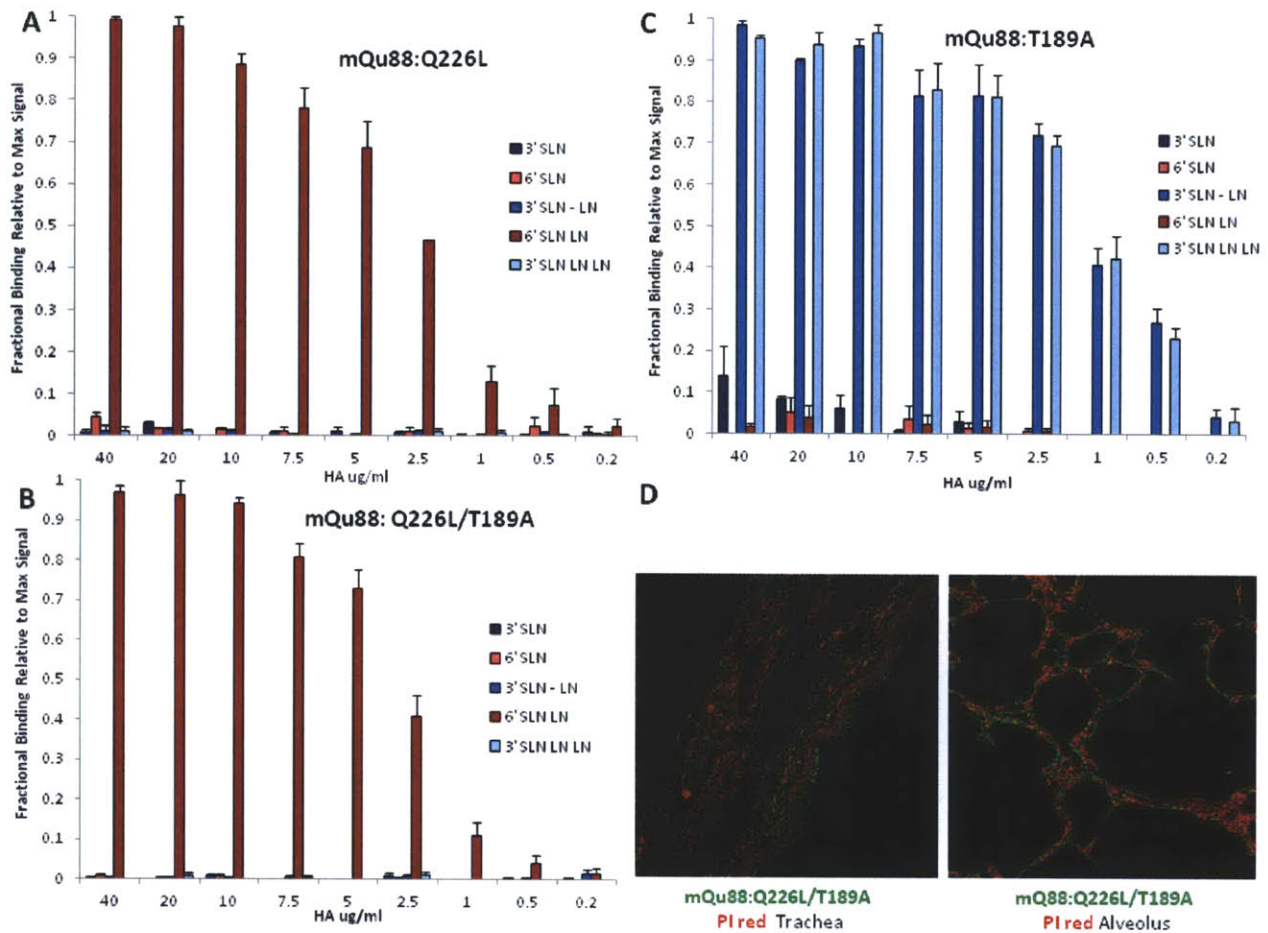
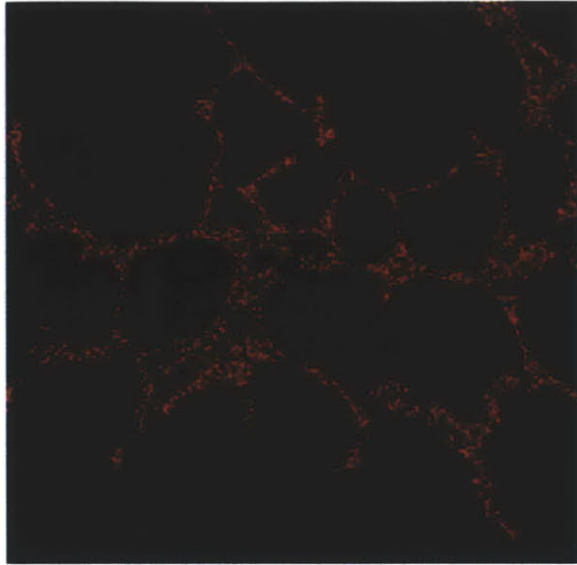
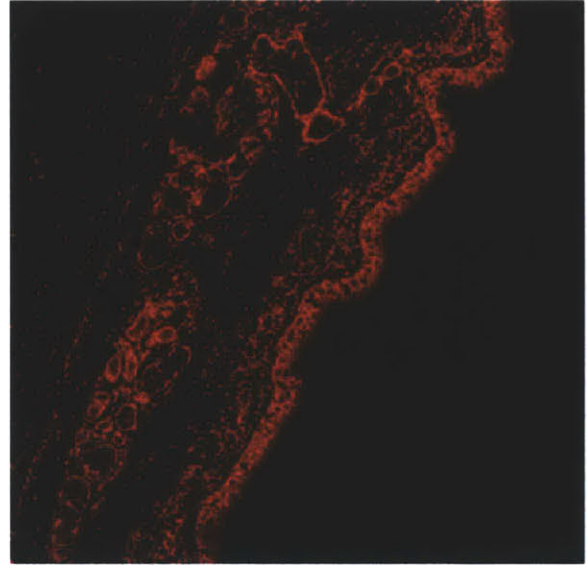


Fig.2.4. Glycan receptor-binding specificity of mQu88:Q226L, mQu88:T189A and double mutant mQu88:Q226L/T189A HA.

A, B show dose-dependent direct glycan array binding of mQu88:Q226L and mQu88:Q226L/T189A respectively. The single Q226L mutation completely changes glycan binding property from avian to human receptor. Additional T189A mutation increases binding specificity for human receptor (6'SLN-LN). **C**, Dose-dependent direct binding of mQu88:T189A shows that this mutant retains avian receptor-binding but specificity for avian receptors is higher when compared to mQu88 HA in **Figure 1B**. **D**, Consistent with glycan array-binding mQu88:Q226L/T189A HA shows extensive staining of apical surface of human tracheal epithelium and mQu88:T189A HA shows extensive staining of human alveolar section. HA (in green) shown against propidium iodide staining (in red).



mQu88 PI Red
Human Alveolus 10x



mQu88:Q226L/T189A PI Red
Human Trachea 10x

Figure 2.5. Sialidase A treated sections of human trachea and alveolus stained with mQu88:Q226L/T189A and mQu88 HA respectively.

No binding to either tracheal or alveolar sections is observable. HA (in green) and propidium iodide (in red).

Glycan	Expanded nomenclature
3'SLN	Neu5Ac α 2-3Gal β 1-4GlcNAc β 1-
6'SLN	Neu5Ac α 2-6Gal β 1-4GlcNAc β 1-
3'SLN-LN	Neu5Ac α 2-3Gal β 1-4GlcNAc β 1-3Gal β 1-4GlcNAc β 1-
6'SLN-LN	Neu5Ac α 2-6Gal β 1-4GlcNAc β 1-3Gal β 1-4GlcNAc β 1-
3'SLN-LN-LN	Neu5Ac α 2-3Gal β 1-4GlcNAc β 1-3Gal β 1-4GlcNAc β 1-3Gal β 1-4GlcNAc β 1-

Table 2.1. Expanded nomenclature of glycans used in the glycan array

Key: Neu5Ac: N-acetyl D-neuraminic acid; Gal: D-galactose; GlcNAc: N-acetyl D-glucosamine. α / β : anomeric configuration of the pyranose sugars. All the sugars are linked via a spacer to biotin (-Sp-LC-LC-Biotin as described in <http://www.functionalglycomics.org/static/consortium/resources/resourcecored5.shtml>)

3 Quantitative Description of Glycan-Receptor Binding of Influenza A Virus H7 Hemagglutinin

3.1 Summary

In the context of recently emerged novel influenza strains through reassortment, avian influenza subtypes such as H5N1, H7N7, H7N2, H7N3 and H9N2 pose a constant threat in terms of their adaptation to the human host. Among these subtypes, it was recently demonstrated that mutations in H5 and H9 hemagglutinin (HA) in the context of lab-generated reassorted viruses conferred aerosol transmissibility in ferrets (a property shared by human adapted viruses). We previously demonstrated that the quantitative binding affinity of HA to $\alpha 2 \rightarrow 6$ sialylated glycans (human receptors) is one of the important factors governing human adaptation of HA. Although the H7 subtype has infected humans causing varied clinical outcomes from mild conjunctivitis to severe respiratory illnesses, it is not clear where the HA of these subtypes stand in regard to human adaptation since its binding affinity to glycan receptors has not yet been quantified. In this study, we have quantitatively characterized the glycan receptor-binding specificity of HAs from representative strains of Eurasian (H7N7) and North American (H7N2) lineages that have caused human infection. Furthermore, we have demonstrated for the first time that two specific mutations; Gln226 \rightarrow Leu and Gly228 \rightarrow Ser in glycan receptor-binding site of H7 HA substantially increase its binding affinity to human receptor. Our findings contribute to a framework for monitoring the evolution of H7 HA to be able to adapt to human host.

3.2 Introduction

Avian influenza virus subtypes known to infect and cause disease in humans include H5N1, H7N7, H7N2, H7N3 and H9N2 strains. These viruses circulate in domestic poultry but have not yet adapted to the human host to establish sustained airborne human-to-human transmission capabilities [31]. One of the characteristic features of human-adapted subtypes such as H1N1, H2N2 and H3N2 is the ability of their viral surface glycoprotein hemagglutinin (HA) to bind preferentially to $\alpha 2 \rightarrow 6$ sialylated glycan receptors (or *human receptors*) that are predominantly expressed in the human upper respiratory epithelium. The HA of influenza viruses isolated from avian species typically binds to $\alpha 2 \rightarrow 3$ sialylated glycans (or *avian receptors*) [44]. Therefore, the gain in the ability of HA from an avian isolate (such as H5, H7, H9, etc.) to preferentially bind to human receptors (high relative binding affinity to human receptor over avian receptor) is implicated as one of the important factors for the human adaptation of the virus [9]. In the past few years, novel influenza strains such as 2009 H1N1 and 2010 H3N2 that naturally emerged from multiple reassortment of viral gene segments between avian, swine and human isolates were able to successfully adapt to human host [29, 39]. In the context of these novel strains, the avian influenza subtypes pose a significant threat of human adaptation [40]. With the human population predominantly naïve to these avian influenza antigens, constant surveillance with particular focus on molecular changes geared towards human host adaptation becomes vital in this era of pandemics [41].

Specific mutations in glycan-receptor binding site (RBS) of H5 and H9 HAs have been shown to correlate with respiratory droplet transmissibility of laboratory-generated reassorted viruses possessing either of these mutant HAs (and internal genes from human-adapted virus) in a ferret animal model[49-51]. Aerosol transmissibility in ferrets, a hallmark property of human-adapted viruses, has been shown to correlate with specificity and quantitative affinity of viral HA binding to human receptors [1, 8]. In fact a single amino acid mutation Gln226 \rightarrow Leu in H2 HA completely shifts its receptor binding preference from avian to human receptors and confers airborne viral transmission in ferrets[52] . Studies on H7 subtype have thus far focused on specific H7N7 and H7N2 strains isolated from infected patients in Eurasia and North America respectively (**Fig. 3.4**). The H7N7 strains were isolated from two patients with very different

clinical conditions during a local highly pathogenic outbreak in the Netherlands in 2003 [53]. One of the strains was isolated from a patient with a conjunctivitis infection (A/Netherlands/230/03 referred to henceforth as CC); which is typical of H7 human infection, and the other was isolated from a patient with acute respiratory illness that eventually resulted in fatality (A/Netherlands/219/03 henceforth referred to as FC); which was the first of its kind. The HAs from both CC and FC comprise of the polybasic sequence between HA1 and HA2 analogous to the highly pathogenic H5N1. The RBS of CC and FC HAs differs by a single amino acid substitution in position 135 (H3 numbering), which is Ala in CC but Thr in FC (**Fig. 3.4**). The presence of Thr in 135 in FC introduces a glycosylation sequon at Asn-133 [54-56].

The H7N2 strain A/New York/107/03 or NY/107 was isolated from a single human case with respiratory infection [53]. The NY/107 HA does not possess the HA1-HA2 polybasic sequence, which is typically associated with high pathogenicity. A dramatically unique feature of NY/107 HA is the complete deletion of the 220-loop region in the RBS (**Fig. 3.4**), which plays a key role in governing glycan receptor-binding specificity of HA [57].

The glycan receptor-binding properties of CC, FC and NY/107 HAS have been characterized by screening the HAs and whole viruses on glycan array platform. These screening assays provide an overall readout in terms of the number and different types of avian and human receptors that bind to the HA (or virus) when analyzed at a high protein concentration or virus titer. A limitation of such screening studies is that they do not quantify the relative binding affinities of HA to avian versus human receptor. It is important to quantify the nuances in relative binding affinities in order to understand how molecular changes in the HA such as deletion of 220-loop and differences in glycosylation at Asn-133 impinge on glycan receptor-binding. We have previously demonstrated that a change in glycosylation at a single site subtly alters human receptor-binding affinity of the pandemic 1918 H1N1 HA[58]. Furthermore we have demonstrated that quantitative parameters derived from a dose-dependent binding of HA to representative human and avian receptors correlated with the respiratory droplet transmissibility of the virus [8, 37, 38].

In this study, we quantify the relative human and avian receptor-binding affinity of CC, FC and NY/107 HA. We also characterized the effect of altering glycosylation at Asn-133 on NY/107 HA

in the context of the deletion of 220-loop on the relative glycan-receptor binding affinities of this HA. Finally we introduced the Gln226→Leu and Gly228→Ser double mutation in the RBS of FC and CC HAs since the Leu-226/Ser-228 combination in the RBS is a hallmark of all the human-adapted H3N2 HAs (belong to the same group 2 clade as H7) and characterize the effect of these mutations on quantitative glycan receptor-binding affinity of these HAs. Our study provides important biochemical insights for monitoring the evolution of H7 HAs as they continue to circulate in avian species and cause sporadic human outbreaks and also pose a constant threat of adapting to human host through reassortment.

3.3 Results

FC, CC and NY/107 HA were recombinantly expressed as described earlier [1, 8, 37, 38]. Given that FC and CC HA differ by a single amino acid change at RBS, CC HA was generated by introducing a Thr135→Ala mutation through site-directed mutagenesis. The wild type and mutant HAs were analyzed on a glycan array platform in a dose-dependent fashion and an apparent binding parameter K_d' was calculated to quantify the relative binding affinities as described earlier [8, 38] (see Methods).

3.3.1 Quantitative glycan-receptor binding affinities of H7N7 CC and FC HAs

FC HA exclusively bound to the avian receptors, 3' SLN, 3'SLN-LN and 3' SLN-LN-LN ($K_d' \sim 25$ pM; based on 3'SLNLN and 3'SLNLNLN; K_d values were similar for binding for both glycans) (**Fig. 3.1A**). The apparent binding affinity of FC HA to avian receptors was comparable to HAs from avian H2N2 and H5N1 strains analyzed in a similar fashion previously [8, 38, 52]. The HA from CC which lacks glycosylation at Asn-133 also showed predominant binding to avian receptors ($K_d' \sim 65$ pM) (based on 3' SLNLN 3'SLNLNLN binding; K_d values were similar for binding for both glycans) (**Fig. 3.1B**). CC showed observable binding to human receptors in a dose dependent fashion although at several orders of magnitude lower than avian receptor binding (K_d' was not calculated since saturation was not reached in the concentration window for avian receptor binding). The presence of glycosylation at Asn-133 therefore appears to increase avian receptor specificity for H7N7 HAs. On the other hand lack of glycosylation at this site appears to increase propensity for binding to human receptors.

3.3.2 Quantitative glycan-receptor binding affinities of H7N2 NY/107 HA

As mentioned earlier, NY/107 HA has a deletion of 8 amino acids in the 220-loop (which is almost the entire loop). The glycan array screening of NY/107 carried out previously showed that this HA shows mixed binding to both avian and human receptors [59]. X-ray crystallography studies of NY/107 HA complexed with avian and human receptors have been solved. The binding of NY/107 HA to avian receptor is clearly observed in terms of resolving the coordinates of the sugar units in the RBS in the X-ray crystal structure [57]. On the other hand, much poorer electron density map and fewer interactions were observed for human receptor in RBS of NY/107 HA [57]. These structural observations do not fully explain the observed mixed binding to both avian and human receptors by this HA.

NY/107 HA showed predominant high affinity binding ($K_d \sim 63$ pM) (Based on 3'SLNLN) to avian receptors and a significantly lower binding to human receptors in our dose-dependent binding analysis (**Fig. 3.1C**). The orders of magnitude higher relative affinity for binding to avian over human receptors by NY/107 HA is consistent with the observed interactions in the X-ray co-crystal structure of HA-glycan complexes[57]. Given that glycosylation at Asn-133 appeared to improve specificity for avian receptors in the H7N7 FC HA, we wanted to test if a similar effect was seen in the case of NY/107 HA specifically in the context of the deletion of the 220-loop. Therefore the Ala135→Thr mutation was introduced on NY/107 HA and this mutant HA showed the identical binding profile in a dose-dependent fashion as that of the wild type HA (**Fig. 3.1D**). This result suggested that the glycosylation at Asn-133 is not likely to affect glycan-receptor binding of H7N2 HAs in which the 220-loop is deleted like in the case of NY/107 HA.

3.3.3 Quantitative glycan-binding affinity of H7N7 HAs double Gln226→Leu/Gly228→Ser mutations

A double Gln226→Leu/Gly228→Ser mutations has quantitatively switched the glycan receptor binding specificity and affinity from avian receptor to human receptors for H3 and H2 HAs[38]. However such a double mutation has not quantitatively switched or increased binding of avian H5 HAs to human receptors[60]. Given that H7 HA belongs to the same phylogenetic clade 2 as H3 HA, we wanted to evaluate the effect of the double mutation on the H7N7 HAs (given that NY/107 HA does not have the 220 loop).

Introducing the double Gln226→Leu/Gly228→Ser mutations on FC (mFC:LS) and CC (mCC:LS) resulted in binding to both avian and human receptors. The human receptor binding affinity ($K_d' \sim 1\text{nM}$) (Based on 6' SLNLN binding) of mFC:LS and mCC:LS HAs was orders of magnitude higher (Figure 2A and 2B) and the human receptor binding observed for H7N7 CC and NY/107 HAs based on the quantitative dose-dependent binding assay. Interestingly the avian receptor binding affinity of mFC:LS ($K_d \sim 70\text{ pM}$) (based on 6' SLNLN) and mCC:LS (for $K_d \sim 225\text{ pM}$) (based on 6'SLNLN) was lower than that of their respective wild type HAs (Fig. 3.2A and 3.2B).

3.3.4 Binding of H7 HAs to human respiratory tissues

To compare observed binding specificities of H7 HAs on the array with their binding to physiological glycan receptors, human tracheal (upper respiratory tract which is main target for human-adapted viruses) and alveolar sections were stained using representative wild type and the mutant HA with the double mutation. mFC:LS showed extensive staining of apical surface of the tracheal epithelium where human receptors are predominantly expressed (Fig. 3.2A). Specifically it also predominantly stained what appear to be non-ciliated (goblet) cells. Extensive staining of goblet cells is a property that we have previously observed to be shared by human adapted 1918 H1N1 and 1958 H2N2 HAs [8,10]. The staining of tracheal epithelium by the mutant HA is consistent with its observed human receptor-binding in the glycan array analysis. On the other hand, the wild-type FC HA showed minimal staining of the apical surface of the human tracheal epithelium (Fig. 3.3B) consistent with its minimal human-receptor binding on the glycan array. Both the wild-type FC and mutant mFC:LS HAs showed extensive staining of the human alveolar section, which predominantly expresses $\alpha 2 \rightarrow 3$ sialylated glycans (Figure 3C and 3D). This staining pattern is consistent with the binding of these HAs to the avian receptors on the glycan array.

3.4 Discussion

The functions of HA in terms of glycan-receptor binding specificity and cleavage sequence for membrane fusion is among the key factors that contribute to the pathogenicity, severity of infection and transmissibility of influenza A virus. In this study we characterized in a

quantitative fashion, the relative binding affinities of H7 HA to avian and human receptors given that some H7 strains especially from the Eurasian lineage are highly pathogenic and have caused human infections. To our knowledge, such a quantitative description of glycan-binding properties of H7 HA has not been reported earlier.

The FC, CC and NY/107 strains were also previously analyzed for their ability to transmit in the ferret animal model NY/107 and the highly pathogenic CC strain showed some transmission via direct contact, however the other highly pathogenic strain isolated from fatal case did not show any transmission. None of the viruses transmitted via respiratory droplets. Since we previously demonstrated that the human receptor-binding specificity and affinity correlates with respiratory droplet transmissibility in ferrets, we sought to investigate any potential mutations that would significantly increase the human-receptor binding of H7 HAs in this study. We demonstrated that the double Gln226→Leu/Gly228→Ser mutation (hallmark changes for human adaptation of H3 and H2 HA) dramatically increased human receptor-binding affinity of FC and CC HA. This study is therefore the first to report mutations in H7 HA that quantitatively increase its human receptor-binding affinity. Although the double mutation increased human receptor binding of FC and CC HAs, the binding affinity of this HA to human receptor was still lower relative to avian receptor. This is not a typical characteristic of human-adapted HAs such as prototypic pandemic 1918 H1N1 and 1958 H2N2 HAs. However a natural variant of 1918 H1N1 HA isolated from humans which has a single amino acid mutation in the RBS (A/New York/1/18) shows a similar relative binding affinity as that of the mCC:LS and mFC:LS HAs. This observation warrants further investigation of the aerosol transmission in ferrets of reassorted viruses carrying these mutant H7 HAs in context of other human adapted genes similar to the previous studies carried out for H9 and H5 subtypes[49, 50].

In summary our results highlight the nuances in biochemical glycan-binding binding affinities of H7 HAs from two very different lineages and also show mutations in the Eurasian lineage that quantitatively increase their human receptor-binding affinity. Our studies would pave way for investigating the effect of these changes in contributing to the human adaptation of H7 HA based on additional ferret transmission studies that need to be performed on viruses carrying these mutant HAs.

3.5 Materials and Methods

3.5.1 Cloning, baculovirus synthesis, expression and purification of HA

Briefly, recombinant baculoviruses with FC or NY/107 gene and mutants off of each background, were used to infect (MOI=1) suspension cultures of Sf9 cells (Invitrogen, Carlsbad, CA) cultured in BD Baculogold Max-XP SFM (BD Biosciences, San Jose, CA). The infection was monitored and the conditioned media was harvested 3–4 days post-infection. The soluble HA from the harvested conditioned media was purified using Nickel affinity chromatography (HisTrap HP columns, GE Healthcare, Piscataway, NJ). Eluting fractions containing HA were pooled, concentrated and buffer exchanged into 1X PBS pH 8.0 (Gibco) using 100K MWCO spin columns (Millipore, Billerica, MA). The purified protein was quantified using BCA method (Pierce). N-glycosylation is known to play an important role in folding and maintaining the three dimensional structure of HA [38]. In order to ascertain that mutation at position 143 did not affect protein stability circular dichroism analysis of the all wild type and mutant HAs was performed alongside H2 HA, A/Albany/6/58 (Alb58) isolated from the 1957-58 pandemic. The circular dichroism spectra of all the mutant proteins were generated between 190nm and 280nm. All the mutants showed similar circular dichroism spectral signatures as that of their wild-type counterparts and Alb58, a H2N2 HA (A/Albany/6/58) (Fig. 3.5).

3.5.2 Dose dependent direct binding of FC, NY/107 and mutant HAs

To investigate the multivalent HA-glycan interactions a streptavidin plate array comprising of representative biotinylated $\alpha 2 \rightarrow 3$ and $\alpha 2 \rightarrow 6$ sialylated glycans was used as described previously [8]. 3'SLN, 3'SLN-LN, 3'SLN-LN-LN are representative avian receptors. 6'SLN and 6'SLN-LN are representative human receptors (Fig. 3.4). The biotinylated glycans were obtained from the Consortium of Functional Glycomics through their resource request program. Streptavidin-coated High Binding Capacity 384-well plates (Pierce) were loaded to the full capacity of each well by incubating the well with 50 μ l of 2.4 μ M of biotinylated glycans overnight at 4°C. Excess glycans were removed through extensive washing with PBS. The trimeric HA unit comprises of three HA monomers (and hence three RBS, one for each monomer). The spatial arrangement of the biotinylated glycans in the wells of the streptavidin

plate array favors binding to only one of the three HA monomers in the trimeric HA unit. Therefore in order to specifically enhance the multivalency in the HA-glycan interactions, the recombinant HA proteins were pre-complexed with the primary and secondary antibodies in the molar ratio of 4:2:1 (HA: primary: secondary). The identical arrangement of 4 trimeric HA units in the pre-complex for all the HAs permit comparison between their glycan binding affinities. A stock solution containing appropriate amounts of Histidine tagged HA protein, primary antibody (Mouse anti 6X His tag IgG) and secondary antibody (HRP conjugated goat anti Mouse IgG (Santacruz Biotechnology) in the ratio 4:2:1 and incubated on ice for 20 min. Appropriate amounts of pre-complexed stock HA were diluted to 250 μ l with 1% BSA in PBS. 50 μ l of this pre-complexed HA was added to each of the glycan-coated wells and incubated at room temperature for 2 hours followed by the above wash steps. The binding signal was determined based on HRP activity using Amplex Red Peroxidase Assay (Invitrogen, CA) according to the manufacturer's instructions. The experiments were done in triplicate. Minimal binding signals were observed in the negative controls including binding of pre-complexed unit to wells without glycans and binding of the antibodies alone to the wells with glycans. The binding parameters, cooperativity (n) and apparent binding constant (Kd'), for HA-glycan binding were calculated by fitting the average binding signal value (from the triplicate analysis) and the HA concentration to the linearized form of the Hill equation:

$$\log\left(\frac{y}{1-y}\right) = n * \log([HA]) - \log(K_d')$$

where y is the fractional saturation (average binding signal/maximum observed binding signal). In order to compare Kd' values, the values reported in this study correspond to the appropriate representative avian (3'SLN-LN or 3'SLN-LN-LN) and human (6'SLN-LN) receptor that gave the best fit to the above equation and the same slope value (n ~1.3).

3.5.3 Binding of recombinant FC and mFC: LS HAs to human tracheal and alveolar tissue sections

Paraffinized human tracheal (US BioChain) tissue sections were deparaffinized, rehydrated and incubated with 1% BSA in PBS for 30 minutes to prevent non-specific binding. HA was pre-complexed with primary antibody (mouse anti 6X His tag, Abcam) and secondary antibody

(Alexa fluor 488 goat anti mouse, Invitrogen) in a molar ratio of 4:2:1, respectively, for 20 minutes on ice. The tissue binding was performed over different HA concentrations by diluting the pre-complexed HA in 1% BSA-PBS. Tissue sections were then incubated with the HA-antibody complexes for 3 hours at RT. The tissue sections were counterstained by propidium iodide (Invitrogen; 1100 in TBST). The tissue sections were mounted and then viewed under a confocal microscope (Zeiss LSM 700 laser scanning confocal microscopy). Sialic-acid specific binding of HAs to tissue sections was confirmed by loss of staining after pre-treatment with Sialidase A (recombinant from *Arthrobacter ureafaciens*, Prozyme), This enzyme has been demonstrated to cleave the terminal Neu5Ac from both Neu5Ac α 2 \rightarrow 3Gal and Neu5Ac α 2 \rightarrow 6Gal motifs. In the case of sialidase pretreatment, tissue sections were incubated with 0.2 units of Sialidase A for 3 hours at 37°C prior to incubation with the proteins.

3.6 References

1. Alexander DJ (2006) Avian influenza viruses and human health. *Dev Biol (Basel)* 124: 77-84.
2. Ge S, Wang Z (2011) An overview of influenza A virus receptors. *Critical reviews in microbiology* 37: 157-165.
3. Shriver Z, Raman R, Viswanathan K, Sasisekharan R (2009) Context-specific target definition in influenza a virus hemagglutinin-glycan receptor interactions. *Chem Biol* 16: 803-814.
4. Neumann G, Noda T, Kawaoka Y (2009) Emergence and pandemic potential of swine-origin H1N1 influenza virus. *Nature* 459: 931-939.
5. Pearce MB, Jayaraman A, Pappas C, Belser JA, Zeng H, et al. (2012) Pathogenesis and transmission of swine origin A(H3N2)v influenza viruses in ferrets. *Proceedings of the National Academy of Sciences of the United States of America* 109: 3944-3949.
6. Malik Peiris JS (2009) Avian influenza viruses in humans. *Revue scientifique et technique* 28: 161-173.
7. Medina RA, Garcia-Sastre A (2011) Influenza A viruses: new research developments. *Nature reviews Microbiology* 9: 590-603.
8. Sorrell EM, Wan H, Araya Y, Song H, Perez DR (2009) Minimal molecular constraints for respiratory droplet transmission of an avian-human H9N2 influenza A virus. *Proc Natl Acad Sci U S A* 106: 7565-7570.
9. Kimble JB, Sorrell E, Shao H, Martin PL, Perez DR (2011) Compatibility of H9N2 avian influenza surface genes and 2009 pandemic H1N1 internal genes for transmission in the ferret model. *Proc Natl Acad Sci U S A* 108: 12084-12088.
10. Imai M, Kawaoka Y (2012) The role of receptor binding specificity in interspecies transmission of influenza viruses. *Curr Opin Virol* 2: 160-167.
11. Srinivasan A, Viswanathan K, Raman R, Chandrasekaran A, Raguram S, et al. (2008) Quantitative biochemical rationale for differences in transmissibility of 1918 pandemic influenza A viruses. *Proc Natl Acad Sci U S A* 105: 2800-2805.
12. Chandrasekaran A, Srinivasan A, Raman R, Viswanathan K, Raguram S, et al. (2008) Glycan topology determines human adaptation of avian H5N1 virus hemagglutinin. *Nat Biotechnol* 26: 107-113.
13. Pappas C, Viswanathan K, Chandrasekaran A, Raman R, Katz JM, et al. (2010) Receptor specificity and transmission of H2N2 subtype viruses isolated from the pandemic of 1957. *PLoS One* 5: e11158.
14. Belser JA, Bridges CB, Katz JM, Tumpey TM (2009) Past, present, and possible future human infection with influenza virus A subtype H7. *Emerg Infect Dis* 15: 859-865.
15. de Wit E, Munster VJ, van Riel D, Beyer WE, Rimmelzwaan GF, et al. (2010) Molecular determinants of adaptation of highly pathogenic avian influenza H7N7 viruses to efficient replication in the human host. *J Virol* 84: 1597-1606.
16. Jonges M, Bataille A, Enserink R, Meijer A, Fouchier RA, et al. (2011) Comparative analysis of avian influenza virus diversity in poultry and humans during a highly pathogenic avian influenza A (H7N7) virus outbreak. *J Virol* 85: 10598-10604.

17. Fouchier RA, Schneeberger PM, Rozendaal FW, Broekman JM, Kemink SA, et al. (2004) Avian influenza A virus (H7N7) associated with human conjunctivitis and a fatal case of acute respiratory distress syndrome. *Proc Natl Acad Sci U S A* 101: 1356-1361.
18. Yang H, Chen LM, Carney PJ, Donis RO, Stevens J (2010) Structures of receptor complexes of a North American H7N2 influenza hemagglutinin with a loop deletion in the receptor binding site. *PLoS Pathog* 6: e1001081.
19. Jayaraman A, Koh, X., Li, J., Raman, R., Viswanathan, K., Shriver, Z., and Sasisekharan, R. (2012) Glycosylation at Asn-91 of H1N1 haemagglutinin affects binding to glycan receptors. *Biochem J*.
20. Jayaraman A, Pappas C, Raman R, Belser JA, Viswanathan K, et al. (2011) A single base-pair change in 2009 H1N1 hemagglutinin increases human receptor affinity and leads to efficient airborne viral transmission in ferrets. *PloS one* 6: e17616.
21. Viswanathan K, Koh X, Chandrasekaran A, Pappas C, Raman R, et al. (2010) Determinants of glycan receptor specificity of H2N2 influenza A virus hemagglutinin. *PLoS One* 5: e13768.
22. Belser JA, Blixt O, Chen LM, Pappas C, Maines TR, et al. (2008) Contemporary North American influenza H7 viruses possess human receptor specificity: Implications for virus transmissibility. *Proc Natl Acad Sci U S A* 105: 7558-7563.
23. Chen LM, Blixt O, Stevens J, Lipatov AS, Davis CT, et al. (2012) In vitro evolution of H5N1 avian influenza virus toward human-type receptor specificity. *Virology* 422: 105-113.

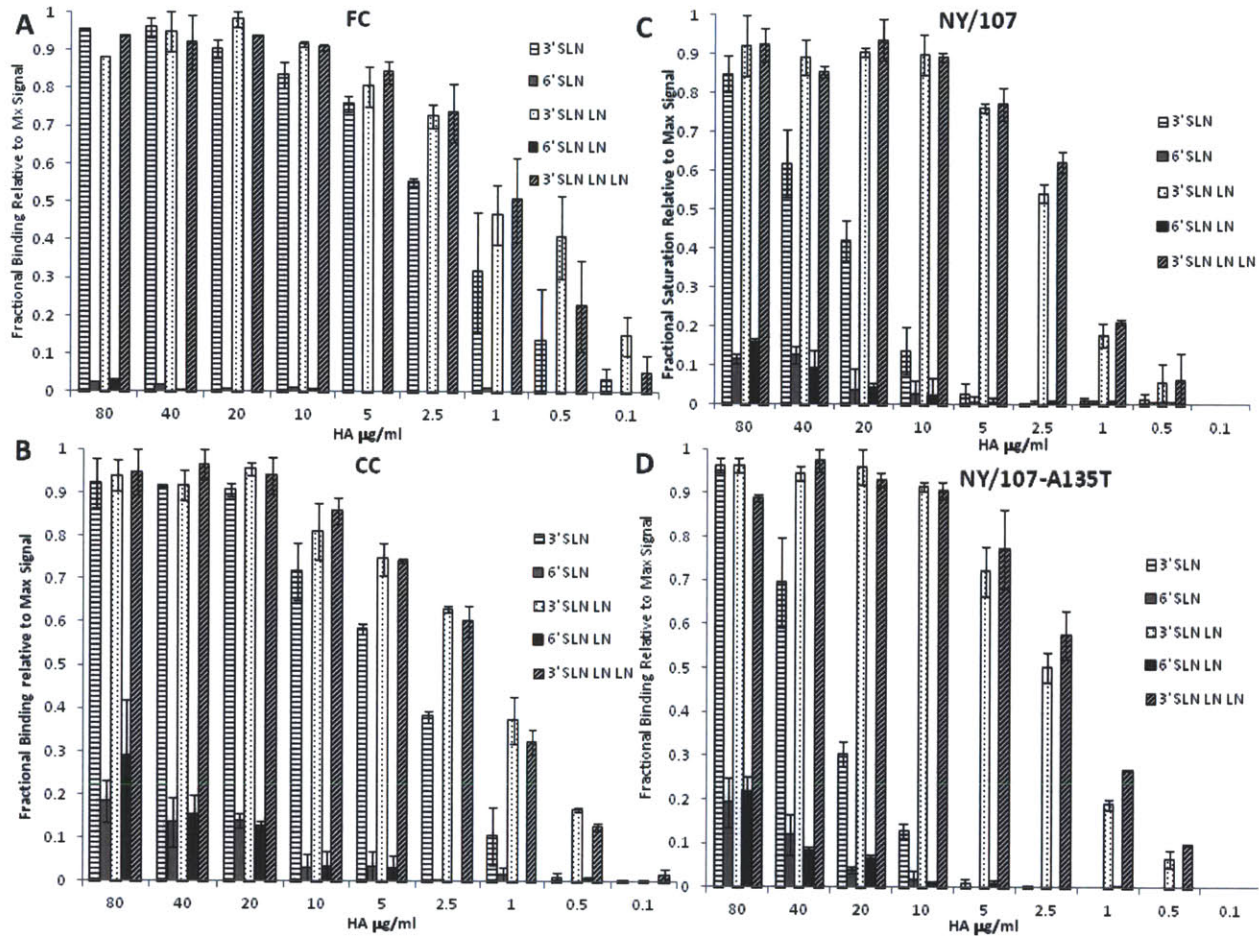


Fig 3.1. Glycan receptor-binding specificity of FC, CC, NY/107 and mNY/107:A135T HA.

A, Dose-dependent direct glycan array binding of FC HA. Specific high affinity binding to avian receptors (3'SLN, 3' SLNLN and 3' SLNLLN) and no binding to human receptors is observed. **B**, shows dose-dependent direct glycan array binding of CC HA. High affinity binding to avian receptors is observed. In comparison with FC, there is observable binding to human receptors (6'SLN-LN and 6'SLN) albeit at orders of magnitude lower affinity than binding to avian receptors. **C**, shows dose-dependent direct glycan array binding of NY/107 HA. High affinity binding to avian receptors (3'SLN-LN and 3'SLN-LN-LN) is observed with binding affinity for 3'SLN lower than that of FC and CC HAs. Binding to human receptor is observed but at much lower affinity (by orders of magnitude) than binding to avian receptors. **D**, shows dose-dependent direct glycan array binding of mutant mNY/107:A135T HA. Introduction of glycosylation sequon at Asn-133 does not seem to alter binding of this mutant HA in relation to the wild-type.

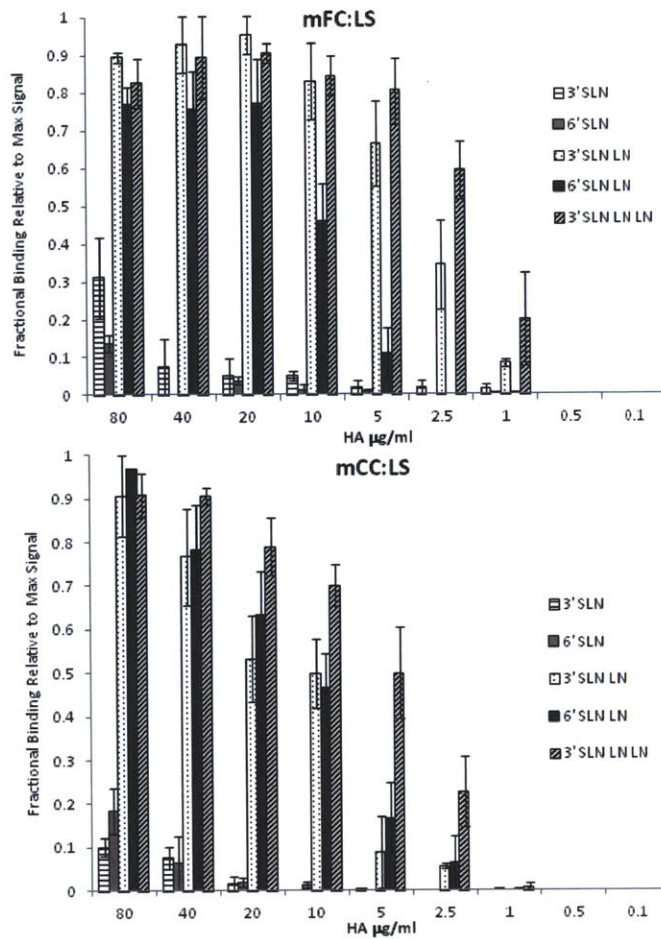


Fig. 3.2. Glycan receptor-binding specificity of Gln226→Leu/Gly228→Ser mutant of FC and CC.

A and B, respectively show dose-dependent direct glycan array binding of mFC: LS and mCC: LS mutant HAs. The double mutation leads to a substantial increase in human-receptor binding signals to a level that allowed calculation of apparent binding affinity parameter K_d' . The double mutation also lowers the avian-receptor binding affinity of mutant HAs relative to the corresponding wild-type HAs.

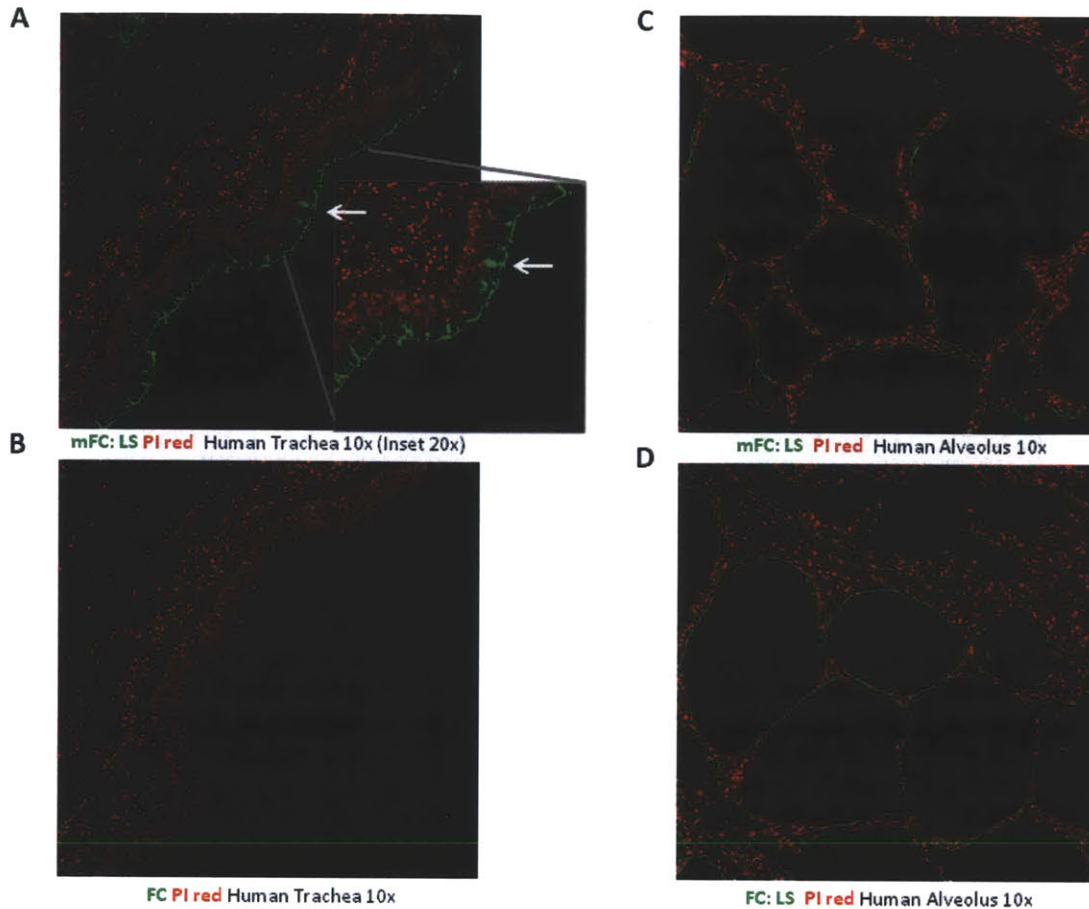


Fig 3.3. Tissue binding specificity of FC and mFC:LS for human tracheal and alveolar sections.

A, Extensive staining of apical surface of human tracheal epithelia for the mFC:LS (green) against propidium iodide staining (in red) is observed. Bright staining of what appears to be goblet cells (inset at 20x magnification; indicated by *white arrow*) by this mutant HA resembles a similar pattern that was previously observed with 1918 H1N1 and 1958 H2N2 HAs. **B**, Shows minimal to no staining of apical surface of tracheal section by FC consistent with its low binding to human receptors on glycan array. **C and D** respectively show intense staining of alveolar section by mFC:LS and FC consistent with their high affinity binding to avian receptors.

```

tk_Italy_02_H7N3      SKGKRTVDLGQCGLLGTITGPPQCDQFLEFSADLIERREGSDVCYPGKQFVNEEALRQIL
Neth_219_03_FC_H7N7  SKGKRTVDLGQCGLLGTITGPPQCDQFLEFSADLIERREGSDVCYPGKQFVNEEALRQIL
Neth_230_03_CC_H7N7  SKGKRTVDLGQCGLLGTITGPPQCDQFLEFSADLIERREGSDVCYPGKQFVNEEALRQIL
NY_107_03_H7N2       TQGKRPTDLGQCGLLGTILIGPPQCDQFLEFSSDLIERREGTDICYGRFTNEESLRQIL
                      :.***.*****:*****:*****:*.***:*.***:*****

                      133 135
tk_Italy_02_H7N3      RESGGIDKETMGFTYSGIRTNGATSACRRSGSSFYAEMKWLLSNTDAAFPQMTKSYKNT
Neth_219_03_FC_H7N7  RESGGIDKETMGFTYSGIRTNGATSACRRSGSSFYAEMKWLLSNTDAAFPQMTKSYKNT
Neth_230_03_CC_H7N7  RESGGINKETMGFTYSGIRTNGATSACRRSGSSFYAEMKWLLSNTDAAFPQMTKSYKNT
NY_107_03_H7N2       RRSGGIGKESMGFTYSGIRTNGATSACRRSGSSFYAEMKWLLSNTDAAFPQMTKAYRNP
                      *.***.***:*****:***** ***** *****:*****:*.*.

                      220 Loop
                      226 228
tk_Italy_02_H7N3      RKDPALIIWGIHHSSTTEQTKLYGSGNKLITVGSSNYQQSFVPSPGARPPQVNGQSGRID:
Neth_219_03_FC_H7N7  RKDPALIIWGIHHSSTTEQTKLYGSGNKLITVGSSNYQQSFVPSPGARPPQVNGQSGRID:
Neth_230_03_CC_H7N7  RKDPALIIWGIHHSSTTEQTKLYGSGNKLITVGSSNYQQSFVPSPGARPPQVNGQSGRID:
NY_107_03_H7N2       RNKPALIIWGVHSESVSEQTKLYGSGNKLITVRSSKYQQSFTPNPGAR-----RID:
                      *.***:****.***** ***** *.***.***.***

```

Fig 3.4: Sequence Alignment of glycan-receptor binding site of H7 HAs.

Shown in the figure is the sequence alignment of HAs used in this study. The tk_Italy_H7N3 HA is also included since its X-ray crystal structure has been solved. The residue positions 133, 135, 226 and 228 are marked given that their properties have been modified through mutagenesis in this study. The deletion of the 220-loop in NY/107 HA is also shown.

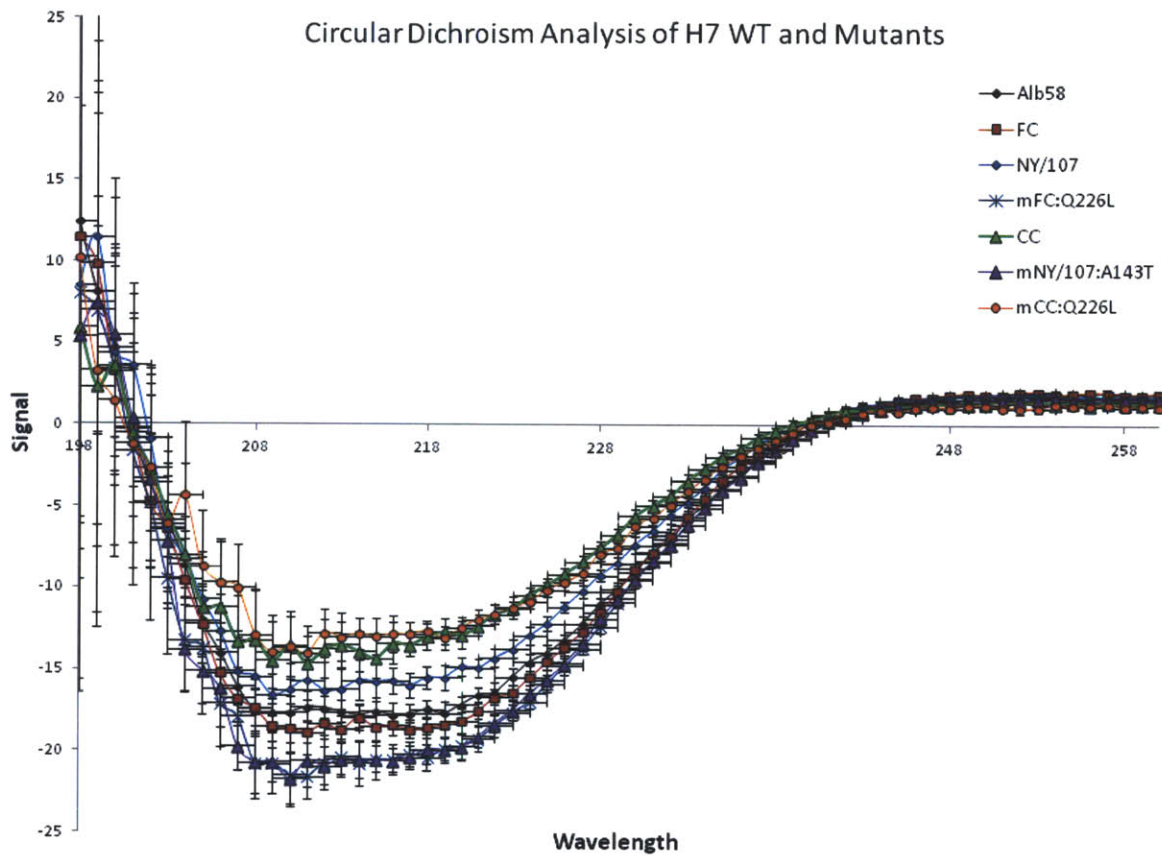


Fig 3.5: Circular Dichroism Analysis of H7 wild type and mutant HAs used in the study.

Circular dichroism spectra for FC, CC, NY/107, mFC: Q226L, mCC: Q226L and Alb58 (A/Albany/6/58; H2N2 HA) are shown as indicated in the legend. All examined HAs show similar spectral signatures indicative of no general misfolding due to amino acid substitutions.

4 Characterization of Viral Escape Mutants by Sequencing and qPCR

4.1 Summary

The evolutionary success of Influenza viruses can be largely attributed to their propensity to rapidly undergo antigenic change to evade detection by the host immune system. Advances in research have led to therapeutics and vaccines for these viruses whose efficacy is shortened due to viral escape mutants rapidly becoming fixed in the population. *In vitro* platforms that mimic antigenic drift and screens for escape mutants, in an effort to map viral evolution under selective pressure, would aid rationalized drug design to combat these viruses.

To this end, the goal was to develop a rapid, quantitative and high throughput method to identify, isolate and characterize viral quasi species (Fig. 4.1).

1. An MDCK cell culture system in 96-well format for passaging virus under varying drug concentrations was optimized.
2. As the next step, a screen for the detection of viral populations that escaped neutralization was developed. This included,
 - a. Quantitative PCR with probes designed against internal genes was used for evaluation of any/all changes in sensitivity to the drug by IC_{50} evaluation.
 - b. Viral genome sequencing for identification of nucleic acid changes in any of the eight genes of the virus that manifested in the phenotype by,
 - i. Isolation of vRNA from the vS/N for cDNA generation.
 - ii. The dsDNA generated was sequenced using gene-specific primers to reveal the substitutions.
3. After identification, the viral proteins were cloned, transfected and expressed using an insect cell expression system and tested for stability, activity and receptor binding (for Influenza Hemagglutinin).
4. An alternate reverse genetics approach to generate mutant whole viruses was attempted in an effort to systematically analyze the ramifications of the substitutions on overall viral fitness.

This approach was validated using commercially available antibodies against the Influenza viral surface protein Hemagglutinin, the primary cause for flu vaccines to be reformulated each year and allowed a systematic exploration of the viral genome to better understand sites that were prone to undergo change reflected in the virus' escape of neutralization.

4.2 Overview and Significance

Results from previous sections of this thesis were derived using recombinant proteins and proved valuable as a first step towards understanding changes that impinge on receptor binding; the orthogonal approach provided a biochemical rationale for transmission seen *in vivo*. The ability to predict mutations that would impinge on transmission followed by validation in ferret models further consolidated the effectiveness of such complementary analyses in understanding receptor binding. However, the question whether such substitutions would be seen in a real world scenario where the virus, constantly exposed to selective pressure evolves in many different ways to evade detection by the host immune system remained unanswered. Recent work has suggested that studying viral evolution of the Influenza HA, through numerous cycles of replication, in a mammalian host could provide valuable insights on sites that are more mutation prone than others, thus paving the way for rationalized drug design impinging on the invariant sites on the viral proteins for better efficacy[6]. However, a method to routinely screen for mutants as a way to map viral evolution, alongside rapid and quantitative *in vitro* ways for isolation and characterization of mutants has not been reported.

To this end, the current section explores using reverse genetics for live virus engineering for function/dysfunctional Influenza mutants designed *in silico*. In conjunction, sequencing and quantitative PCR for screening for escape mutants are tools that could be used iteratively to examine how viral replication under selective pressure leads to selection of viral progeny with specific characteristics.

This thesis focuses on the role of influenza HA in transmission and using the aforementioned paradigm in mapping the evolution of this particular glycoprotein is discussed. The glycan array was used as an “activity” assay for phenotypic characterization of the mutant/s isolated. It is believed that such an approach could be extended to understand the variability in other viral components.

4.3 Introduction

With a mutation rate of one change per replication per genome, influenza viruses generate vast numbers of quasi species. Such substitutions consequently lead to small but permanent changes in the RBS of HA that have implications in vaccine and therapeutic development.

Molecular-based techniques including reverse transcriptase-PCR, real-time PCR, microarrays and other nucleic acid sequencing-based amplifications for detecting influenza viruses have become an integral component of human and animal surveillance programs, outbreak management, diagnosis and treatment of influenza viruses [61-72]. Passaging of the virus in a ferret model has been used to discern mutants under immune pressure although performing such animal studies on a regular basis for therapeutics in parallel would be cost prohibitive. This section elaborates on tying quantitative PCR and reverse genetics with cell based assay platforms to understand binding of HA when presented as a trimer on a mature virion to glycan receptors and map the “natural” variants of the protein.

Such a platform would enable prediction of mutations likely to emerge *in vivo*. Further, the novel HA mutations detected would be analyzed on the glycan array to quantitatively measure changed HA binding affinity thus furthering our understanding of the possible mutations in the HA RBS that facilitate human adaptation while simultaneously looking at the probability of such mutations arising *in vivo*.

Finally, this platform is designed and presented in a fashion that makes it extendable to any of the 11 other proteins in the viral genome.

4.4 Results

Quantitative PCR and genome sequencing as a screen for detection of escape mutants of Influenza viruses in response to pressure from neutralizing compounds

4.4.1 Method Development

4.4.1.1 Overview

MDCK cells in 96 well plates were used for passaging the Influenza virus (A/Puerto Rico/8/34 H1N1). IC₅₀ was determined using PCR. In parallel, the vS/N was processed for RNA extraction, cDNA and dsDNA generation and sequencing of the genome (**Fig 4.1**). Then, neutralizing compounds were added to vS/N and IC₅₀ changes monitored. Changes in viral genome that resulted in IC₅₀ alterations could be identified via the sequencing paradigm. This protocol was validated using C179, a commercial antibody against the viral hemagglutinin.

4.4.1.2 Quantitative PCR

Quantitative PCR protocols as described by Suarez et al., [73] with primer and probe sequences for Taq-man based PCR. The protocol was validated using C179, a commercially available monoclonal antibody that has previously been shown to broadly cross-neutralize H1 and H2 Influenza viruses was chosen to provide selective pressure[74-77]. The virus chosen was A/Puerto Rico/8/34 H1N1 virus Pr8 that was purchased from ATCC. IC₅₀ for the neutralizing antibody (nAb) C179 at MOI = 0.005 of the H1 N1 virus Pr8 was determined using qRT-PCR. This value is in agreement with previous reports for this monoclonal antibody whose epitope lies within the stem region of HA [76, 78].

4.4.1.3 Selection of neutralization escape mutant

The H1N1 virus Pr8 was propagated in MDCK cells for 72h in the presence of varying concentrations (1-20 ug/ml) of the nAb C179. The internal genes and NA were sequenced as described. Positive control for the assay was Pr8 in the absence of the antibody at the same MOI. Plaques isolated from vS/N passaged in similar fashion allowed calculation of viral titer that matched the original titer of virus. Viral titer was also calculated using qRT-PCR and sequencing confirmed that the virus had not undergone any amino acid changes during the

passaging. As a negative control the assay was repeated in the absence of virus. C179 was non toxic to the cellular monolayer at ~100 fold higher concentrations than what was used in the assay. qRT-PCR confirmed the absence of a viral titer.

4.4.1.4 Reverse Genetics and Plaque Isolation

A method to generate whole infectious viral particles from cDNAs of individual viral genes was first described by Palese and colleagues in 1989[79-82]. Hoffmann et al., were pioneers in provide a simple tool kit for generation of infectious virions after transfection of 8 plasmids into the host cells eliminating the need for helper viruses that was a significant advancement. High titers 1×10^8 PFU/ml was reproducibly generated using this new method [83-85]. This thesis does not attempt to provide a detail overview of the advancements made in the field or the applications of reverse genetics but refers the reader to several excellent reviews on the subject [16, 24, 25, 27, 82, 86-98].

The ability to reconstruct any strain of Influenza viruses via reverse genetics provides a tool for systematic analysis of pathogenesis, virulence and transmission apart from receptor binding. Whole infectious virions or viral-like particles generated via transfection of plasmids corresponding to all 8 viral genes or a smaller subset would present a more physiologically relevant HA to the glycans on the array allowing a more biologically relevant interpretation for the affinity calculated. To this end, it was attempted to establish a reverse genetics platform using HEK293 and MDCK cells as described in the original Hoffman et al., publication [84, 85]. However, despite availability of the original plasmids the tissue culture based system ran aground due to technical difficulties.

4.5 Discussion

Key gaps exist in our understanding of the evolution of Influenza virus HA in the presence of antigenic pressure notwithstanding the advances that have been made in our understanding of these viruses. The need to understand the changes that HA may undergo in the presence of antibodies generated upon vaccination and/or previous exposure to other Influenza strains would have implications on how the HA would evolve as seen from an immune perspective.

Platforms for screening for escape mutants are essential for ascertaining the probability of a given subset of mutations emerging *in vivo*. Advances in reverse genetics allows live engineering of the virus based on mutations designed *in silico* and qRT-PCR and sequencing allows for screening of mutants in tandem with the glycan array assay to map the evolution of the viral surface protein and determine whether the mutations predicted to enhance human receptor binding could be expected to emerge *in vivo*.

4.6 Materials and Methods

4.6.1 Infection: Calculations for Passage 1

MDCK cells were seeded 18-20h before the infection at 3×10^4 cells/well in a 96 well plates in a 100 ul volume of 1x MEM. MOI of orig. virus Pr8 purchased from ATCC equaled 3×10^6 pfu/ml (This was previously determined via plaque assay and verified by qRT-PCR). This was diluted 1/100x in 1x MEM to give MOI = 1. The virus-antibody mixture was pre-incubated in a 20 ul volume on ice. 2 ul of 100x diluted virus was added to 20 ul of 1x MEM containing antibody effectively diluting the virus concentration by another 10x. C179 in lyophilized form was re-constituted in DNase/RNase free water to a final concentration of 2 ug/ul and further 10x diluted to give 0.2 ug/ul in 1x MEM. 2 ul of this 0.2 ug/ul C179 was used for preincubation. 2ul C179 (0.2 ug/ul) + 2 ul Pr8 (MOI 0.1) + 16 ul media (1x MEM) make a final volume of 20 ul that is incubated for 1h on ice. The mixture is then diluted 20x to give a total volume of 400 ul that was added 50ul/well making the final MOI 0.005 and antibody concentration 1 ug/ml.

Infection was allowed for 1h at 37C, after which add 3ml of avicel overlay was added per well. Plates were returned to 37C and left undisturbed for 72h. At the end of the incubation the avicel was carefully removed from the wells and discarded and the plates immunostained for a titer estimation via plaque assay.

Alternately, if the virus were being passaged on MDCK cells, then the virus-antibody mixture is carefully pipetted out of the wells and antibody diluted in 1x MEM with TPCK trypsin made to a final concentration of 1 ug/ml (100ul/well). Plates are returned to the incubator for 48h. At the end of this time interval, the vS/N is removed and processed for whole genome sequencing.

The MDCK monolayer is stained with crystal violet to check for intactness viz failure to neutralize virus by antibody would result in loss of cell monolayer and cell death.

4.6.2 Processing of vS/N for qRT-PCR and genome sequencing (Fig 4.2; Fig. 4.3 and 4.4 provide finer details)

4.6.2.1 vS/N harvest

RNA/cDNA/dsDNA generation was optimized for vS/N obtained from a single well~100 ul (Fig. 4.3). Aliquots can be frozen upon harvest (-80C) and RNA extracted later. Freeze/thaw of RNA repeatedly is not recommended. QiAamp Viral RNA Mini Kit (Qiagen Cat # 52906) was used for extraction. Briefly, vS/N collected from each well were spun down at 1500g for 10min to pellet the floating cells and transferred to fresh tubes. At this stage the vS/N could be frozen at -80C until further use. Upon thawing, recentrifuge at 1500g for 10 min (To pellet any cells in vS/N and to ensure that there is no cellular DNA contamination). Prepare carrier RNA and aliquot into smaller volumes and freeze at -20C. Freeze-thawing of carrier RNA is not recommended more than 3times. Prepare buffer AVL-carrier RNA according to the number of samples. The extraction and purification protocol is optimized for a sample volume of 140 ul. Adjust sample volume to 140ul with PBS. Ratio of the sample volume (140 ul) to buffer AVL-carrier RNA (560 ul) is maintained. The remainder protocol is as provided in the handbook with the reagents. Elution is done twice, each at a volume of 40 ul instead of a single elution in 60 ul volume (Fig. 4.3).

4.6.2.2 Quantitative PCR

qRT-PCR based on the matrix gene using taq man probes was optimized for the Qiagen OneStep RT-PCR kit. PCR primers and probe were HPLC purified. Primers and probes were centrifuged briefly to ensure that the DNA pellet is at the bottom of the tube before opening and reconstitution. Nuclease-free water was used for reconstitution and concentrated stock solutions stored at -80C. Primer stock solutions were at 200 uM and probe stock solutions made to 120 uM. Working dilutions for primer and probe were 20 pmol/ul and 6 pmol/ul and these were stored at 4C. Primer and probe sequences described in Suarez et al., were used [73].

4.6.2.3 Real-Time RT-PCR reaction

The reverse transcription step is one cycle of 30 mins at 50C and 15min at 94C. Heat activation of the taq polymerase is a 15 min 94C step. The PCR phase of the cycle for influenza specific primers and probes is 45 cycles of 94C for 1s and 60C for 20s [73].

4.6.3 Processing of vRNA for sequencing the virus genome (Fig. 4.2, 4.3 and 4.4)

4.6.3.1 1st strand generation (cDNA)

Use of fresh RNA is recommended. 9ul of the elutant is optimal. Add 9ul of vRNA, 2 ul of Uni12 HA primer (Uni12 HA primer- AGC AAA AGC AGG) and 1 ul of 10mM dNTP mix into a Rnase-free tube and incubate mixture (12ul) for 5 mins @ 65C (PCR machine). Then add 5ul cDNA synthesis buffer, 1 ul 0.1M DTT, 1ul RNase OUT (40 units/ul) and 1 ul water and 1 ul Thermoscript (15U/ul) to the same tube. Returned the tube to the PCR machine for 1h at 65C. This should be immediately followed by incubation at 85C for 5 mins. Contents of the tube are briefly centrifuged to spin down contents. 20 ul of cDNA (1st strand) is generated. (Fig 4.3)

4.6.3.2 Digestion with RNASE H.

Add 1 ul of RNASE H to the cDNA reac of 20 ul and incubate for 20mins at 37C before proceeding to PCR. This cDNA can immediately be used to generate dsDNA via PCR. (Fig. 4.4)

4.6.3.3 dsDNA Synthesis

Use 45ul of High Fidelity PCR MIX (Invitrogen Catalog # 12532-016 or # 10790-020) and add 1-2 ul each of forward and reverse primers with 3 ul of the cDNA to make 50 ul volume PCR reaction. The thermocycler conditions are 94C – 2min, (94C – 30s, 55C – 30s, 68C – 2 min) Repeat for 32 cycles followed by annealing at 68C – 7 min. Primer stocks are prepared at 200 picomoles/ul. This stock is 10 fold diluted to give a working conc of 20 picomoles/ul. (Fig 4.4)

4.6.3.4 Agarose gel electrophoresis

Run a 1% agarose gel with the samples. Load 30 ul of the PCR reaction/well. Run at 120V for 1h. This should give good separation. Cut out the portion of the gel required. (Fig 4.4)

4.6.3.5 Gel Purification

Use the Invitrogen Gel Purification Kit to extract DNA. 400 mg is a typical band weight of gel which requires 1.2 ml of the gel solubilization buffer supplied in the kit. Use a water bath set to 50C for gel solubilization. This should generate ~15-20 ng/ul of dsDNA which is sequenced (**Fig 4.4**).

4.6.3.6 Primer Sequences

As outlined in **Table 4.1**. The usefulness of these primers in amplifying specific gene segments was validated (**Fig 4.5 and 4.6**). Gel purified products were sent out for sequencing and sequence alignments with sequences was used to discern for changes if any sustained upon passaging.

4.7 References

- 1 Hensley, S. E., Das, S. R., Bailey, A. L., Schmidt, L. M., Hickman, H. D., Jayaraman, A., Viswanathan, K., Raman, R., Sasisekharan, R., Bennink, J. R. and Yewdell, J. W. (2009) Hemagglutinin receptor binding avidity drives influenza A virus antigenic drift. *Science*. **326**, 734-736
- 2 Tang, Q., Wang, J., Bao, J., Sun, H., Sun, Y., Liu, J. and Pu, J. (2012) A multiplex RT-PCR assay for detection and differentiation of avian H3, H5, and H9 subtype influenza viruses and Newcastle disease viruses. *J Virol Methods*. **181**, 164-169
- 3 Agrawal, A. S., Sarkar, M., Chakrabarti, S., Rajendran, K., Kaur, H., Mishra, A. C., Chatterjee, M. K., Naik, T. N., Chadha, M. S. and Chawla-Sarkar, M. (2009) Comparative evaluation of real-time PCR and conventional RT-PCR during a 2 year surveillance for influenza and respiratory syncytial virus among children with acute respiratory infections in Kolkata, India, reveals a distinct seasonality of infection. *J Med Microbiol*. **58**, 1616-1622
- 4 Crossley, B. M., Hietala, S. K., Shih, L. M., Lee, L., Skowronski, E. W. and Ardans, A. A. (2005) High-throughput real-time RT-PCR assay to detect the exotic Newcastle Disease Virus during the California 2002--2003 outbreak. *J Vet Diagn Invest*. **17**, 124-132
- 5 Eladl, A. E., El-Azm, K. I., Ismail, A. E., Ali, A., Saif, Y. M. and Lee, C. W. (2011) Genetic characterization of highly pathogenic H5N1 avian influenza viruses isolated from poultry farms in Egypt. *Virus Genes*. **43**, 272-280
- 6 Daum, L. T., Canas, L. C., Schadler, C. A., Ujimori, V. A., Huff, W. B., Barnes, W. J. and Lohman, K. L. (2002) A rapid, single-step multiplex reverse transcription-PCR assay for the detection of human H1N1, H3N2, and B influenza viruses. *J Clin Virol*. **25**, 345-350
- 7 Druce, J., Tran, T., Kelly, H., Kaye, M., Chibo, D., Kosteci, R., Amiri, A., Catton, M. and Birch, C. (2005) Laboratory diagnosis and surveillance of human respiratory viruses by PCR in Victoria, Australia, 2002-2003. *J Med Virol*. **75**, 122-129
- 8 Duitama, J., Kumar, D. M., Hemphill, E., Khan, M., Mandoiu, II and Nelson, C. E. (2009) PrimerHunter: a primer design tool for PCR-based virus subtype identification. *Nucleic Acids Res*. **37**, 2483-2492
- 9 Ecker, D. J., Massire, C., Blyn, L. B., Hofstadler, S. A., Hannis, J. C., Eshoo, M. W., Hall, T. A. and Sampath, R. (2009) Molecular genotyping of microbes by multilocus PCR and mass spectrometry: a new tool for hospital infection control and public health surveillance. *Methods Mol Biol*. **551**, 71-87
- 10 Ellis, J., Iturriza, M., Allen, R., Bermingham, A., Brown, K., Gray, J. and Brown, D. (2009) Evaluation of four real-time PCR assays for detection of influenza A(H1N1)v viruses. *Euro Surveill*. **14**
- 11 Ellis, J. S., Fleming, D. M. and Zambon, M. C. (1997) Multiplex reverse transcription-PCR for surveillance of influenza A and B viruses in England and Wales in 1995 and 1996. *J Clin Microbiol*. **35**, 2076-2082
- 12 Ellis, J. S., Smith, J. W., Braham, S., Lock, M., Barlow, K. and Zambon, M. C. (2007) Design and validation of an H5 TaqMan real-time one-step reverse transcription-PCR and

- confirmatory assays for diagnosis and verification of influenza A virus H5 infections in humans. *J Clin Microbiol.* **45**, 1535-1543
- 13 Ellis, J. S. and Zambon, M. C. (2001) Combined PCR-heteroduplex mobility assay for detection and differentiation of influenza A viruses from different animal species. *J Clin Microbiol.* **39**, 4097-4102
- 14 Martinez-Sobrido, L. and Garcia-Sastre, A. (2010) Generation of recombinant influenza virus from plasmid DNA. *J Vis Exp*
- 15 Hoffmann, E., Krauss, S., Perez, D., Webby, R. and Webster, R. G. (2002) Eight-plasmid system for rapid generation of influenza virus vaccines. *Vaccine.* **20**, 3165-3170
- 16 Lipatov, A. S., Gitelman, A. K. and Smirnov Yu, A. (1997) Prevention and treatment of lethal influenza A virus bronchopneumonia in mice by monoclonal antibody against haemagglutinin stem region. *Acta Virol.* **41**, 337-340
- 17 Smirnov Iu, A., Lipatov, A. S., Okuno, I. and Gitel'man, A. K. (1999) [A common antigenic epitope in influenza A virus (H1, H2, H5, H6) hemagglutinin]. *Vopr Virusol.* **44**, 111-115
- 18 Smirnov, Y. A., Lipatov, A. S., Gitelman, A. K., Claas, E. C. and Osterhaus, A. D. (2000) Prevention and treatment of bronchopneumonia in mice caused by mouse-adapted variant of avian H5N2 influenza A virus using monoclonal antibody against conserved epitope in the HA stem region. *Arch Virol.* **145**, 1733-1741
- 19 Okuno, Y., Matsumoto, K., Isegawa, Y. and Ueda, S. (1994) Protection against the mouse-adapted A/FM/1/47 strain of influenza A virus in mice by a monoclonal antibody with cross-neutralizing activity among H1 and H2 strains. *J Virol.* **68**, 517-520
- 20 Smirnov, Y. A., Lipatov, A. S., Gitelman, A. K., Okuno, Y., Van Beek, R., Osterhaus, A. D. and Claas, E. C. (1999) An epitope shared by the hemagglutinins of H1, H2, H5, and H6 subtypes of influenza A virus. *Acta Virol.* **43**, 237-244
- 21 Rohani, P., Breban, R., Stallknecht, D. E. and Drake, J. M. (2009) Environmental transmission of low pathogenicity avian influenza viruses and its implications for pathogen invasion. *Proc Natl Acad Sci U S A.* **106**, 10365-10369
- 22 Sawabe, K., Tanabayashi, K., Hotta, A., Hoshino, K., Isawa, H., Sasaki, T., Yamada, A., Kurahashi, H., Shudo, C. and Kobayashi, M. (2009) Survival of avian H5N1 influenza A viruses in *Calliphora nigribarbis* (Diptera: Calliphoridae). *J Med Entomol.* **46**, 852-855
- 23 Fodor, E., Devenish, L., Engelhardt, O. G., Palese, P., Brownlee, G. G. and Garcia-Sastre, A. (1999) Rescue of influenza A virus from recombinant DNA. *J Virol.* **73**, 9679-9682
- 24 Palese, P. (2006) Making better influenza virus vaccines? *Emerg Infect Dis.* **12**, 61-65
- 25 Neumann, G., Watanabe, T., Ito, H., Watanabe, S., Goto, H., Gao, P., Hughes, M., Perez, D. R., Donis, R., Hoffmann, E., Hobom, G. and Kawaoka, Y. (1999) Generation of influenza A viruses entirely from cloned cDNAs. *Proc Natl Acad Sci U S A.* **96**, 9345-9350
- 26 Hoffmann, E., Stech, J., Guan, Y., Webster, R. G. and Perez, D. R. (2001) Universal primer set for the full-length amplification of all influenza A viruses. *Arch Virol.* **146**, 2275-2289
- 27 Ozawa, M. and Kawaoka, Y. (2011) Taming influenza viruses. *Virus Res.* **162**, 8-11
- 28 Taubenberger, J. K. and Kash, J. C. (2011) Insights on influenza pathogenesis from the grave. *Virus Res.* **162**, 2-7
- 29 Wang, R. and Taubenberger, J. K. (2010) Methods for molecular surveillance of influenza. *Expert Rev Anti Infect Ther.* **8**, 517-527

- 30 Kiraly, J. and Kostolansky, F. (2009) Reverse genetics and influenza virus research. *Acta Virol.* **53**, 217-224
- 31 Horimoto, T. and Kawaoka, Y. (2009) Designing vaccines for pandemic influenza. *Curr Top Microbiol Immunol.* **333**, 165-176
- 32 Belak, S., Kiss, I. and Viljoen, G. J. (2009) New developments in the diagnosis of avian influenza. *Rev Sci Tech.* **28**, 233-243
- 33 Rao, S. S., Styles, D., Kong, W., Andrews, C., Gorres, J. P. and Nabel, G. J. (2009) A gene-based avian influenza vaccine in poultry. *Poult Sci.* **88**, 860-866
- 34 Suarez, D. L., Das, A. and Ellis, E. (2007) Review of rapid molecular diagnostic tools for avian influenza virus. *Avian Dis.* **51**, 201-208
- 35 Brown, I. H. (2006) Advances in molecular diagnostics for avian influenza. *Dev Biol (Basel).* **124**, 93-97
- 36 Huang, Y. W., Li, L. and Yu, L. (2004) [The reverse genetics systems for human and animal RNA viruses]. *Sheng Wu Gong Cheng Xue Bao.* **20**, 311-318
- 37 Marsh, G. A. and Tannock, G. A. (2005) The role of reverse genetics in the development of vaccines against respiratory viruses. *Expert Opin Biol Ther.* **5**, 369-380
- 38 Subbarao, K. and Katz, J. M. (2004) Influenza vaccines generated by reverse genetics. *Curr Top Microbiol Immunol.* **283**, 313-342
- 39 Neumann, G. and Kawaoka, Y. (2004) Reverse genetics systems for the generation of segmented negative-sense RNA viruses entirely from cloned cDNA. *Curr Top Microbiol Immunol.* **283**, 43-60
- 40 Schickli, J. H., Flandorfer, A., Nakaya, T., Martinez-Sobrido, L., Garcia-Sastre, A. and Palese, P. (2001) Plasmid-only rescue of influenza A virus vaccine candidates. *Philos Trans R Soc Lond B Biol Sci.* **356**, 1965-1973
- 41 Rimmelzwaan, G. F. and Osterhaust, A. D. (2001) Influenza vaccines: new developments. *Curr Opin Pharmacol.* **1**, 491-496
- 42 Neumann, G. and Kawaoka, Y. (2001) Reverse genetics of influenza virus. *Virology.* **287**, 243-250
- 43 Garcia-Sastre, A. and Palese, P. (1995) Influenza virus vectors. *Biologicals.* **23**, 171-178

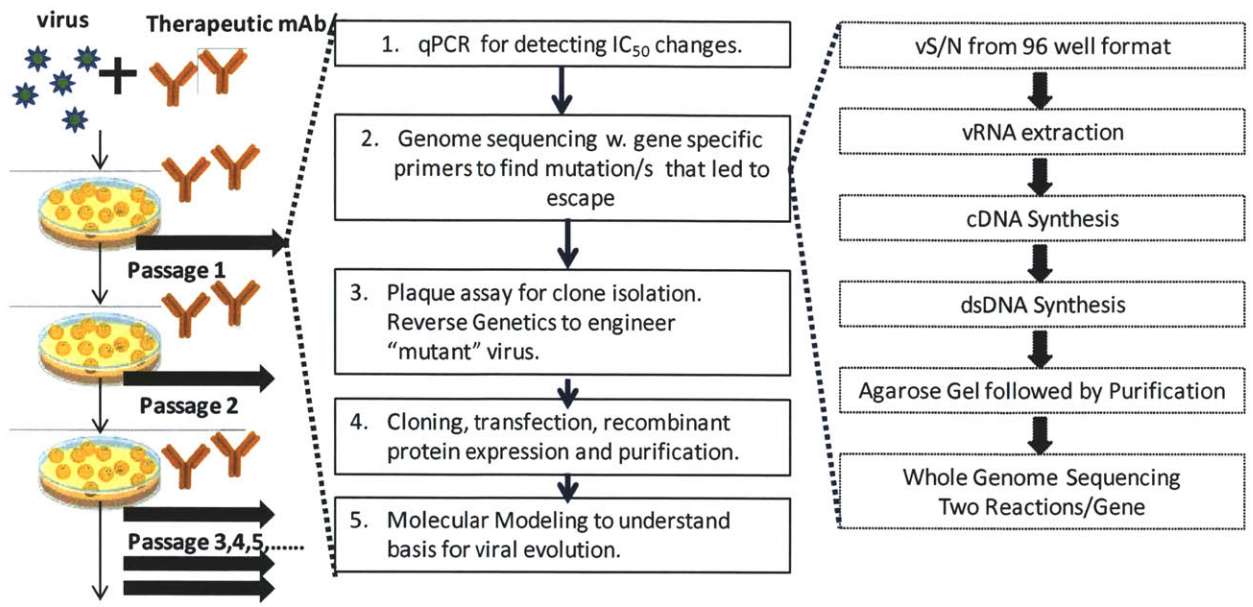


Fig 4.1 Characterization of viral escape mutants to understand viral evolution under selective pressure.

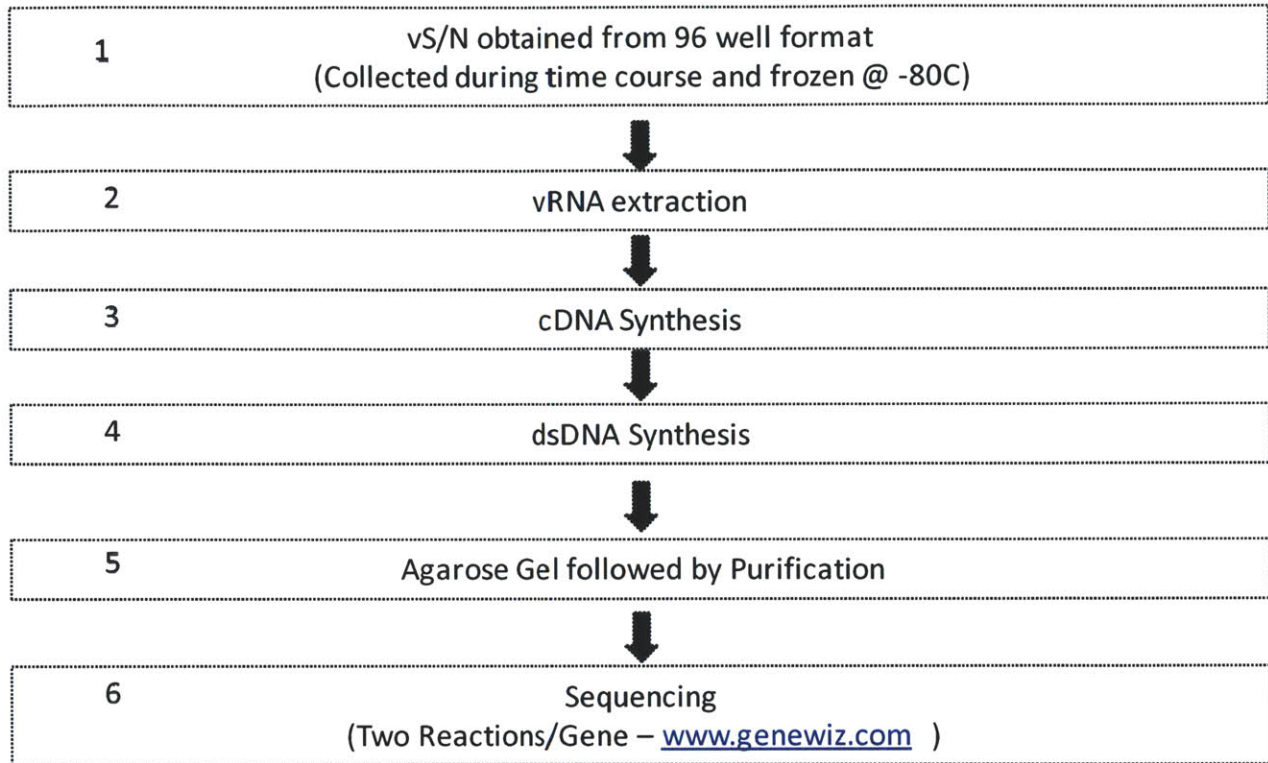


Fig 4.2 Rapid PCR based screen platform for detection of escape mutants to therapeutic pressure for Influenza Viruses.

Outlined are the steps for: Generation of dsDNA from vS/N that could be used for HA (& other viral genes) sequencing.

1. vS/N harvest

- The escape mutant generation assays were designed and performed in 96 well format and hence rna/cdna/dsDNA generation were all optimized for vS/N obtained from a single 96 well.
- Volume – 50 -100 ul of vS/N.
- Aliquots can be frozen upon harvest (-80C) and RNA extracted later.
- *It would be a good idea NOT to freeze/thaw RNA repeatedly and hence best to collect vS/N and cumulatively extract RNA and proceed immediately to cDNA/dsDNA generation.*
- *dsDNA can be stably stored for up to 6months if reqd.*

2. vRNA Extraction

- Use the Qiagen kit & elution volume is 80ul.
- QiAamp Viral RNA Mini Kit Cat # 52906

3. cDNA synthesis.

- Use of fresh RNA is recommended. 9ul of the

Component	12 ul	Component	Vol.
v RNA (from a total of 80 ul)	9 ul	5x cDNA synthesis buffer	4ul
Uni 12 Primer (20 pmol)	1 ul	0.1 M DTT	1 ul
10 mM dNTP	2 ul	Rnase OUT (40 units/ul)	1 ul
		Water	1 ul
		ThermoScript (15U/ul)	1 ul

- Step 1 – **GREEN** TABLE
 - Add components in Rnase-free tube and incubate mixture (12ul) for 5 mins
- STEP 2 – **BLUE** TABLE
 - Add the remaining components and place the reaction mixture in the PCR machine at 65C for 1 hour.
 - This should be immediately followed by 85C for 5 mins.
 - Then spin down the contents of the tube to obtain 20ul of cDNA.

- **Uni12 HA primer- AGC AAA AGC AG**

Fig. 4.3 Expanding on the first three steps as outlined in Fig 4.2 viz 1. vS/N Harvest 2. vRNA Extraction and 3. cDNA Synthesis

4. Digestion w. RNASE H.

- Add 1 ul of RNASE H to the cDNA reac of 20 ul and incubate for 20mins at 37C before proceeding to PCR.
- This cDNA can immediately be used to generate dsDNA via PCR.

4. dsDNA Synthesis

- Use 45ul of High Fidelity PCR MIX (Invitrogen Catalog # 12532-016 or # 10790-020) and add 1-2 ul each of forward and reverse primers. **RED** Table.
- A stock for each primer is prepared at a conc of 200 picomoles/ul. This stock is 10x diluted to give a working conc of 20 picomoles/ul.

5. Agarose Gel Electrophoresis

- Run a 1% agarose gel with the samples.
- Use broad frame which takes in about 30 ul of the PCR reaction/well.
- Run at 120V for 1h. This should give good separation.
- Cut out the portion of the gel required.
 - Gel Purification
- Use the Invitrogen Gel Purification Kit to extract DNA.
- This after purification gives around 15-20 ng/ul of dsDNA which is sequenced.
- 400 mg is a typical band weight of gel which requires 1.2 ml of the gel solubilization buffer supplied in the kit. Use a water bath set to 50C for gel solubilization.

94C – 2min

94C – 30s
55C – 30s
68C – 2 min

Repeat for 32 cycles

68C – 7 min

Component	Volume
PCR SuperMix High Fidelity	45 ul
Primer (Use 20 picomoles/ul conc)	1ul For + 1 ul Rev
cDNA	3 ul
Total	50 ul

Fig 4.4 Details on Steps 4 and 5 as outlined in Fig 4.2. (viz 4. Rnase H Digestion; ds DNA generation and 5. Agarose gel eletrophoresis and gel purification).

HA (EF467821.1) (1-1778 bases)	HA-1	AGC AAAA GCA GGGG AAAA TAA
	HA-1778R	AGT AGA AAC AAG GGT GTTTT
NA (EF467823.1) (1-1413 bases)	NA - FOR 1	AGC GAA AGC AGG AGT TTA AAA TGA
	NA - 1413 REV	AGT AGA AAC AAG GAG TTT TTT GA
M(EF467824.1) (1-1023 bases)	M-8-FOR	5- GAA GGT AGA TAT TGA AAG ATG -3
	M-1023-REV	5- GAA ACA AGG TAG TTT TTT ACT C -3
PA (EF467820.1) (1-2233 bases)	PA 1 FOR	AGC GAA AGC AGG TAC TGA TCC
	PA 2233 CREV	AGT AGA AAC AAG GTA CTT TTT TGG ACA
NS (EF467817.1) (1-890 bases)	NS 1 FOR	AGC AAA AGC AGG GTG ACA AA
	NS 890 Rev	AGT AGA AAC AAG GGT GTT TTT T
NP (EF467822.1)	NP-1FOR	<u>AGC AAA AGC AGG GTA</u> GAT AAT CA Underlined – Hoffmann Purple – Primer3
	NP-1565REV	AGT AGA AAC AAG GGT ATT TTT Reverse Comp : <u>AAA AAT ACC CTT GTT TCT ACT</u>
	NP-1557REV	CAA GGG TAT TTT TCT TTA ATT GTC G Reverse Comp: C GAC AAT TAA AGA AAA ATA CCC TTG <u>Underlined part is common between the two reverse primers</u>
PB2 (EF467818.1)	PB2-1FOR	<u>AGC GAA AGC AGG TCA</u> ATT ATA TTC Underlined Region is common w. Hoffmann et al.,
	PB2-2332REV	AAG GTC GTT TTT AAA CTA TTC GAC A Reverse Complement – T GTC GAA TAG TTT AAA AAC GAC CTT
	PB2-2341REV	AGT AGA AAC AAG GTC GTT TT Reverse Complement – AA AAC GAC CTT GTT TCT ACT
	PB2-2341REV	<u>AGT AGA AAC AAG GTC GTT TTT AAA C</u> Reverse Complement - GTTAAAAACGACCTTGTCTACT Underlined Region is common w. Hoffmann et al.,

Table 4.1. Sequencing Primers for the viral genome.

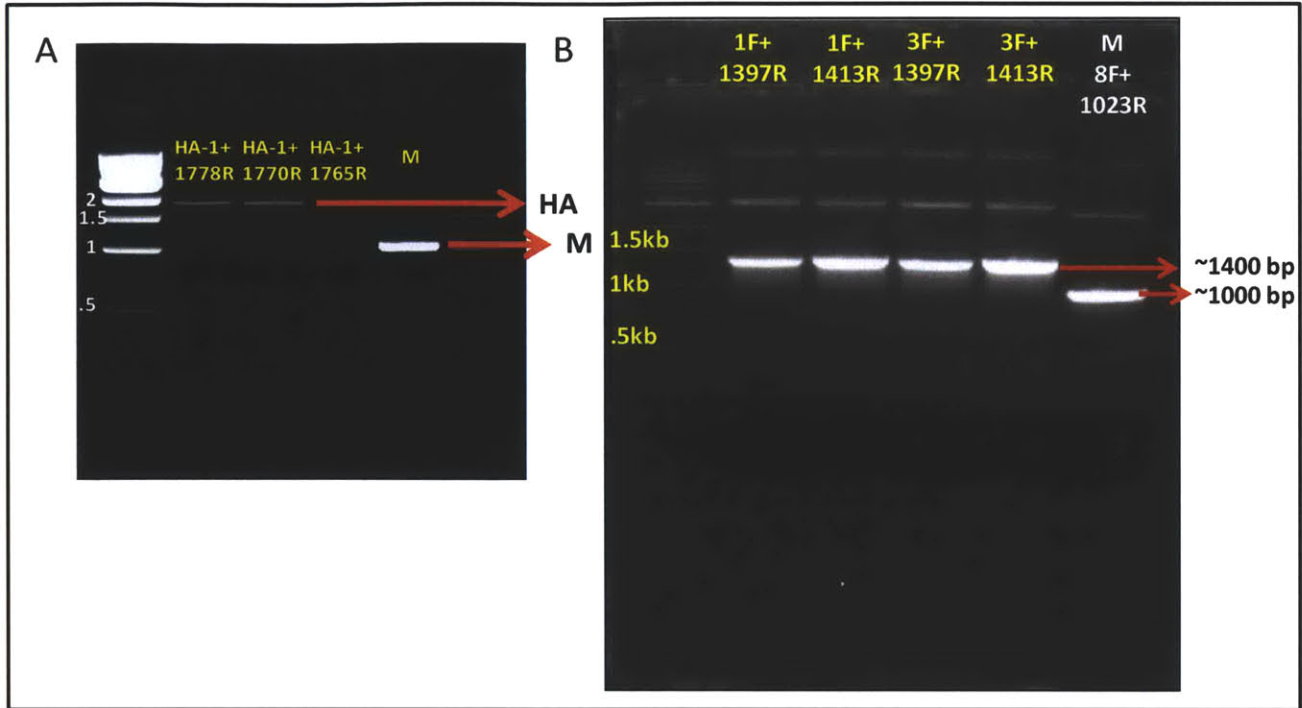


Fig 4.5 A. HA gene amplified after processing vS/N. B. Validation of NA Primers.

Gel Purified Products were sent out for sequencing. Note : HA-1770R (+HA1) provided shorter sequence read (the difference cannot be visualized on the gel). HA-1778R (+HA1) was chosen for the longest sequence length).

- A.
1. Check validity of primers (A +ve Control for Reverse Genetics)
 - Use Plasmids with primers designed and PCR
 - 2ul of each primer + 3 ul plasmid + 45 ul PCR platinum super mix
 - Run on gel and you should see product bands
 2. Gene-specific primers to amplify plasmids in S/N
 - Use S/N (~2-3 ul) after 1x media change post-transfection as the DNA template and verify product formation.
 - Run on gel and see product band

Note: If you do have infectious particles in the S/N then extract RNA and proceed to generate cDNA and dsDNA.
 3. Verify Sequences
 - Use the gene-specific Primers and sequence dsDNA generated from Step #2
 - (Sequences should show alignment to the Pubmed sequences of Pr8 EF467817-EF467824).
 - HA Primers
 - HA-1 (FORWARD) and HA-1778R (REVERSE).
 - M Primers
 - M-8 (FORWARD) and M-1023R (REVERSE).
 - NA Primers
 - NA-1 FORWARD and NA-1413 (REVERSE)
- B.
- 5ul of vS/N after syringe filtering using 0.45 um filter. 48h samples were tested.
 - HA, M and NA primers were used.
 - HA-1For + HA1778 Rev
 - ~1.8 kb
 - M – M-FOR + M-1023REV
 - ~1 kb
 - NA – 1For + 1413Rev
 - ~1.4 kb



Fig. 4.6 A. Sequencing guidelines in the context of Reverse Genetics. B. Amplification of HA, NA and M plasmids from v S/N of transfection reaction

5 Decoding Pectins – Establishment of a structure-function relationship for complex glycans in cancer.

5.1 Summary

The use of pectins, natural polysaccharides derived from plant sources as anti-cancer agents have offered promising results [99, 100]. Studies suggest that the pectic oligosaccharides generated by enzyme digestion have a greater protective effect than untreated pectins and imply that specific components of pectic oligosaccharides (i.e., galactan and structures released by enzymatic degradation) may provide therapeutic efficacy. However, defining specific structural motifs responsible for this observed activity would be crucial to develop pectin based therapeutics. Biochemical binding assays to determine specific activities and *in vivo* experiments to test more rigorously this therapeutic potential of the natural carbohydrates would need to follow. To this end, outlined in this section is a detailed research plan for isolation, *in vitro* screening and structural characterization of pectic oligosaccharide fractions (POFs) with anti cancer properties. Preliminary work on developing protocols for generation of pectin fragments after enzymatic and acid based digestion were contributed by a former postdoc Toomas Haller in the lab. The *in vitro* and *in vivo* approaches outlined were developed by a former graduate student David Evarone. Under the tutelage of both Tom and Dave, I learnt the basis of dissecting pectins for a more biological read out and have outlined a proposal based on Integration of known approaches that would aid in the establishment of a structure-function relationship for complex glycans in cancer.

5.2 Introduction

5.2.1 Structural complexity of pectins

Pectin is a complex carbohydrate network composed predominantly of galacturonic acid rich polysaccharides and a major component of all primary cell walls. Pectin is loosely composed of “smooth” and “hairy” regions [101, 102]. Smooth regions are defined by homogalacturonan, a linear polymer of poly 1-4 linked α -D-galacturonic acid (GalA) moieties with varying degrees of carboxymethylation (**Fig.5.1**). The hairy regions of pectin are divided into two distinct components known as Rhamnogalacturonan I and II. Rhamnogalacturonan I is composed of homogalacturonan randomly interspersed with α -L-rhamnose (Rha) residues, adjacent to GalA residues[103]. Each of these Rha residues is a potential branch point for side chains. Rhamnogalacturonan II is the most complex form of pectin, possessing multiple branch points containing various sugars [104]. Pectin is a classic example of a complex sugar which contains a variety of individual monosaccharides, diverse glycosidic linkages and many chemical modifications like methylation and acetylation. Given the heterogeneity and complexity of pectins, many approaches have been used to degrade the pectins derived from the natural source to produce pectic oligosaccharide fractions (referred to henceforth as POFs). Although these POFs are also heterogeneous mixtures of oligosaccharide, they are more strictly defined in terms of their structural attributes such as the distribution of oligosaccharide chain lengths, chemical composition and branching patterns, etc. Pectins and POFs are achieving prominence as potential anti-cancer agents [105-110]. Specifically, there are promising studies that have demonstrated the anti-tumor action of low molecular weight pectins (LMPs) derived citrus fruit pectins using a two-step base and acid hydrolysis [105-107, 110]. These complex polysaccharides offer tremendous potential for development of various therapeutic strategies. A series of proof-of-principle experiments demonstrating that the combination of analytical tools and biological assays can lead to a substantial structure-function understanding of pectins demonstrated that this approach can be used to produce a pectin-derived mixture (LMP) which has potent anti-tumor activity in addition to extending this analytical platform to structurally characterize LMP-derived fragments [111-113].

5.2.2 *In vitro* and *in vivo* inhibition of cancer cell growth with LMP treatment

Various concentrations of LMP (0-666 mg/ml) were used to treat B16F10 cells in a 96-well plate format. A dose-dependent decrease in the number of viable cells was observed over the 2 day exposure to LMP. Using this assay, an LD₅₀ for the drug was calculated to be 116±5 mg/ml (Fig. 5.2). Treatment of the cells with PBS produced no changes in cell viability (data not shown) and suggested that the observed effect was directly attributable to LMP. This dose-dependent decrease in B16F10 cell viability confirmed this as a legitimate model for studying the cellular biology underlying the anti-tumor effect of LMP. Additionally, a similar effect in other cell lines, including SK-ES-3 murine osteosarcoma cells (LD₅₀ of 275 mg/ml) and Lewis lung carcinoma cells (LD₅₀ 53 mg/ml) was observed suggesting that LMP is capable of producing a dose-dependent decrease in cell viability in diverse tumor cell lines.

Further, this observed dose-dependent response is typical of what is seen with a variety of standard chemotherapeutic agents designed to specifically target proliferating cells through mechanisms such as irreversible DNA damage [114]. Such a defined, reproducible response was surprising for LMP given its structural heterogeneity and no real *a priori* cellular target or mechanism of action. Other polysaccharide polymers, including unmodified pectin, polygalacturonic acid, and heparin do not produce such a response when used to treat B16F10 tumor cells in this model (data not shown). This confirmed a specific sugar motif exposed during the generation of LMP that directly produces the cell mortality observed and a specific interaction at the cell surface that initiates a signal transduction cascade leading to observed cellular response.

Encouraged by the *in vitro* response of the B16F10 cell line to LMP, an initial experiment was performed to test the effect of the therapeutic in an *in vivo* tumor model. Primary tumors were initiated by the subcutaneous injection of B16F10 melanoma cells into the rear flank of syngeneic mice. The mice were treated with daily tail vein injections of 4 mg/kg, 10 mg/kg LMP, or PBS control beginning on Day 7 when tumors first became palpable. Treatment continued for 15 days before the mice were sacrificed. Tumor-bearing mice treated with 4 mg/kg LMP showed a 75% decrease in overall tumor volume while mice treated with 10 mg/kg demonstrated a 95% decrease in tumor volume in comparison with the PBS controls (Fig. 5.3).

There was a significant, dose-dependent decrease in tumor size over the period of treatment when compared to mice treated with PBS alone (Fig. 5.4). There were no deaths or observed changes in overall body weight, as well as no observed cell death in tissue surrounding the tumors upon the administration of the LMP which confirmed that LMP was not toxic to the mice at the current doses over the period of administration (results not shown).

These pilot experiments that were developed to monitor the anti-tumor effects of LMP revealed that LMP treatment leads to a decrease in B16F10 cell viability *in vitro* and to an inhibition of primary tumor growth *in vivo* thus serving as a biological platform to elucidate the structure-function relationship of pectin structures that possess anti-cancer properties.

5.2.3 Analytical tools to elucidate pectin structure

In parallel with the development of the *in vitro* and *in vivo* assays, Toomas Haller began to apply experience with the structural analysis of GAGs to the study of LMP. The first step in this analysis was to demonstrate that enzymatically could degrade LMP and analyze its products using a CE-based approach similar to that used to study GAGs. Pectin lyase (PL) was employed to begin these enzymatic studies because, like the heparinases and chondroitinases, it leaves behind a $\Delta^{4,5}$ double bond that serves as an internal chromophore ($\lambda_{\max} = 232$ nm) in the reaction products [115]. With minor modifications to the CE methodology developed for the analysis of GAGs, Dr. Haller was able to detect the PL-generated products of LMP (data not shown). Unsurprisingly, the primary peak in the electropherogram was identified as GalA by co-migration with known standards. PL specifically cleaves the homogalacturonan regions of LMP, regardless of methylation and leaves behind GalA monosaccharides and larger, intact “hairy” regions. In the future other HPLC-based analytical techniques could be used to isolate these remaining hairy regions and examine their structure and biological activity.

Further, LMP was degraded using polygalacturonase (PG), a hydrolytic enzyme specific for regions of unmethylated homogalacturonan [116, 117]. Since PG digestion does not result in products containing the $\Delta^{4,5}$ double bond, the enzymatic reaction products were end-labeled using 1-aminopyrene-3,6,8-trisulfonate (APTS). In addition to being a chromophore ($\lambda_{\max} = 488$ nm), APTS-labeling introduces a negatively charged trisulfonate residue onto the reducing end of the reaction products [118]. This redistribution in the aggregate charge in the mono- and

oligosaccharides necessitated development of a novel CE methodology for the adequate separation of the PG reaction products [119]. PG digestion of LMP reveals multiple GalA-containing products, ranging from simple to higher order oligosaccharides (Fig. 5.5). MALDI_MS was used for further, examination of the PG-generated mono- and oligosaccharides [120, 121]. Similar to the CE results, the presence of mono- to multimeric GalA-containing saccharides, consistent with the degradation of the homogalacturonan regions of LMP was observed (data not shown).

These initial experiments served as initial proof-of-principle that the tools developed for the analysis of GAGs could be extended to the structural analysis of the pectic fractions generated as outlined in the research design.

5.3 An integrated research design for the isolation, *in vitro* screening and structural characterization of pectic oligosaccharide fractions (POFs) with cancer inhibiting properties

5.3.1 Rationale

The goal would be to develop a robust structure-function framework for generating POFs as potential inhibitors for cancer. To accomplish this goal the first objective would be to develop chemical and enzymatic methodologies for the controlled and reproducible degradation of citrus pectin to obtain different POFs that would then be tested for activity using quantitative biochemical assays. From these results biochemical studies, the POFs with notable antagonist activities would then be subjected to detailed structural characterization using a combination of analytical methods such as composition by capillary electrophoresis (CE), linkage determination and degree of substitution, such as methylation, by nuclear magnetic resonance (NMR) and mass/chain length by mass spectrometry (MS). The structural attributes will then be used to generate theoretical structural models of individual oligosaccharide(s) representing the predominant attributes of a given POF or mixtures. Cognizant that the properties of a distribution of oligosaccharides are mapped to a representative oligosaccharide in this approach, multiple 'modeled' oligosaccharides for a given POF would then be generated. The models will be used as a framework to identify the specific structural attributes that contribute

to anticancer activity as well as to provide feedback to modify the POF-generating methods to enhance these structural attributes in the oligosaccharide mixture. The overall strategy shown in Fig. 5.6 is described below in detail.

5.3.2 Strategy

5.3.2.1 Enzymatic and chemical degradation of pectins to generate POFs

5.3.2.1.1 Developing and using enzymatic tools for precise degradation of pectins

There are three broad classes of enzymes that degrade pectin: 1) enzymes that cleave the homogalacturonan backbone; 2) enzymes that degrade the backbone of “hairy” regions; and 3) enzymes that selectively degrade the neutral side chains off the rhamnose branch points (Fig. 5.7). The first class of enzymes includes pectin lyase (PL) and polygalacturonase (PG) used extensively in preliminary studies to characterize the pectic oligosaccharide fragments constituting LMP. As previously mentioned, PL and PG differ in their ability to cleave carboxymethylated homogalacturonan regions of pectin, with PG being refractory to a high degree of methylation in the pectin backbone. By incubating these enzymes for different durations with pectin starting material, we will be able to generate POFs comprising homogalacturonan oligosaccharides with diverse chain length and composition (GalA vs. methylated GalA).

Rhamnogalacturonan lyases (RGL) represent the second class of pectin degrading enzymes. This class of enzymes specifically cleaves bonds in the rhamnose-interspersed backbone found in the “hairy” regions of pectin [122]. RGLs specifically cleave the 1→4 bond between Rha and GalA in the hairy region backbone leaving the neutral sugar side chain of the Rha residue intact (Fig. 5.7). Similar to pectin lyase, RGL leaves a $\Delta^{4,5}$ double bond, which increases its utility for studying reaction kinetics and monitoring product formation., since the product absorbs UV light at approximately 230 nm. Two RGLs (designated RGL A and B) have been isolated and cloned from *Aspergillus aculeatus* [123]. Other members of the *Apergillus* genus are also reported to be rich sources of pectin degrading enzymes, including different RGLs [124]. In varying incubation times of pectin with RGL A and B, we will be able to liberate the smooth

regions from the branched neutral side chains, enabling generation of POFs with distinct structural attributes including enrichment in the branched neutral galactan chains.

Finally, pectin-degrading enzymes, such as β -galactosidase, arabinase and galactanase, can be used to selectively degrade components of the neutral sugar side chains found in the “hairy” regions of pectin [125, 126]. Together these enzymatic tools will be critical to the generation as well as structural investigation of a reasonable number of POFs with distinct structural attributes that will then be screened for anti cancer activities.

5.3.2.1.2 Chemical methods to generate POFs:

Chemical methods viz., high temperature and alkaline treatment of the starting material have been used to derive LMPs. We will first try using. High temperature treatment of pectin, without a pH change, catalyzes chain fragmentation via acid-based hydrolysis, generating smaller oligosaccharides. Alkaline conditions favor the chemical processes of demethylation and depolymerization of the homogalacturonan backbone [127]. Conversely, acidic treatment under controlled conditions will favor the liberation of long chains of polygalacturonic acid due to the preferential cleavage of glycosidic bonds in hairy regions [128]. In addition to generating POFs using these chemical methods coupling chemical approaches with enzyme digestion by treating enzyme digested POFs with specific temperature and pH schemes would produce POFs with a greater diversity in the structural attributes that will be used in screening studies.

5.3.2.2 Testing pectic derivatives for Anti Cancer Activity

5.3.2.3 Development of analytical tools for structural characterization of POFs

The POFs demonstrating significant antagonist activities will be structurally characterized using a combination of analytical techniques including CE, MALDI-MS, HPLC and NMR (**Fig. 5.8**). A critical component of the analysis of mono- and oligosaccharides derived from the POFs will be labeling the reducing end of the saccharide with a chromophore to enable its detection using a diode array detector. In initial experiments the enzymatically derived reaction products were end-labeled with APTS to promote their separation and detection using CE [129]. We will employ a variety of other charged and hydrophobic labels previously used for the end-labeling of carbohydrates including 2-anthralilic acid (2-AA), 2-aminoacridone (AMAC), and 8-

aminonaphthalene-1,3,6-trisulfonic acid (ANTS) as application specific tags for the separation and detection of LMP-derived fragments [118, 130-132]. ^1H and ^{13}C , 1D NMR analysis of the POFs would provide valuable information on the relative abundance of modifications such as methylation and acetylation of the oligosaccharide chains, average chain length and abundance of unsaturated uronic acids (derived from β -elimination of GalA). In addition to CE, MALDI-MS and NMR techniques for the analysis for the fine structure of the POFs, HPLC-based separation analysis of different enzymatic and chemically generated fractions. We will use both size exclusion (SEC-HPLC) and strong anion exchange (SAX-HPLC) methods to separate the constituent oligosaccharides in POFs based on size and charge respectively. These techniques allow for the separation of the larger components of enzymatic digests, and provide a suitable compliment to the use of CE that allows for the detection and fingerprinting of smaller reaction products. Finally, we will interface HPLC with electrospray ionization mass spectrometry (LC-ESI-MS) to enable the separation and online mass identification of the various components of enzymatically and chemically generated POFs. For this application, we will rely on C18 reverse phase chromatography to separate the oligosaccharide components of the POFs based on their hydrophobicity. Labels such as AMAC will be introduced to increase the overall hydrophobicity of the oligosaccharides and to provide a facile means of detection [131]. We will also perform MS/MS analysis on the oligosaccharide component to derive defined sequence information of the parent molecule. Combining this technique with CE, MALDI-MS, and a variety of HPLC separation techniques, we will be able to provide a more comprehensive understanding of the structural attributes of POFs that will be valuable for understanding their structure-function roles in cancer inhibition.

5.3.2.4 Modeling approaches with pectic oligosaccharides

Although these POFs comprise a heterogeneous mixture of oligosaccharides, the modeling of oligosaccharide structures which possess a representative set of the predominant structural attributes will enable the correlation of these attributes to the cancer inhibiting properties of the POFs. The Sasisekharan lab has performed several studies involving structural and conformational analysis of glycan-protein interactions including the recent study demonstrating the key role that glycan structural topology plays in determining the binding specificity of

influenza A virus hemagglutinin to its sialylated glycan receptors [1]. A modeling approach will also provide a feedback mechanism for the POF generation process to enrich specific structural attributes that enhance their cancer inhibition properties.

In summary, the enzymatic as well as chemical methods will not only be useful for the generation and structural characterization of diverse POFs; but they will be critical tools that will also be used in an iterative fashion to generate distinct POFs. Positive hits and other feedback from our screening assays along with structural information on promising POFs are critical constraints for glycan-protein modeling studies. The glycan-protein structural investigation will help us refine the sample space of distinct POFs that will be further generated and tested. Once promising pectic oligosaccharides are generated, further optimization using the above tools, will be undertaken (this logic is schematically shown in **Fig. 5.9**). Such an iterative approach has been previously implemented by the lab in the generation of more defined low molecular weight heparins as well as LMPs. This strategy has led to the successful development of a polysaccharide that is a clinical candidate currently in Phase II trials in humans [14].

5.4 Experimental Methods

5.4.1 Production of pectic derivatives by temperature and pH:

Temperature treatment is performed by incubating a solution of purified pectin in an incubation oven, ranging from 40-80°C for 0.5-3 hours. Treatment with pH is performed by addition of NaOH to achieve a final pH value ranging from 7-12.

5.4.2 Capillary electrophoresis (CE)

For CE studies analyzing monosaccharide composition, pectins are first hydrolyzed into their monosaccharide constituents by 72-hour incubation in 200mM trifluoroacetic acid (TFA) at 80°C. To ensure complete hydrolysis, the samples are then incubated with 2U of pre-dialyzed pectinases (Sigma-Aldrich) for 48 hours in 60 mM sodium acetate buffer, pH 5 at 45°C. After lyophilization, the hydrolyzed pectins (and reference monosaccharides) are labeled with the APTS fluorophore [118], using a 3:1 molar ratio of APTS: pectin. The samples are then analyzed with 40mM sodium tetraborate running buffer using a Beckman Coulter P/ACE MDQ

instrument. Peak assignment is determined by spiking samples with known standards of labeled monosaccharides. For CE analysis of pectin lyase products, the samples are monitored by absorbance at 232 nm using the same running conditions. The polygalacturonase products are labeled with APTS, as described above, and run under the same conditions using laser induced fluorescence (LIF). For both enzyme degradation products, assignments of peaks are determined by co-migration of known standards.

5.4.3 MALDI-MS

Mass spectral analysis is performed using a Voyager Workstation instrument. Sample preparation was performed by mixing pectin samples with the matrix 2,5-dihydroxybenzoic acid (DHB), a commonly utilized matrix for MALDI-MS of oligosaccharides [133]. The samples are then analyzed using linear negative mode.

5.4.4 NMR

¹H-NMR is performed by using pectin samples at 10 mg/ml in D₂O. Data collection is done at 80°C using 500 scans with a 400 MHz Bruker instrument. ¹³C-NMR is performed in the same manner except spectrum acquisition is completed at room temperature and with 20,000 scans. Given the heterogeneity of pectins, the generation of POFs in a controlled and reproducible fashion is a sizeable undertaking which offers several potential challenges. For example, the same generation method could result in POFs with variations in the structural attributes such as distribution of chain lengths or relative abundance of different monosaccharide units. We have observed similar issues with heparin and have been able to address this effectively. Thus, we anticipate the need to evaluate the effect of these variations in the competitive binding of the POFs to the cancer cells in the inhibition assay. This evaluation will be further refined using our modeling approach to determine if the variation of a specific attribute is likely to cause significant perturbation to the molecular contacts with the glycan binding site.

5.5 Acknowledgements

I would like to acknowledge the help of fellow graduate student Luke Robinson and research scientist Rahul Raman in the generation of this part of my thesis on pectins that we originally

used as a grant. As first year and second year graduate students (Luke and I resp.) we were provided preliminary instructions on the analytical procedures outlined by Dr. Haller. I would also like to express my gratitude to Dr. Raman for the help provided with developing the modeling rationale.

5.6 References

- 1 Wong, T. W., Colombo, G. and Sonvico, F. (2011) Pectin matrix as oral drug delivery vehicle for colon cancer treatment. *AAPS PharmSciTech.* **12**, 201-214
- 2 Glinsky, V. V. and Raz, A. (2009) Modified citrus pectin anti-metastatic properties: one bullet, multiple targets. *Carbohydr Res.* **344**, 1788-1791
- 3 Mohnen, D. (2008) Pectin structure and biosynthesis. *Curr Opin Plant Biol.* **11**, 266-277
- 4 Gunning, A. P., Bongaerts, R. J. and Morris, V. J. (2008) Recognition of galactan components of pectin by galectin-3. *Faseb J*
- 5 Willats, W. G., McCartney, L., Mackie, W. and Knox, J. P. (2001) Pectin: cell biology and prospects for functional analysis. *Plant Mol Biol.* **47**, 9-27
- 6 Ishii, T., Matsunaga, T., Pellerin, P., O'Neill, M. A., Darvill, A. and Albersheim, P. (1999) The plant cell wall polysaccharide rhamnogalacturonan II self-assembles into a covalently cross-linked dimer. *J Biol Chem.* **274**, 13098-13104
- 7 Pienta, K. J., Naik, H., Akhtar, A., Yamazaki, K., Replogle, T. S., Lehr, J., Donat, T. L., Tait, L., Hogan, V. and Raz, A. (1995) Inhibition of spontaneous metastasis in a rat prostate cancer model by oral administration of modified citrus pectin. *J Natl Cancer Inst.* **87**, 348-353
- 8 Inohara, H. and Raz, A. (1994) Effects of natural complex carbohydrate (citrus pectin) on murine melanoma cell properties related to galectin-3 functions. *Glycoconj J.* **11**, 527-532
- 9 Platt, D. and Raz, A. (1992) Modulation of the lung colonization of B16-F1 melanoma cells by citrus pectin. *J Natl Cancer Inst.* **84**, 438-442
- 10 Jackson, C. L., Dreaden, T. M., Theobald, L. K., Tran, N. M., Beal, T. L., Eid, M., Gao, M. Y., Shirley, R. B., Stoffel, M. T., Kumar, M. V. and Mohnen, D. (2007) Pectin induces apoptosis in human prostate cancer cells: correlation of apoptotic function with pectin structure. *Glycobiology.* **17**, 805-819
- 11 Guess, B. W., Scholz, M. C., Strum, S. B., Lam, R. Y., Johnson, H. J. and Jennrich, R. I. (2003) Modified citrus pectin (MCP) increases the prostate-specific antigen doubling time in men with prostate cancer: a phase II pilot study. *Prostate Cancer Prostatic Dis.* **6**, 301-304
- 12 Nangia-Makker, P., Hogan, V., Honjo, Y., Baccarini, S., Tait, L., Bresalier, R. and Raz, A. (2002) Inhibition of human cancer cell growth and metastasis in nude mice by oral intake of modified citrus pectin. *J Natl Cancer Inst.* **94**, 1854-1862
- 13 Guerrini, M., Beccati, D., Shriver, Z., Naggi, A., Viswanathan, K., Bisio, A., Capila, I., Lansing, J. C., Guglieri, S., Fraser, B., Al-Hakim, A., Gunay, N. S., Zhang, Z., Robinson, L., Buhse, L., Nasr, M., Woodcock, J., Langer, R., Venkataraman, G., Linhardt, R. J., Casu, B., Torri, G. and Sasisekharan, R. (2008) Oversulfated chondroitin sulfate is a contaminant in heparin associated with adverse clinical events. *Nat Biotechnol*
- 14 Guerrini, M., Guglieri, S., Naggi, A., Sasisekharan, R. and Torri, G. (2007) Low molecular weight heparins: structural differentiation by bidimensional nuclear magnetic resonance spectroscopy. *Semin Thromb Hemost.* **33**, 478-487
- 15 Sasisekharan, R., Raman, R. and Prabhakar, V. (2006) Glycomics approach to structure-function relationships of glycosaminoglycans. *Annu Rev Biomed Eng.* **8**, 181-231

- 16 Herzig, M. C., Rodriguez, K. A., Trevino, A. V., Dziegielewski, J., Arnett, B., Hurley, L. and Woynarowski, J. M. (2002) The genome factor in region-specific DNA damage: the DNA-reactive drug U-78779 prefers mixed A/T-G/C sequences at the nucleotide level but is region-specific for long pure AT islands at the genomic level. *Biochemistry*. **41**, 1545-1555
- 17 Nedjma, M., Hoffmann, N. and Belarbi, A. (2001) Selective and sensitive detection of pectin lyase activity using a colorimetric test: application to the screening of microorganisms possessing pectin lyase activity. *Anal Biochem*. **291**, 290-296
- 18 Daas, P. J., Voragen, A. G. and Schols, H. A. (2000) Characterization of non-esterified galacturonic acid sequences in pectin with endopolygalacturonase. *Carbohydr Res*. **326**, 120-129
- 19 Daas, P. J., Boxma, B., Hopman, A. M., Voragen, A. G. and Schols, H. A. (2001) Nonesterified galacturonic acid sequence homology of pectins. *Biopolymers*. **58**, 1-8
- 20 Guttman, A., Chen, F. T., Evangelista, R. A. and Cooke, N. (1996) High-resolution capillary gel electrophoresis of reducing oligosaccharides labeled with 1-aminopyrene-3,6,8-trisulfonate. *Anal Biochem*. **233**, 234-242
- 21 Zhang, Z., Pierce, M. L. and Mort, A. J. (1996) Detection and differentiation of pectic enzyme activity in vitro and in vivo by capillary electrophoresis of products from fluorescent-labeled substrate. *Electrophoresis*. **17**, 372-378
- 22 van Alebeek, G. J., Zabolina, O., Beldman, G., Schols, H. A. and Voragen, A. G. (2000) Structural analysis of (methyl-esterified) oligogalacturonides using post-source decay matrix-assisted laser desorption/ionization time-of-flight mass spectrometry. *J Mass Spectrom*. **35**, 831-840
- 23 Daas, P. J., Arisz, P. W., Schols, H. A., De Ruiter, G. A. and Voragen, A. G. (1998) Analysis of partially methyl-esterified galacturonic acid oligomers by high-performance anion-exchange chromatography and matrix-assisted laser desorption/ionization time-of-flight mass spectrometry. *Anal Biochem*. **257**, 195-202
- 24 Mutter, M., Renard, C. M., Beldman, G., Schols, H. A. and Voragen, A. G. (1998) Mode of action of RG-hydrolase and RG-lyase toward rhamnogalacturonan oligomers. Characterization of degradation products using RG-rhamnohydrolase and RG-galacturonohydrolase. *Carbohydr Res*. **311**, 155-164
- 25 Kofod, L. V., Kauppinen, S., Christgau, S., Andersen, L. N., Heldt-Hansen, H. P., Dorreich, K. and Dalboge, H. (1994) Cloning and characterization of two structurally and functionally divergent rhamnogalacturonases from *Aspergillus aculeatus*. *J Biol Chem*. **269**, 29182-29189
- 26 McKie, V. A., Vincken, J. P., Voragen, A. G., van den Broek, L. A., Stimson, E. and Gilbert, H. J. (2001) A new family of rhamnogalacturonan lyases contains an enzyme that binds to cellulose. *Biochem J*. **355**, 167-177
- 27 Pitson, S. M., Voragen, A. G., Vincken, J. P. and Beldman, G. (1997) Action patterns and mapping of the substrate-binding regions of endo-(1->5)-alpha-L-arabinanases from *Aspergillus niger* and *Aspergillus aculeatus*. *Carbohydr Res*. **303**, 207-218
- 28 Christgau, S., Sandal, T., Kofod, L. V. and Dalboge, H. (1995) Expression cloning, purification and characterization of a beta-1,4-galactanase from *Aspergillus aculeatus*. *Curr Genet*. **27**, 135-141

- 29 Renard, C., and Thibault, J.F. (1996) Degradation of pectins in alkaline conditions: kinetics of demethylation. *Carbohydr Res.* **286**, 139-150
- 30 Thibault, J.-F., Renard, C.M.G.C., Axelos, M., Roger, P., and Crepeau, M.J. (1993) Studies on the length of homogalacturonic regions in pectins by acid-hydrolysis. *Carbohydr Res.* **238**, 271-286
- 31 Hamai, A., Hashimoto, N., Mochizuki, H., Kato, F., Makiguchi, Y., Horie, K. and Suzuki, S. (1997) Two distinct chondroitin sulfate ABC lyases. An endoeliminase yielding tetrasaccharides and an exoeliminase preferentially acting on oligosaccharides. *J Biol Chem.* **272**, 9123-9130
- 32 Mort, A. J. and Chen, E. M. (1996) Separation of 8-aminonaphthalene-1,3,6-trisulfonate (ANTS)-labeled oligomers containing galacturonic acid by capillary electrophoresis: application to determining the substrate specificity of endopolygalacturonases. *Electrophoresis.* **17**, 379-383
- 33 Militopoulou, M., Lamari, F. N., Hjerpe, A. and Karamanos, N. K. (2002) Determination of twelve heparin- and heparan sulfate-derived disaccharides as 2-aminoacridone derivatives by capillary zone electrophoresis using ultraviolet and laser-induced fluorescence detection. *Electrophoresis.* **23**, 1104-1109
- 34 Bigge, J. C., Patel, T. P., Bruce, J. A., Goulding, P. N., Charles, S. M. and Parekh, R. B. (1995) Nonselective and efficient fluorescent labeling of glycans using 2-amino benzamide and anthranilic acid. *Anal Biochem.* **230**, 229-238
- 35 Chandrasekaran, A., Srinivasan, A., Raman, R., Viswanathan, K., Raguram, S., Tumpey, T. M., Sasisekharan, V. and Sasisekharan, R. (2008) Glycan topology determines human adaptation of avian H5N1 virus hemagglutinin. *Nat Biotechnol.* **26**, 107-113
- 36 Papac, D. I., Wong, A. and Jones, A. J. (1996) Analysis of acidic oligosaccharides and glycopeptides by matrix-assisted laser desorption/ionization time-of-flight mass spectrometry. *Anal Chem.* **68**, 3215-3223

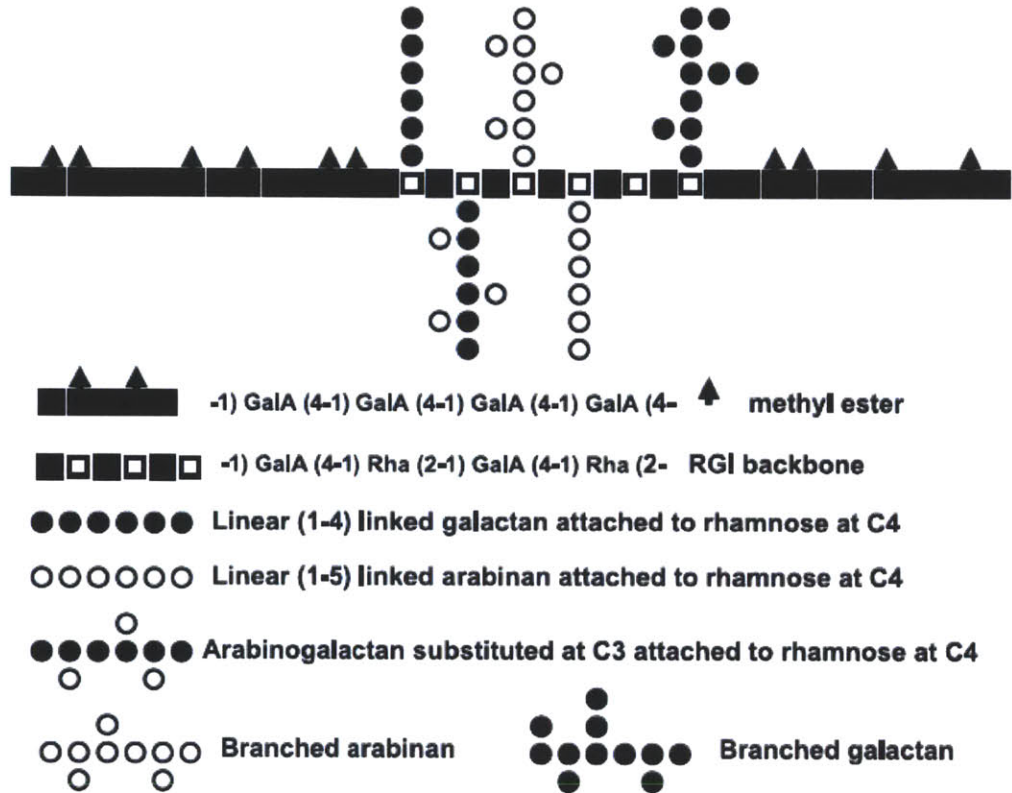


Figure 5.1: Structural complexity of pectins (adapted from Gunning et al)

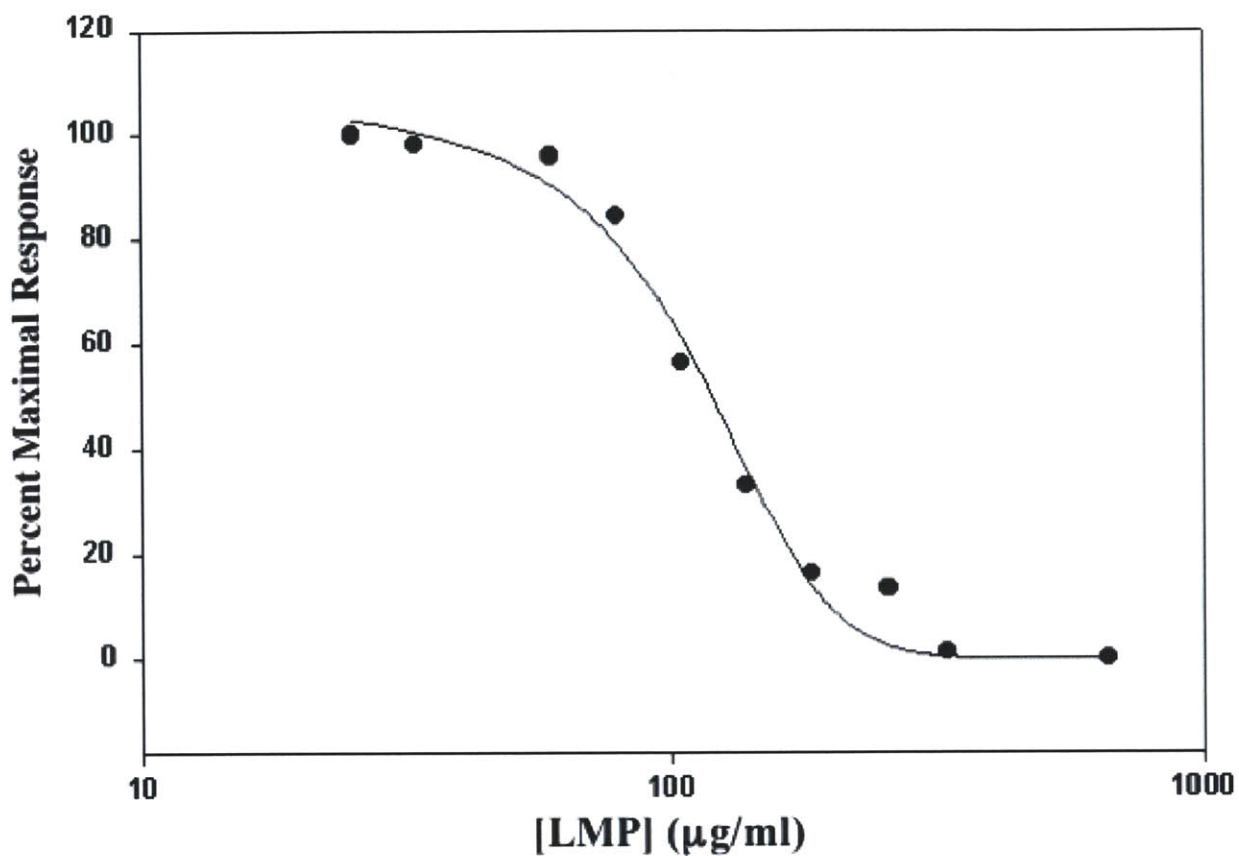


Figure 5.2: LMP inhibits B16F10 cell growth *in vitro*.

B16F10 cells were treated with LMP in a 96 well plate. Cell viability was quantified using the CellTiter reagent (Promega). The LD50 calculated using this assay was 116 ± 5 µg/ml LMP. This graph represents one of the experiments used in calculating the LD50 (n=6).

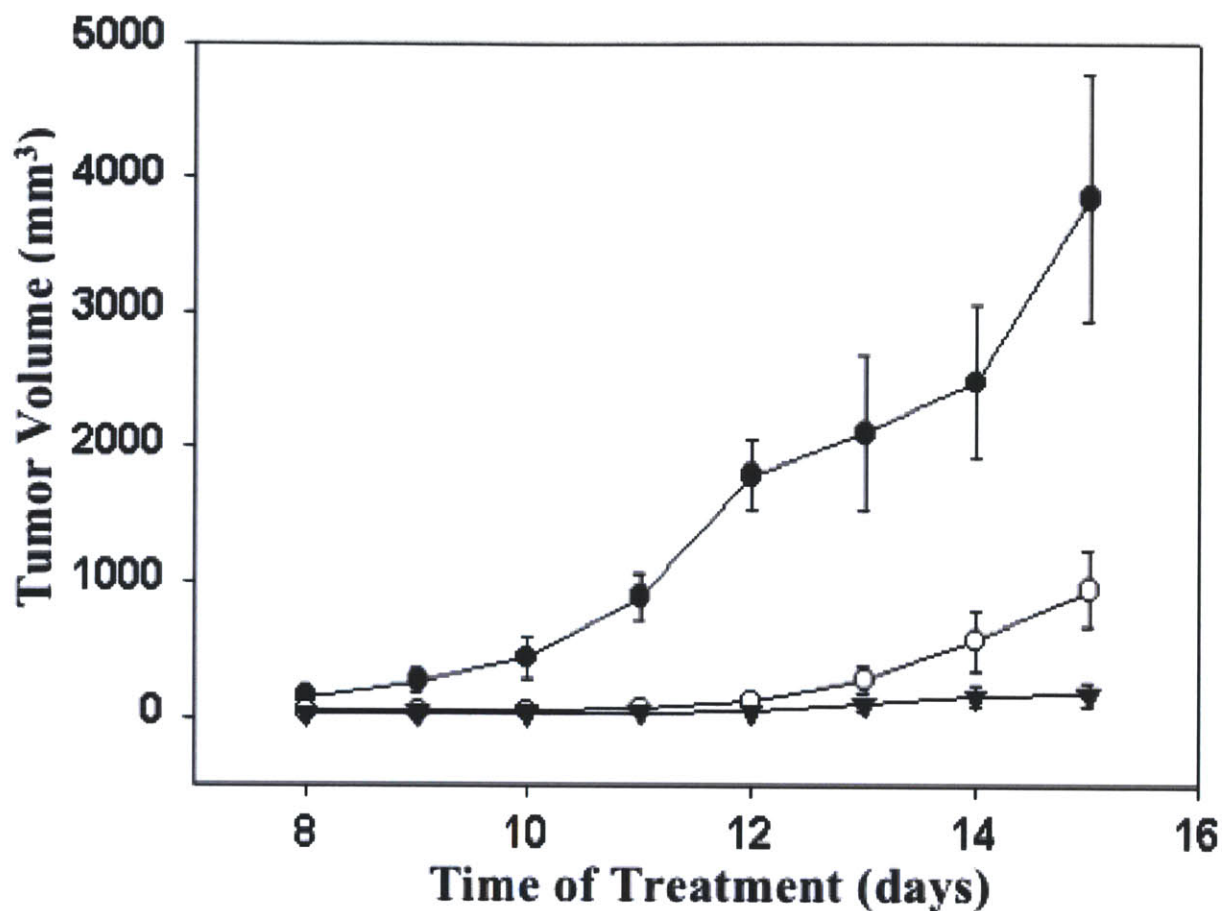


Figure 5.3. Inhibition of primary tumor growth by LMP.

Primary tumors were initiated by subcutaneous injection of B16F10 melanoma cells into syngeneic mice were measured daily with calipers. Animals were treated daily with PBS (●), 4 mg/kg LMP (○), and 10 mg/kg LMP (▼) via i.v. administration. LMP produced a dose-dependent inhibition in primary tumor growth.



Figure 5.4: LMP treatment inhibits tumor growth *in vivo*.

Comparison of two tumor-bearing mice (*top*) treated with PBS (left) and 10 mg/kg LMP (right), respectively. Gross comparison of the primary tumors (*bottom*) of the mice from (A). After 15 days of treatment, LMP significantly inhibited the growth of primary B16F10 tumors and led to an increase of leaky blood vessels in the tumor bed.

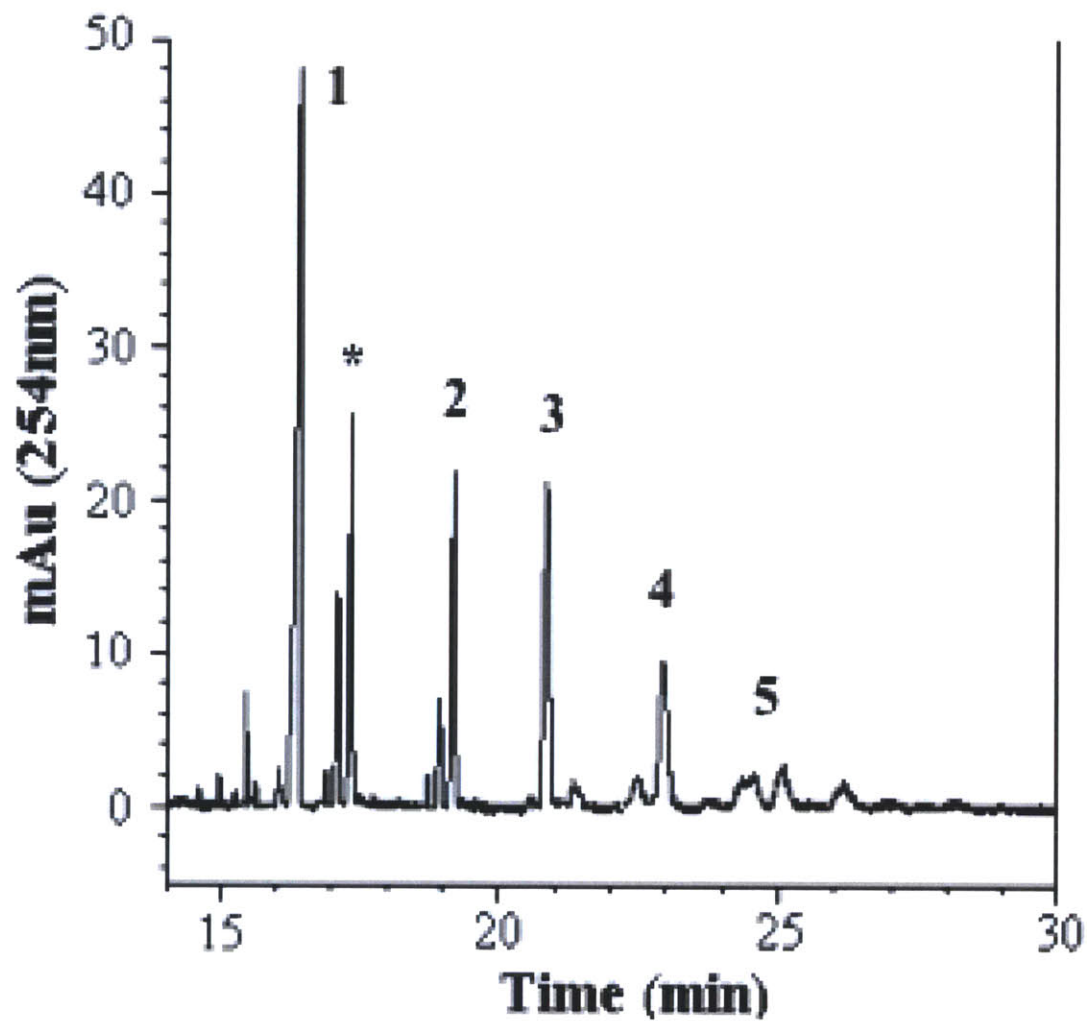


Figure 5.5. CE analysis of APTS-labeled oligosaccharides from LMP.

LMP was degraded with PG, end-labeled with APTS, and products were separated using CE. Each of the labeled peaks represents $(\text{GalA})_n$ where $n = 1-5$. The peak * is observed in both the sample digest and the GalA standard control.

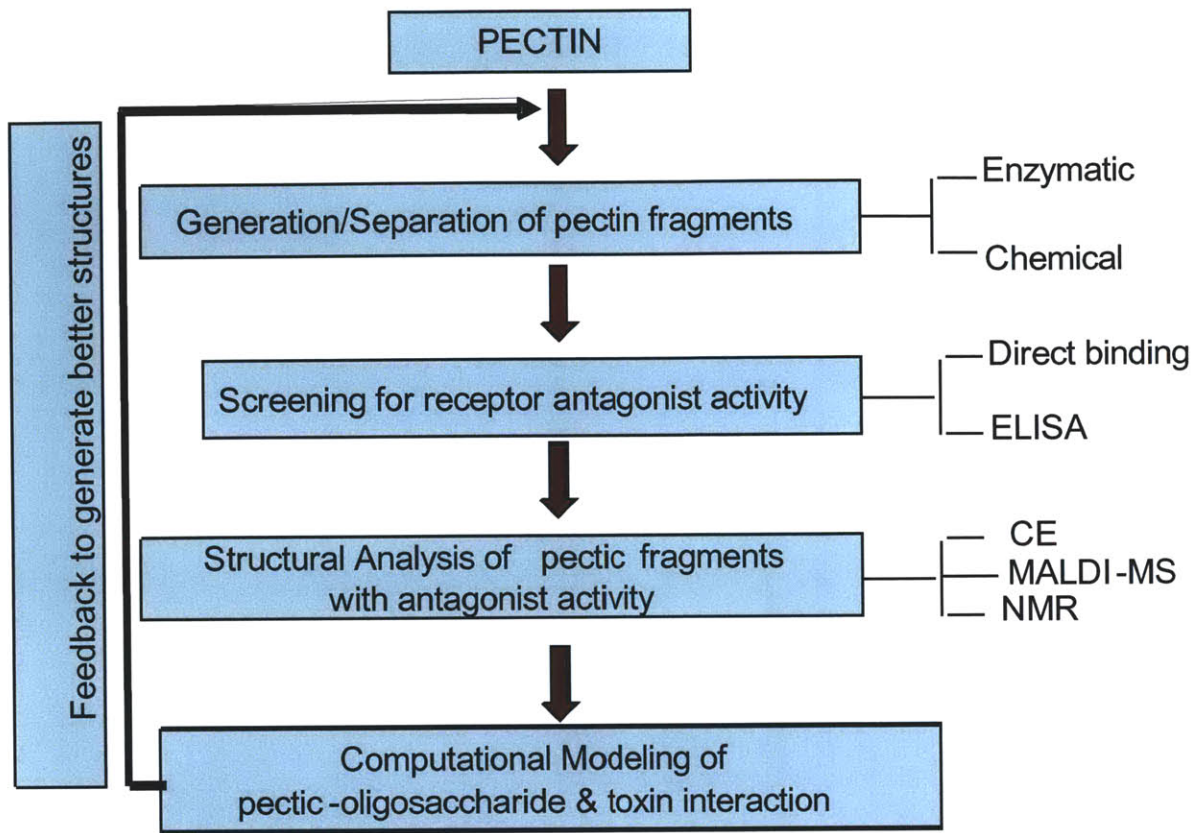


Figure 5.6. Flow chart of the strategy for Specific Aim 1.

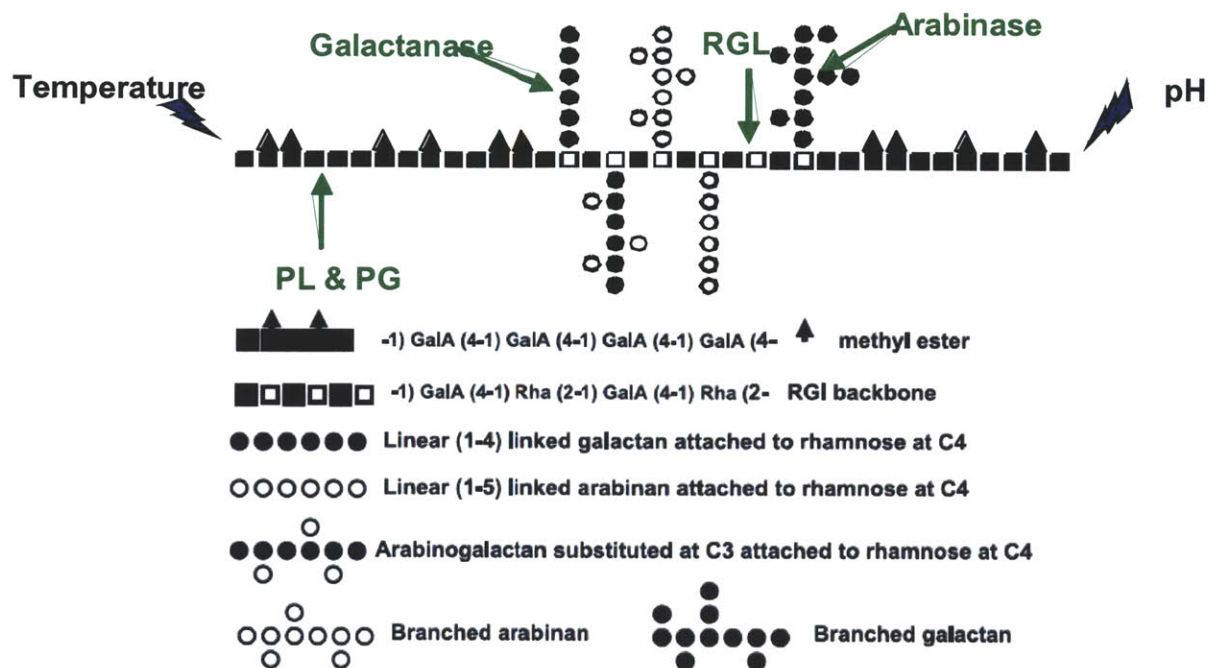


Figure 5.7. Overview of pectin-degrading enzymes (adapted from Gunning et al. [35]).

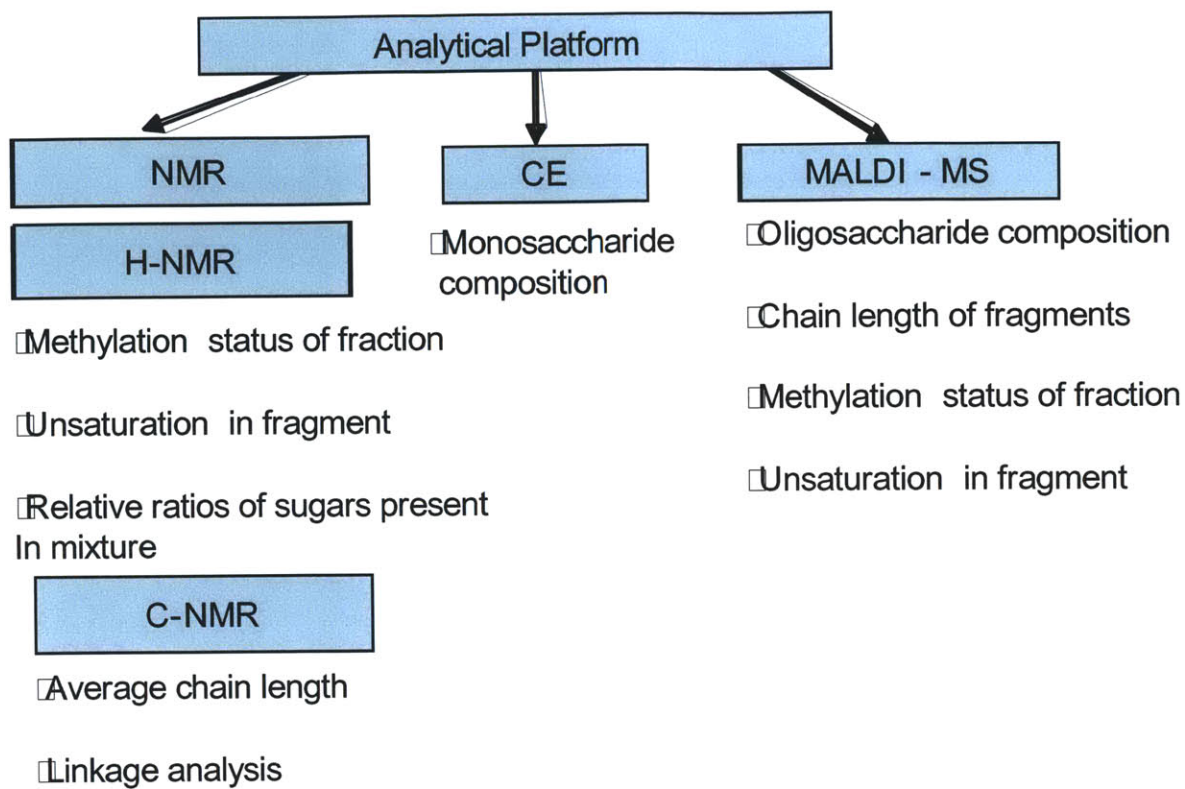


Figure 5.8. Overview of structural information garnered from analytical techniques.

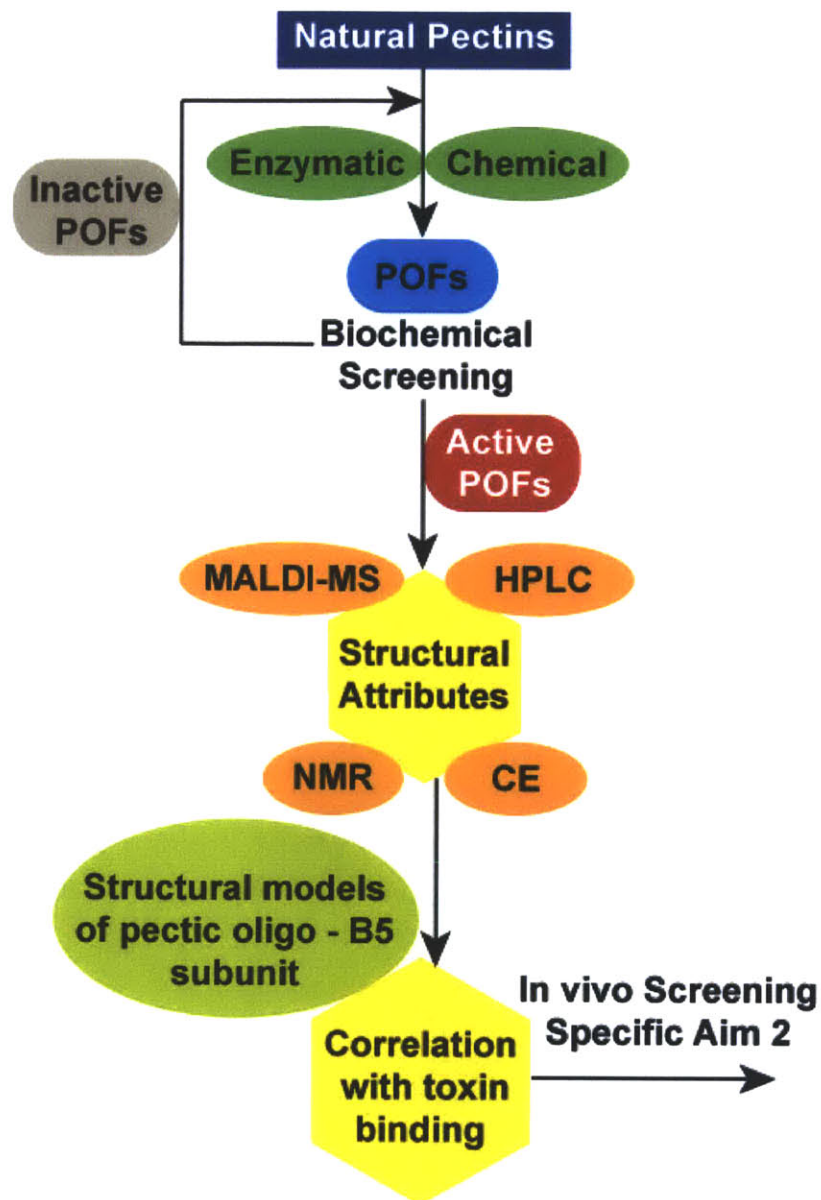


Figure 5.9. Schematic of transition.

6 Summary and Significance of Thesis Research

6.1 Is Pandemic Influenza predictable?

A 1931 editorial in the *Journal of the American Medical Association*[134] stated, “. . . it does not seem possible, with our present knowledge, to make any prediction as to whether or not an epidemic might be expected in the near future.” Unfortunately, despite more than nine decades of intensive study of influenza virus biology since this editorial was written, and almost two hundred years after the question was first posed by the German Physician Georg Friedrich Most[135], we are still unable to predict future pandemics, as evidenced by the completely unexpected emergence of the 2009 swine-origin H1N1 virus[35, 136, 137].

6.2 Avian influenza viruses and the continuing risk of a future pandemic

The past decade has been witness to the spread and establishment of stable lineages of both HPAI (H5 and H7) and LPAI Influenza virus strains (H9N2) in poultry leading to repeated human infections and consequently broad interest in pandemic prediction [138, 139]. Although overshadowed by H5N1, major poultry epizootics have occurred caused either by H7 subtype or H9N2 viruses resulting in human infections and rare human fatalities [31, 140]. Of all known avian influenza strains only H5 and H7 viruses are known to acquire the requisite polybasic insertional mutation at the HA cleavage site that makes them highly pathogenic to poultry. The last four human pandemics caused by H1 (1918, 1977, 2009), H2 (1957), and H3 (1968) subtypes, were by definition not HPAI viruses. Neither is there evidence that a human pandemic or even an epidemic has been caused by any of the many other HPAI viruses making finding the answer to whether the HPAI H7 strains in circulation could become human adapted even more pertinent. As with H5N1 [139], different genetic lineages of H9N2 have been established primarily due to prolonged circulation in domestic birds like the water fowl and quail. Some H9N2 viruses have even acquired enhanced specificity for the human form of the HA receptor[141] but whether these viruses possess sustained human-to-human transmission and consequently true pandemic potential is still unclear.

Finally, with research that shows that the most devastating of the flu pandemics, the 1918 Spanish flu rose de novo after the human adaptation of a hitherto avian strain underscoring the

need to monitor all strains of the continuously evolving virus in both wild and domestic bird populations with focus on those that have either established stable lineages in poultry and/or known to cause sporadic human respiratory infections.

Despite significant research, fundamental questions about how influenza A viruses switch hosts from wild avian species to domestic poultry and mammals, and subsequently to human hosts, remain unanswered. To cause a pandemic, an avian virus would have to adapt at least to human HA receptors and acquire human transmissibility properties; a challenge that is rarely met by most influenza A viruses.

6.3 Role of HA in Human Adaptation

Host restriction is partly mediated by the viral surface glycoprotein hemagglutinin (HA) which binds to sialylated glycan receptors, complex glycans terminated by N-acetylneuraminic acid (Neu5Ac) expressed on the host cell surface. Glycans terminating in Neu5Ac that is $\alpha 2 \rightarrow 6$ -linked to the penultimate sugar are predominantly expressed in human upper respiratory epithelia and serve as receptors for human-adapted influenza A viruses. Binding to human receptors consequently allows the virus to replicate in the respiratory epithelium in addition to allowing the virus to be conveyed via respiratory droplets when the infected individual sneezes. On the other hand, glycans terminating in Neu5Ac that is $\alpha 2 \rightarrow 3$ -linked to the penultimate sugar residue, serve as receptors for the avian-adapted influenza viruses and are typically found to replicate in the gastrointestinal tract of birds allowing these avian strains to spread via fecal-to-oral route [19, 20]. Recent studies from the Sasisekharan lab have shown that high affinity binding to human receptors correlates with transmission in vivo. A biochemical rationale for transmission capabilities of H9N2 and H7 HA containing strains of avian influenza viruses has not been reported. Further recent publications elucidating transmission capabilities for the H5N1 strains emphasize the need for similar analysis on other avian strains that pose a significant threat of becoming human adapted. Just as for H5N1 a thorough investigation of the molecular determinants of H9 and H7 subtype viruses to gain a permanent foothold in the human population is crucial for pandemic preparedness. This thesis is an analysis of the of the H9 and H7 HAs and an evaluation of their pandemic potential using a variety of techniques to provide a quantitative rationale for transmission observed in vivo for these strains.

6.4 Developing general rules for human adaptation, applicable to any Influenza strain

Only few mutations in the receptor-binding site were required to convert the avian/swine H1, H2, and H3 HAs counterparts from displaying avian receptor-binding patterns to human receptor-binding patterns [8]. Mutations to H5 HA that now afford to the human form of the receptor have now been reported; with some significant advances being made very recently [60, 142]. Changes in HA receptor binding during host adaptation are complex, and differ from subtype to subtype. The avian H5, H7 and H9 viruses and other avian subtypes may well face biological barriers in achieving efficient binding to human receptors. The approaches outlined in this thesis aim to address the aforementioned need to develop a broad set of rules that would aid in the surveillance of novel strains for human adaptation capabilities. Apart from endorsing a complementary set of techniques including quantitative biochemical characterization of binding affinity to glycan receptors, tissue staining and molecular modeling to facilitate comparison with strains already human adapted for ascertaining how far or how close the HA is from becoming human adapted; the development of quantitative PCR and reverse genetics as elegant tools for in vitro interrogation of the whole infectious virion provides an elegant route to segway into conducting in vivo studies for the transmissibility of the strains.

Ultimately, can we predict when/whether a particular avian strain will acquire sustained human-to-human transmission capabilities using the entire repertoire of tools outlined in this thesis? Answers to questions raised would also aid in development of general rules that govern human adaptation applicable to strains beyond ones currently under study and therein lays the true significance and impact of this work.

6.5 References

- 1 Editor. (1931) Occurrence of epidemic influenza in cycles. JAMA
- 2 Most, G. F. (1820) Influenza Europaea, oder die Größeste Krankheits-Epidemie der neuern Zeit Hamburg: Perthes und Besser. .:
- 3 Morens, D. M., Taubenberger, J. K. and Fauci, A. S. (2009) The persistent legacy of the 1918 influenza virus. N Engl J Med. **361**, 225-229
- 4 Taubenberger, J. K., Morens, D. M. and Fauci, A. S. (2007) The next influenza pandemic: can it be predicted? JAMA. **297**, 2025-2027
- 5 Taubenberger, J. K. and Morens, D. M. (2009) Pandemic influenza--including a risk assessment of H5N1. Rev Sci Tech. **28**, 187-202
- 6 Webster, R. G. and Govorkova, E. A. (2006) H5N1 influenza--continuing evolution and spread. N Engl J Med. **355**, 2174-2177
- 7 Guan, Y., Poon, L. L., Cheung, C. Y., Ellis, T. M., Lim, W., Lipatov, A. S., Chan, K. H., Sturm-Ramirez, K. M., Cheung, C. L., Leung, Y. H., Yuen, K. Y., Webster, R. G. and Peiris, J. S. (2004) H5N1 influenza: a protean pandemic threat. Proc Natl Acad Sci U S A. **101**, 8156-8161
- 8 Choi, Y. K., Ozaki, H., Webby, R. J., Webster, R. G., Peiris, J. S., Poon, L., Butt, C., Leung, Y. H. and Guan, Y. (2004) Continuing evolution of H9N2 influenza viruses in Southeastern China. J Virol. **78**, 8609-8614
- 9 Alexander, D. J. (2006) Avian influenza viruses and human health. Dev Biol (Basel). **124**, 77-84
- 10 Chen, F., Yan, Z. Q., Liu, J., Ji, J., Chang, S., Liu, D., Qin, J. P., Ma, J. Y., Bi, Y. Z. and Xie, Q. M. (2012) Phylogenetic analysis of hemagglutinin genes of 40 H9N2 subtype avian influenza viruses isolated from poultry in China from 2010 to 2011. Virus Genes
- 11 Ge, S. and Wang, Z. (2011) An overview of influenza A virus receptors. Crit Rev Microbiol. **37**, 157-165
- 12 Viswanathan, K., Chandrasekaran, A., Srinivasan, A., Raman, R., Sasisekharan, V. and Sasisekharan, R. (2010) Glycans as receptors for influenza pathogenesis. Glycoconj J. **27**, 561-570
- 13 Srinivasan, A., Viswanathan, K., Raman, R., Chandrasekaran, A., Raguram, S., Tumpey, T. M., Sasisekharan, V. and Sasisekharan, R. (2008) Quantitative biochemical rationale for differences in transmissibility of 1918 pandemic influenza A viruses. Proc Natl Acad Sci U S A. **105**, 2800-2805
- 14 Chen, L. M., Blixt, O., Stevens, J., Lipatov, A. S., Davis, C. T., Collins, B. E., Cox, N. J., Paulson, J. C. and Donis, R. O. (2012) In vitro evolution of H5N1 avian influenza virus toward human-type receptor specificity. Virology. **422**, 105-113
- 15 Amendola, A., Ranghiero, A., Zanetti, A. and Pariani, E. (2011) Is avian influenza virus A(H5N1) a real threat to human health? J Prev Med Hyg. **52**, 107-110